Prenatal Hydrocephalus: Prenatal Diagnosis

Dario Paladini and Roee Birnbaum

Contents

D. Paladini (✉) · R. Birnbaum
Fetal Medicine and Surgery Unit, G. Gaslini Children's Hospital, Genoa, Italy
e-mail: dpaladini49@gmail.com; roebirn@gmail.com

G. Cinalli et al. (eds.), *Pediatric Hydrocephalus*,
https://doi.org/10.1007/978-3-319-27250-4_47

Abstract

This chapter comprises three parts: (1) embryology of the central nervous system, (2) normal ultrasound appearance of the brain from the embryonic period to term of pregnancy, and (3) ultrasound prenatal diagnosis of primary and secondary ventriculomegaly/hydrocephalus. In particular, the first part of the chapter represents a thorough description of the early development of the brain in the human fetus, including an interesting sono-anatomic correlation since when the embryonic brain can be explored with ultrasound, i.e., from the 7th gestational week. The second part is meant to illustrate to non-experts in fetal neurology how ultrasound is able to follow the dramatic changes in the brain appearance and anatomy due to the various phases of cerebral development (from the normally *lissencephalic* brain of the 2nd trimester to the 3rd trimester process of neuronal proliferation and migration). The last part describes in details the diagnostic criteria to establish in the fetus a diagnosis of primary (aqueductal stenosis) versus secondary ventriculomegaly, the latter related to a wide range of genetic and developmental disorders.

Keywords

Fetal hydrocephalus · Ventriculomegaly · Prenatal diagnosis · Neurosonography · Brain development · Primary ventriculomegaly · Secondary ventriculmegaly · Congenital brain malformations

Introduction

In a reference book on pediatric hydrocephalus, the chapter dealing with fetal hydrocephalus has to take into consideration the fact that most of the readers will not be fetal medicine experts but professionals involved in the diagnosis and treatment of hydrocephalus in the neonatal and pediatric patient. Hence, we need to convey in this premise a series of key concepts in order to facilitate the interpretation of the whole chapter sections.

A Premise: The Fetus and the Cerebrospinal Fluid Circulation

1. *Embryology and brain developmental changes*. It is well-known that the human central nervous system (CNS) undergoes dramatic changes across all ages, from birth to death. However, the extent of the architectural and anatomical modifications occurring from the embryonic to the neonatal age is outstanding. This concept has important diagnostic consequences for the accuracy of prenatal diagnosis. As an example, some anomalies such as holoprosencephaly (Fig.1a) can be detected as early as 10 weeks of pregnancy; on the other hand, migration and proliferation abnormalities such as cortical malformations or microcephaly can be diagnosed only in the 3rd trimester of pregnancy in the majority of cases (Fig. 1b, c).
2. *Cerebrospinal fluid circulation*. Another field in which the uncertainties are frustratingly numerous is the issue of cerebrospinal fluid (CSF) production, circulation, and reabsorption. In fact, this very crucial topic is still but unresolved. In some studies, it has been demonstrated that the Pacchioni granules are scant and barely functional in the fetus (Mack et al. 2009). At the same time, we have still to understand why in the fetal Blake's pouch cyst, at a time when neither the Magendie nor the Luschka foramina are patent (<26 weeks), and, hence, there is apparently no communication whatsoever between the ventricular system and the subarachnoid spaces, there is no ventriculomegaly (Paladini et al. 2012).
3. *Association with other genetic or developmental abnormalities*. In the fetus, the risk of association with severe genetic and phenotypic conditions is much higher than in the newborn or child. This is due to the fact that severely affected fetuses may die spontaneously in utero or, more often, undergo termination of pregnancy, at least in those countries in which this option is available by law.
4. *CNS imaging in the fetus*. The size of the fetal brain is such that imaging – no matter if

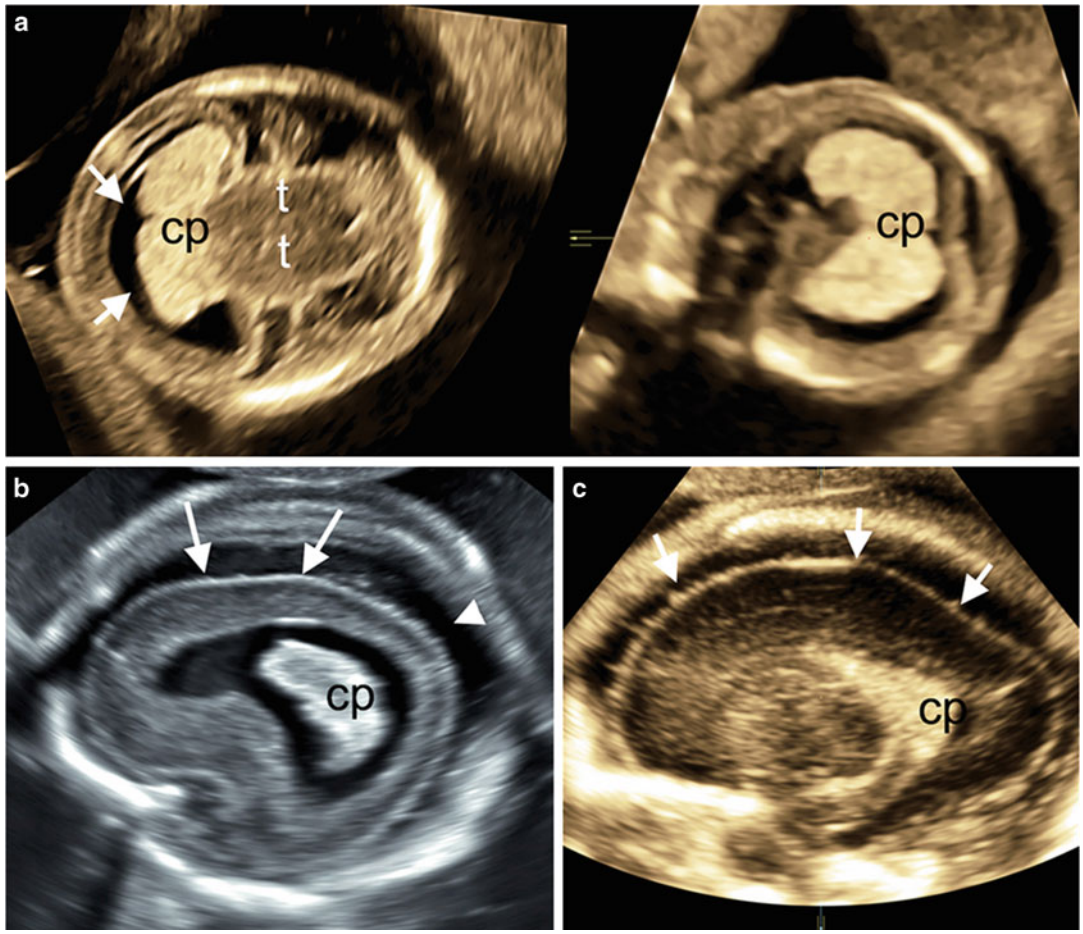

Fig. 1 The earliest time of recognition of a cerebral malformation depends on the timing of the cerebral development. (**a**) **Holoprosencephaly** diagnosed at 13 gestational weeks. On the left, the axial view shows fusion of the thalami (t) and absence of the falx with a single ventricle (arrows) and a single choroid plexus (cp): on the right, the coronal view of the same fetus confirms the absence of the falx with a single ventricle and a single choroid plexus (cp). (**b**) **Lissencephaly** can only be detected in the 2nd part of gestation, when migration should occur. In this case, the parasagittal view shows the abnormally smooth convexity cortex of one hemisphere (arrows) (cp: choroid plexus). Note also the slightly increased subdural spaces (arrowhead). (**c**) Another case of lissencephaly at 26 gestational weeks. Parasagittal view showing also in this case an abnormally smooth convexity cortex (cp: choroid plexus)

ultrasound or MR – cannot provide the extent of information that postnatal MRI can. However, detailed ultrasound imaging can be carried out from the earliest weeks of pregnancy, allowing to visualize the various steps of the CNS development almost from the beginning. It should be considered here that the small size of the fetal brain and the occurrence of fetal movements represent a major drawback limiting the accuracy of MRI evaluation before 24–25 weeks of pregnancy. Hence, before that period ultrasound information are often much more reliable that MRI ones, whereas in the 3rd trimester the two techniques – ultrasound and MRI – become complementary, evenly contributing to a thorough evaluation of fetal CNS anatomy (Paladini et al. 2014).

To provide an idea of the dramatic changes in the appearance of the brain during prenatal life,

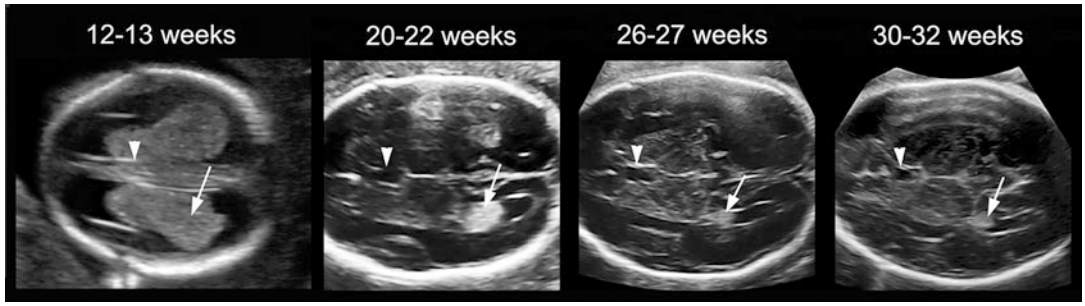

Fig. 2 Axial views of the fetal brain at 12–13, 20–22, 26–27, and 30–32 gestational weeks. Note the progressive apparent reduction in the dimensions of the choroid plexus (arrow) in relation to the width of the atrium. Also, note how the cavum septi pellucidi (arrowhead) is absent at 12–13 weeks, appearing around 17 weeks; it then begins to shrink at 30–32 weeks to disappear by 35 weeks leaving the septum pellucidum, with the two leaflets juxtaposed

it suffices to follow the development of the choroid plexuses (CPs) from the late embryonic stage, at 9–10 weeks onward, assisting at their progressive reduction in comparison with the growing fetal brain (Fig. 2). The ventricular system is obviously deeply involved in these changes.

5. *Epidemiology of CNS abnormalities in the fetus*. For any expert dealing with the differential diagnosis of congenital anomalies, one of the first steps is to consider the prevalence of the various conditions in prenatal life. Professionals dealing with the postnatal patient, widely defined, from neonate to pediatric age, deal with a completely different epidemiological scenario, due to the abovementioned high termination and mortality rates of affected fetuses.

The Developing Human Brain: From Embryology to Sonoembryology

In this first part of the chapter, we summarize the current knowledge on the development of the human brain adding a sonoembryologic anatomic correlation part from when high-frequency ultrasound may effectively show the developing brain structure.

Introduction

The *embryonic* period, defined as the first 8 weeks following fertilization, is characterized by a continuum of morphological changes of both the external and internal anatomical features, whereas the *fetal* period is characterized by elaboration of existing structures (O'Rahilly and Muller 2005). Conveniently, in obstetric practice, pregnancy dating begins on the first day of the last menstrual period (LMP) and counted in gestational (menstrual) weeks (GW). Since ovulation and fertilization are commonly considered close events, and menses commence presumably 14 days prior to ovulation, in the first fortnight of gestation (the 2 weeks prior to the embryonic period), the embryo has not yet formed. Hence, the embryological term "8 weeks' embryo" is commonly referred to by the obstetrician as "10 gestational weeks."

One of the most commonly used staging system of the developing human brain, called the "Carnegie stages," was first introduced by Streeter in the 1940s and later modified by O'Rahilly and Muller in 1987 (1987). According to the Carnegie system, embryonal brain development is subdivided into 23 morphologically distinct stages of both the internal and external characteristic. For each stage, an approximate embryonic length and postfertilization age are described and should solely be used as guidelines, since variability exists between the morphological stage and the mere length or age of the embryo (O'Rahilly and Muller 2010). Key features of the developing human brain based on both the Carnegie staging system and the work published by Bayer and Altman (2008) in their comprehensive atlas on

human central nervous system development represent the bases for the following text. The objective of this text is to provide an overview of the human brain development, from the fetal medicine specialist's point of view, highlighting the developmental dynamics of brain structures commonly imaged on neurosonography throughout pregnancy, in both normally and abnormally developed brain, with a specific insight into fetal ventriculomegaly and hydrocephalus.

Early Organization

Nervous system development is termed neurulation. The first morphologic sign of the primary neurulation appears in stage 8 of the Carnegie system (approximately 23 days postfertilization, 5 GW) when the epiblast layer is being transformed, as a result of inductive influence, into a thickened neuroectoderm, giving rise to the neural plate. In the following stages, the edges of the plate create two parallel longitudinal neural folds, bending medially over the developing neural groove. At stage 9 (approximately 26 days postfertilization, 5.5 GW), despite the fact that the neural tube has not yet closed, the three primary divisions of the future brain are distinguishable: prosencephalon (forebrain), mesencephalon (midbrain), and rhombencephalon (hindbrain), cranial to caudal, respectively. Also, at this stage, the first flexure of the neural tube appears at the level of the mesencephalon. It has been suggested that both longitudinal and transverse patterns of gene expression contribute to the formation of a grid-like array of cells' primordia in a process termed regionalization (Rubenstein et al. 1998). At this stage, the rhombencephalon is subdivided into four rhombomeres (i.e., transverse subdivisions of the neural folds and groove at the level of the rhombencephalon) termed A–D, cranial to caudal, respectively. Rhombomere D represents the level where the first somite pair appears in the mesoderm (Müller and O'Rahilly 2003), indicating the future cerebrospinal junction (Fig. 3). The two neural folds begin to fuse at the level of the rhombencephalon when five somitic pairs are present (stage 10, approximately

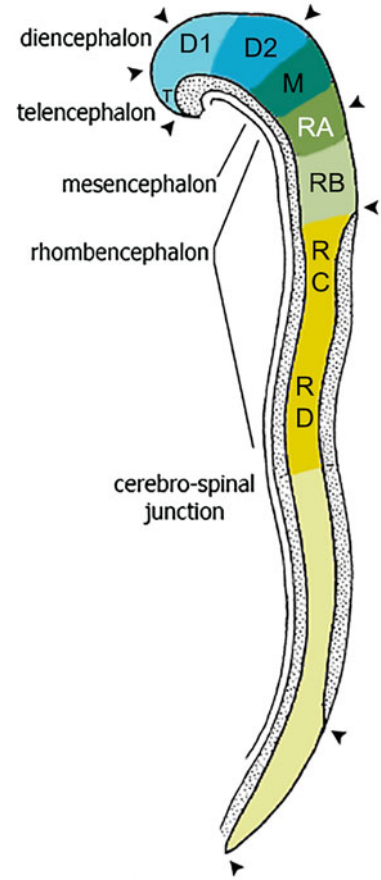

Fig. 3 Embryonal brain development. Approximately 5.5 gestational weeks. The two neuropores are open (arrowheads); the primary subdivisions of the brain are distinguished by different colors. Letters identify the different brain subdivisions (T, telencephalon, D1 and D2, diencephalon, M, mesencephalon, RA-D, rhombomeres A to D). Note rhombomere D at the cerebrospinal junction. (Modified from O'Rahilly and Müller 1987)

29 postfertilizational days, 6 GW). From this point, fusion will continue in a bidirectional pattern, both caudally and cranially. This is followed by the appearance of a second fusion point at the cranial most end of the neural plate, at the level of the prosencephalon, called the "terminal lip," by means of a unidirectional fusion. The gradually closing gap between the two unfused folds is termed the anterior neuropore, whereas the open region between the two neural folds at the caudal end is termed the posterior neuropore. Closure of the terminal lip of the anterior neuropore gives rise to the floor of the telencephalon, representing the

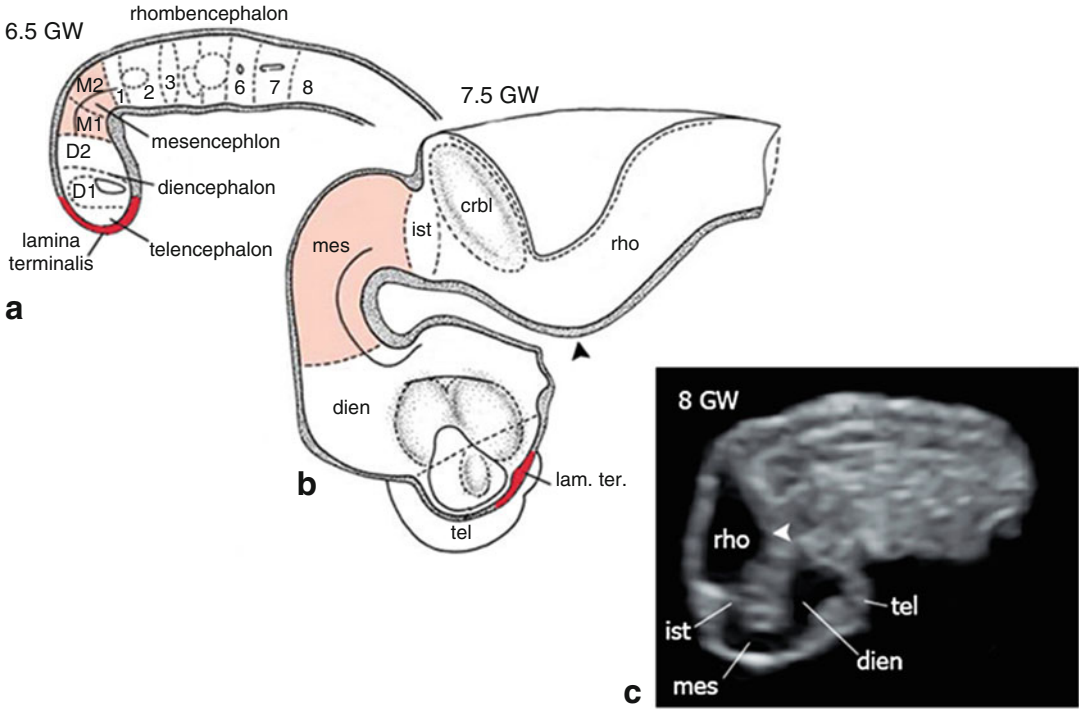

Fig. 4 Different stages in embryonic brain development. (**a**) Approximately 6.5 gestational weeks, following the closure of the anterior neuropore. The brain subdivisions are shown. Note the lamina terminalis (in red) at the rostral end of the telencephalon, representing the site of neuropore closure. (**b**) Approximately 7.5 gestational weeks. The pontine flexure is more pronounced (arrowhead); the isthmus rhombencephali is evident rostral to the future cerebellum. Budding of the right telencephalic vesicle is visible. (**c**) Ultrasound image of 8 gestational weeks' embryo. Midsagittal view. The subdivisions of the brain are shown (rho, rhombencephalon; crbl, cerebellum; ist, isthmus rhombencephali; mes, mesencephalon; dien, diencephalon; tel., telencephalon; lam. Ter, lamina terminalis). (Modified from O'Rahilly and Müller 1999)

area of the future *lamina terminalis* and its commissural plate. As fusion progresses, a farther neuromeric subdivision of the brain is distinguished: the prosencephalon gives rise to the telencephalon and the diencephalon (rostral to caudal, respectively); the mesencephalon enlarges, becomes a more tubular structure, and further subdivides into mesencephalic neuromas (M1, M2); the rhombencephalon will further subdivide into eight different rhombomeres (Fig. 4a).

During 6–7 GW, the neuropores close, beginning with the cranial neuropore at stage 11, followed by the caudal neuropore at stage 12 (approximately 6.5 GW). This represents the end of the primary neurulation and the beginning of the secondary. Also during this period, the pontine flexure appears as a bulge in the ventral surface of the rhombencephalon (Fig. 4b). From this point onward, ultrasound may document the further steps of the secondary neurulation (Fig. 4c). Once the neural tube closure completes, its lumen disconnects from the amniotic cavity, giving rise to the future ventricular system of the brain. By stage 15 of development (7 GW), the five precursors of the brain and spinal cord can be distinguished (commonly termed the *brain vesicles*): telencephalon (future hemispheres and part of basal nuclei), diencephalon (future thalamus and its subdivisions and part of the basal nuclei), mesencephalon (future midbrain), metencephalon (future cerebellum and pons), and myelencephalon (future medulla oblongata). It should be noted that, bridging between the mesencephalon and the rostral part of the metencephalon (i.e.,

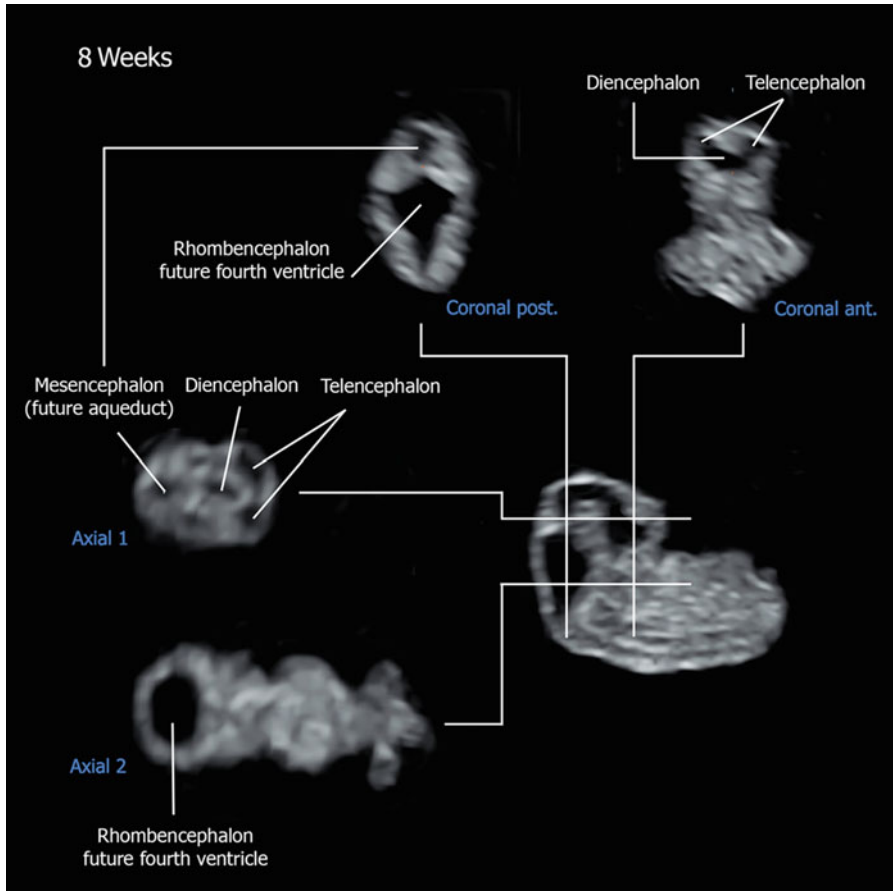

Fig. 5 Three-dimensional multiplanar sonographic imaging (coronal and axial planes) of the main brain subdivisions in an 8 GW embryo. The hypoechoic (darker) areas are fluid-filled cavities representing different luminal segments of the future ventricular system; echogenic (brighter) areas represent the developing brain tissue (ant, anterior; post, posterior). Note how self-explanatory are the images (see text)

rhombomere 1), a new neuromere is distinguished at stage 13 (approximately 6.5 GW), termed the isthmus rhombencephali (Fig. 4b, c). The cerebellum, as discussed later, will evolve from both the isthmus and the rostral part of the metencephalon.

The use of three-dimensional multiplanar sonographic reconstruction imaging provides a reliable demonstration of the main brain subdivisions (Fig. 5). In this way, the embryonic brain development may be followed closely. Figure 6 shows a plane to plane correlation between an 8- and a 10-GW-old fetus. Note that by 10 GW (i.e., the end of embryonic period), both the brain's five subdivisions and the early ventricular system are clearly demonstrated.

Brain Hemispheres

The two brain hemispheres emerge bilaterally from the telencephalon, in an "outpouching" fashion, on both sides of the neural tube (beginning at stage 14, approximately 6.5 GW). As development proceeds, the two telencephalic vesicles begin to follow their *frontal* and *occipital* growth poles, and by stage 22 (approximately 9.5 GW), the *temporal* pole starts to develop, too. The growing hemispheres approach each other at the midline, dorsal to the roof of the diencephalon and mesencephalon, progressively enclosing deeper brain structures (Fig. 6). It is worth mentioning that by the end of the embryonic period (10 GW), the two hemispheres cover most of

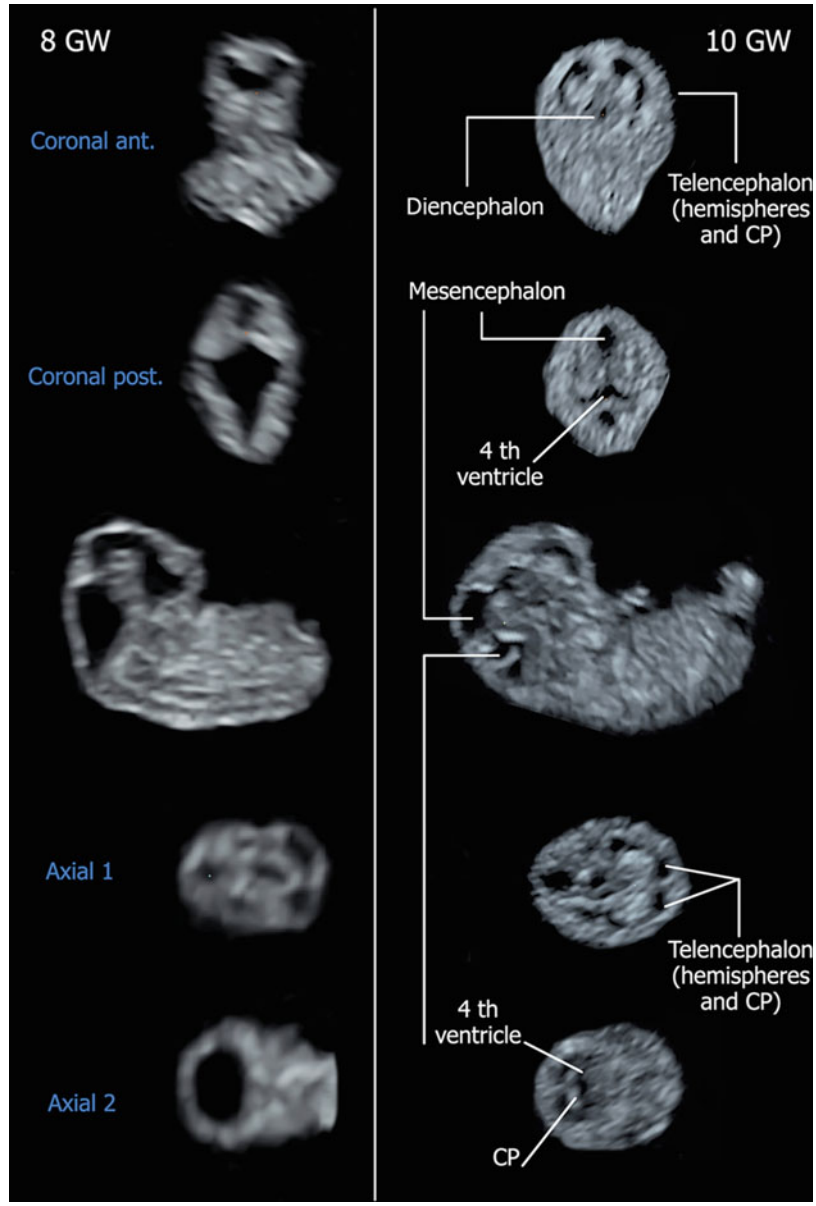

Fig. 6 Plane-to-plane correlation of the developing embryonic brain, 8 versus 10 gestational weeks. Note that by 10 GW, both the brain's five subdivisions and the early ventricular system are clearly visualized on ultrasound

the diencephalon, separated in the midline by the longitudinal fissure, which, at this stage, ends at the roof of the 3rd ventricle. Another important note is that at 10 GW the surface of the hemispheres is smooth with only the beginning of the insular indentation, bordered by the growing anterior and temporal growth poles. As development continues, this indentation will become the Sylvian fissure. At 12 GW, the brain hemispheres have gained their midline separation represented by the echogenic falx and their three growth poles giving the hemispheres their characteristic C shape configuration (Fig. 7). The insular cortex will get progressively buried under the folds of the developing surrounding cortex from frontal, temporal, and frontoparietal areas, in a process called operculization (see text and images below in section on "Cortical Development").

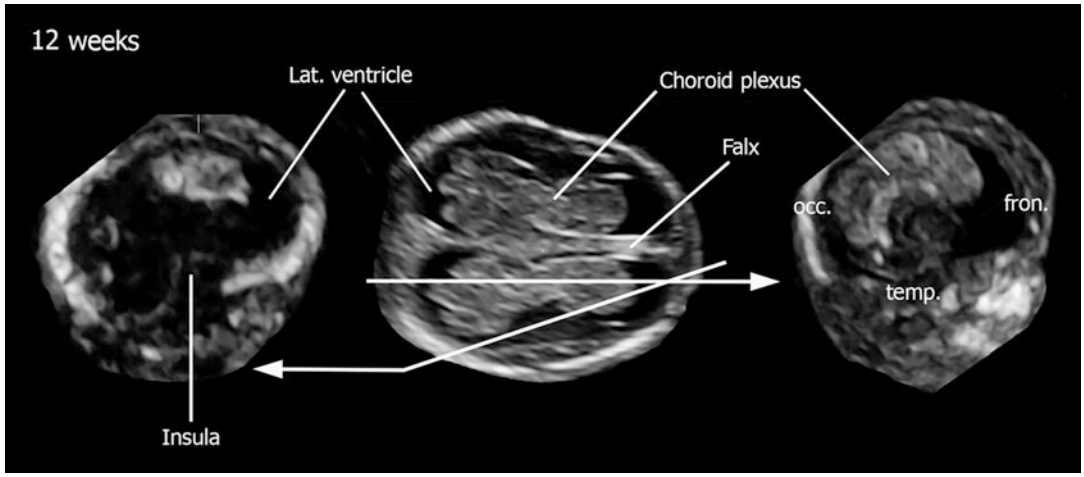

Fig. 7 Twelve gestational weeks' fetus. Three-dimensional multiplanar ultrasound imaging. The two lateral images show planes highlighted in the central image with the white lines. Middle image: axial view of the two brain hemispheres. Note the large choroid plexuses (echogenic "butterfly" structure) of the lateral ventricles and the thin hemispheric walls representing the early cortex. Right image: three growth poles and "C"-shaped choroid plexus of the lateral ventricle. Left image: cut through the developing insular cortex and the Sylvian indentation (front, frontal; occ, occipital; temp, temporal)

The Ventricular System and Choroid Plexus

As mentioned in the previous section, the ventricular system first appears when the neural tube closes and its lumen disconnects from the amniotic cavity. At this point, the fluid trapped within this cavity is an "embryological CSF" derived from the lining neuroepithelium, until the later appearance of the choroid plexuses. It has been suggested that this early CSF has a major role in early brain growth and morphogenesis (Gato and Desmond 2009). As development continues, the ventricular system will fold and shape, guided by the development of the surrounding brain structures, while maintaining its luminal continuity. During early stages of development, including the beginning of the fetal period, the walls of the growing hemispheres, designated to become the future neocortex, are relatively thin, and as a result, the lumen of the ventricular system is prominent, most notably in the lateral ventricles. The different segments of the developing ventricular system are termed according to their anatomic relations with the surrounding structure; the lateral ventricles of the telencephalic vesicles are connected to the 3rd ventricle of the diencephalon and telencephalon medium (the midline segment of the telencephalon) through the interventricular foramina of Monro. The lumen of the mesencephalon, i.e., the future aqueduct of Sylvius, together with the lumen of the isthmus rhombencephali, termed the isthmal canal, tunnels between the 3rd and the 4th ventricle of the rhombencephalon. The progressive development of the ventricular system can be seen in Figs. 8 and 9.

The ventricular lumen continues from the 4th ventricle to the central canal of the spinal cord, and the CSF circulates out from the ventricular system into the subarachnoid space, from where it is eventually absorbed back into the venous system of the brain. It has been suggested that the middle (Magendie) and the two lateral (Luschka) foramina, located in the roof and lateral recesses of the 4th ventricle, develop at approximately 8 and 26 GW, respectively (Brocklehurst 1969). However, a final confirmation on the timing of opening of the foramina is still lacking (for further discussion see section on "Rhombencephalon"). As for all the other brain structures, the ventricular system changes dramatically during gestation. These changes are illustrated in the

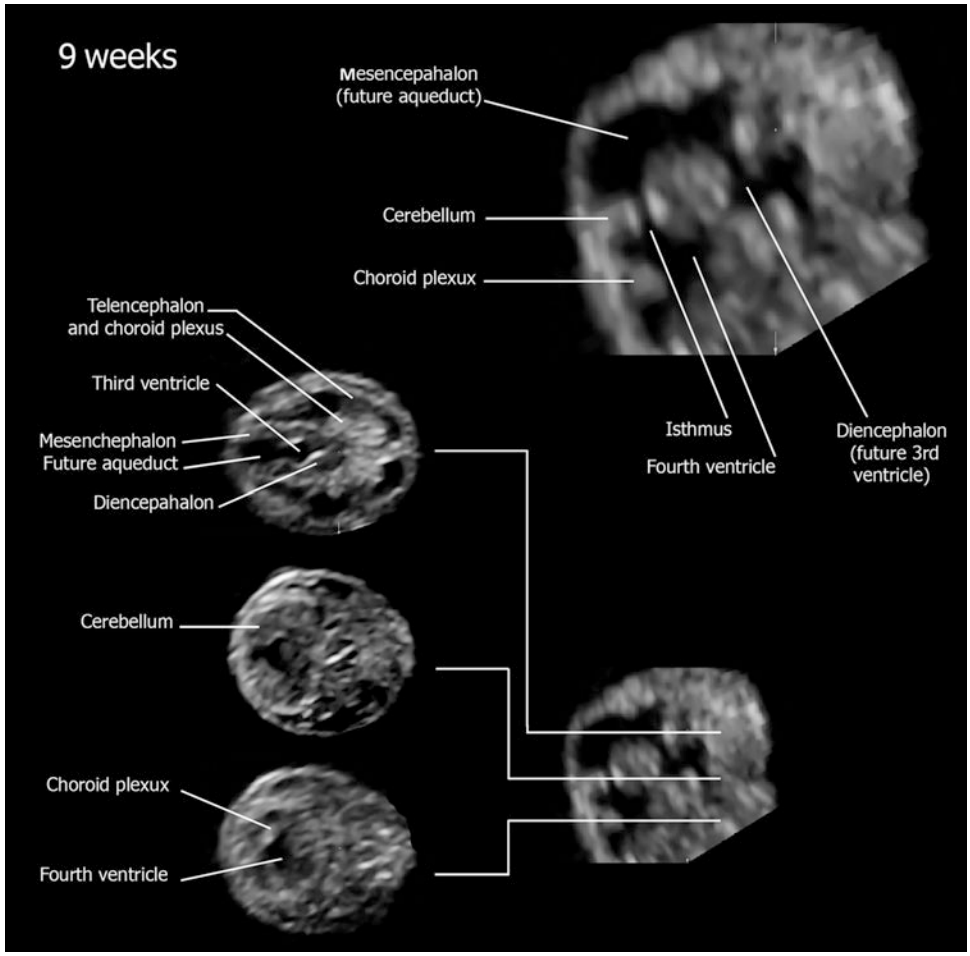

Fig. 8 Early ventricular system in a 9-gestational-week-old fetus. Right upper image: midsagittal view. Lower images: sequential axial views of the brain. Note that by this stage, both the 3rd ventricle and the future aqueduct are quite wide in contrast to their slit-like configuration in a more advanced gestational age

next section on *sonographic anatomy of the ventricular system and choroid plexus*.

The choroid plexus (CP) consists of an outer epithelial layer, derived from the neuroepithelium, which surrounds a core of capillaries and connective tissue derived from mesenchymal cells commonly referred as the *tela choroidea*. The CP creates a papillary structure, invaginating the ventricular lumen, functioning as an interface between the blood and the cerebrospinal fluid (CSF) secreted by its cells. The first to appear is the CP located in the roof of the 4th ventricle at stage 19 (approximately 44 postfertilizational days, 8 GW). It is followed by the formation of the CP of the lateral ventricles that becomes continuous with the CP located at the roof of the 3rd ventricle by passing through the IVF, 1 and 2 weeks later, respectively. Between 9 and 17 GW, the CP is considerably large with respect to the ventricle, whereas after that period it progressively regresses, so that beyond 29 GW the CP is fairly small compared with the ventricular lumen (Fig. 2) (Lun et al. 2015; Mortazavi et al. 2014; Strazielle and Ghersi-Egea 2000). On ultrasound, the CPs appear as hyperechoic structures inside the anechoic ventricles. At 9 GW the CPs

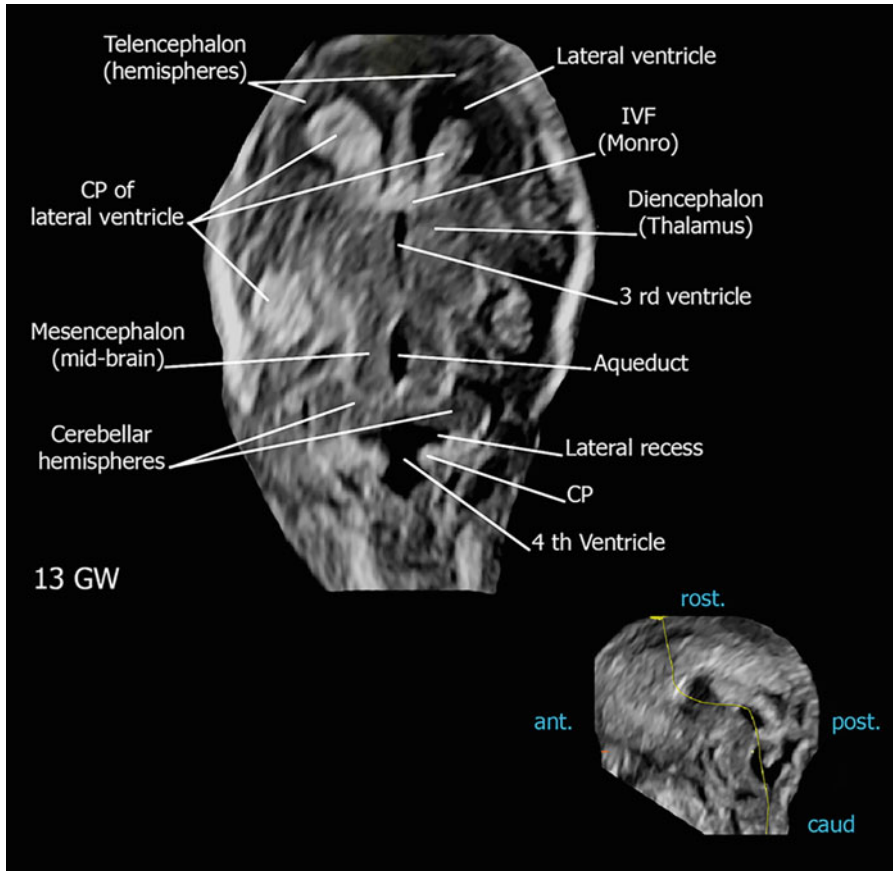

Fig. 9 The ventricular system and neighboring structures in a 13-gestational-week-old fetus. Three-dimensional ultrasound image reconstruction. The upper image shows the whole ventricular system and corresponds to the curvilinear cut shown in the right bottom image. Note the prominent aqueduct and the rhomboid-shaped 4th ventricle (ant, anterior; caud, caudal; CP, choroid plexus; IVF, interventricular foramen; post, posterior; rost, rostral)

are well visualized both in the fourth and lateral ventricles (Figs. 8 and 10).

Cortical Development

The neocortex develops from the dorsolateral walls of the telencephalic vesicles. The earliest sign of cortex formation is the emergence of the cortical plate (CoP), the layer where the first wave of postmitotic neurons migrated to and accumulates in. The CoP first appears at the most lateral part of the rostral telencephalon at approximately *9 GW* (50 postfertilizational days), and in about 1 week it spreads throughout the hemispheres, moving in a rostro-lateral to dorso-caudal direction. The initiation of migration and the appearance of the cortical plate establish a new, transient laminar configuration to the cerebral wall. The following zones are distinguished, inner-to-outer (ventricle to subarachnoid space): ventricular zone, subventricular zone, intermediate zone (IZ), subplate (SP), CoP, and marginal zone (MZ). The IZ is a heterogeneous zone, containing both radially and tangentially migrating neurons and neural axons, and it contains neither precursors nor post-migratory cells. The white matter of the brain evolves within, and eventually replaces, this layer (Bystron et al. 2008). The SP contains heterogeneous cellularity associated with an

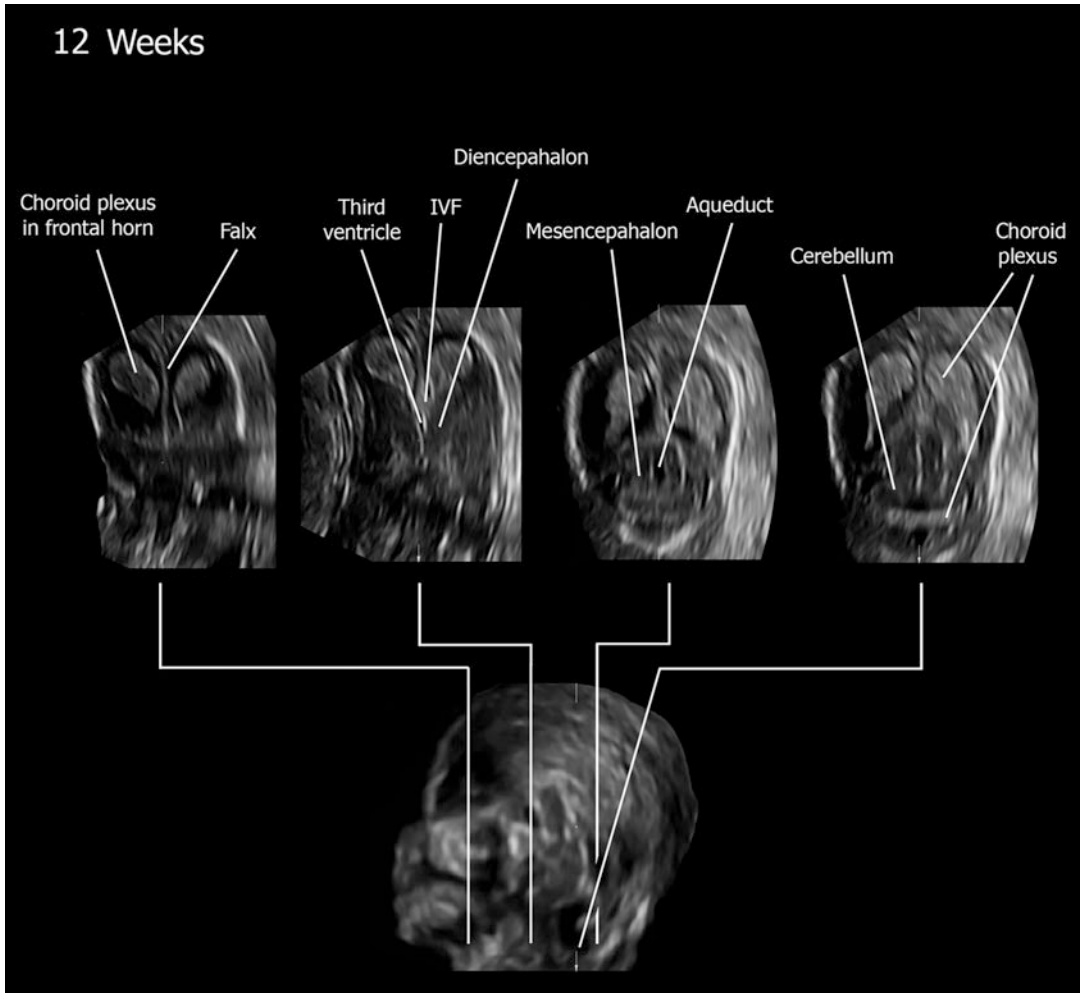

Fig. 10 Twelve-gestational-week-old fetus. Three-dimensional multiplanar image reconstruction showing sequential coronal planes of the fetal brain. Note the bright choroid plexuses in the lateral ventricles as well as in the 4th ventricle (IVF, interventricular foramen)

abundant hydrophilic extracellular matrix that reaches its maximus thickness by 26–27 GW and gradually regresses thereafter (Pugash et al. 2012). The MZ, the future layer 1 of the six-layered cortex, contains cells that have mostly migrated tangentially and involve in the arrest of migration of radially migrating neurons (Rakic and Zecevic 2003).

Neuronal migratory activity peaks between *12* and *20 GW* and is completed gradually through the 3rd trimester of pregnancy. During this period of peak migratory activity, the cortical plate thickens and expands radially, maintaining a smooth surface until approximately mid-gestation. The progressive accumulation of new neurons in the cortical plate sets the ground for the final process in cortical maturation, establishment of cortical connections between various brain regions, commonly termed neuronal differentiation and connectivity formation. It is through this period, beginning after 22 GW and culminating in the 3rd trimester, that the brain's surface area increases considerably, as reflected by the sequential formation of sulci and gyri, and the progressive appearance of the characteristic six-layered cortex, while neuronal migration

gradually subsides. The sonographic description of this gradual process is presented in the section below on *Cortical development – normal gyration and sulcation*.

Rhombencephalon

As mentioned previously, the cerebellum develops from the isthmus rhombencephali and the metencephalon. At stage 18 (approximately 44 postfertilizational days), the primordium of the cerebellar hemispheres (the flocculus) can be distinguished as two bilateral swellings at the level of the metencephalon, protruding both internally (i.e., facing the lumen) and externally. The dorsal surface of the rhombencephalon, caudal to the level of the developing cerebellum, i.e., the roof of the 4th ventricle, is formed by a thin layer called the medullary velum. The transition point between the thin "roof" and the developing "wall" of the rhombencephalon is termed the rhombic lip, an area that will markedly contribute to the formation of the cerebellar hemispheres. As the pontine flexure deepens (stage 21, approximately 9 GW), the two developing cerebellar hemispheres grow laterally, creating the two lateral recesses of the 4th ventricle, which give the rhombencephalon its diamond-shaped appearance on the dorsal view. At this stage, the hemispheres are connected in the midline only by the rostral part of the medullary velum. This section of the medullary velum is commonly termed the anterior membranous area (AMA). Bordering between the anterior and the more caudal, posterior membranous area (PMA) of the medullary velum is a transverse invaginating fold, called the *plica choroidea*, arching over the 4th ventricle (perpendicular to the long axis of the neural tube) indicating the budding site of the future choroid plexus of the 4th ventricle (Fig. 11). The fusion of the two cerebellar hemispheres begins with the fusion of the two floccular regions, at the midline nodule, forming the flocculonodular lobe, i.e., the archicerebellum (distinguished at the end of embryonic period, approximately 10 GW). From the end of the embryonic period, the growth of the cerebellar hemispheres will lead to their fusion, initiating the vermian formation from the anterior membranous area. This will lead to the eversion of the evolving cerebellar hemispheres on top of the floccule, and to lengthening of the vermis in a caudal direction, over the nodule, replacing the anterior membranous area (Fig. 12). As evident in Fig. 13, the two cerebellar hemispheres are still not fully fused, and the vermis is yet barely evident. The progressive growth caudal of the cerebellar vermis and its relationships with the other structures of the posterior fossa from 12 to 30 GW are shown in Fig. 12.

As briefly mentioned earlier, the midline foramen of Magendie is thought to develop at approximately 8 GW (Brocklehurst 1969). It has been suggested by Blake (1900) and later supported by Wilson (1937) that the formation of the Magendie begins as a temporary dorsal outpouching of the PMA into the developing cisterna magna, which since this description has been named *Blake's pouch*. At around 10 weeks, it is believed that this digit-like evagination eventually opens, connecting the 4th ventricle to the subarachnoid space. The appearance of the lateral foramina of Luschka seems to take place later in pregnancy, according to some authors at about 26 GW (Brocklehurst 1969).

Corpus Callosum and Cavum Septi Pellucidi

As mentioned earlier, closure of the anterior neuropore of the neural tube gives rise to the embryonic *lamina terminalis*, the rostro-medial part of the telencephalon. Within the lamina terminalis, the commissural plate (ComP) seems to provide the infrastructure for the commissures of the brain. The largest commissure of the brain, the *corpus callosum (CC)* is composed of axons destined to connect corresponding cortical areas of the two cerebral hemispheres. The CC develops bidirectionally from a budding area representing the anterior part of the body, both posteriorly giving rise to the body and splenium and anteriorly giving rise to the genu and eventually the rostrum (Kier and Truwit 1996). By 12 GW the first fibers of the CC can be

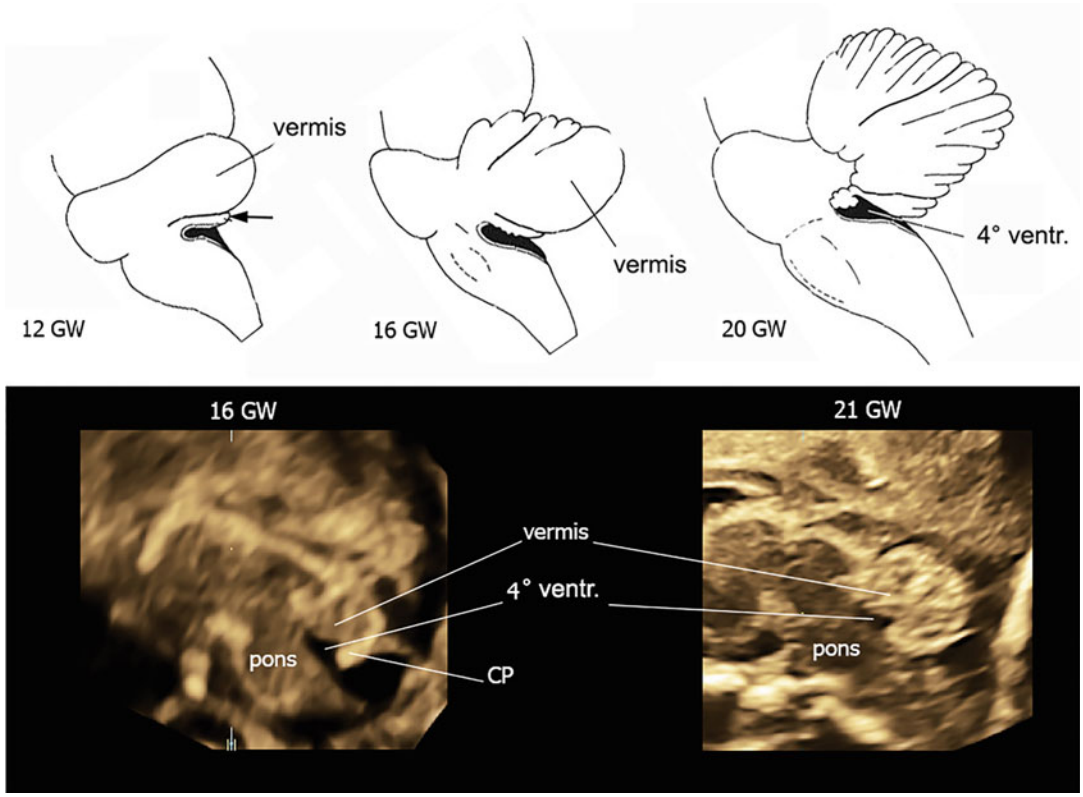

Fig. 11 Development of the rhombencephalon. Upper row illustrates the developmental changes at 12, 16, and 20 gestational weeks, shown from a lateral view. Note the cerebellar vermis enclosing over the flocculonodular lobe (arrow) and the 4th ventricle. As the cerebellum develops, fissures and folia start to appear. Lower row shows ultrasound images of the corresponding gestational weeks on the midsagittal view. The 4th ventricle is shown, in close relationship with the fastigium (CP, choroid plexus). (Modified from Streeter 1911)

recognized in pathological specimens. At about 15 GW, the anterior most part of the body is developed, roofing over the anterior section of the 3rd ventricle. From this gestational age, the corpus callosum will grow rapidly so that by midpregnancy its complete structure is visible on the midsagittal view of the fetal brain (Fig. 14). The development of the *cavum septi pellucidi* (CSP), assumed to develop by necrosis within the commissural plate, takes place at the same time as that of the corpus callosum. The CSP begins to develop at approximately 15 GW, and its caudal continuation, the *cavum vergae*, is visualized on the sagittal and coronal vies of the brain (Fig. 14).

Normal Two- and Three-Dimensional Ultrasound Anatomy of the Brain and the Ventricular System in the Fetus

1. *Ultrasound equipment, techniques, and scanning approach*. There are two different levels of approach to the sonographic examination of the fetal brain: screening and diagnosis. The former is meant to be carried out in low-risk pregnant women and relies on the visualization of two basic sonographic axial planes – transventricular and trans-cerebellar (ISUOG 2007) (Fig. 15) – which will be illustrated in the

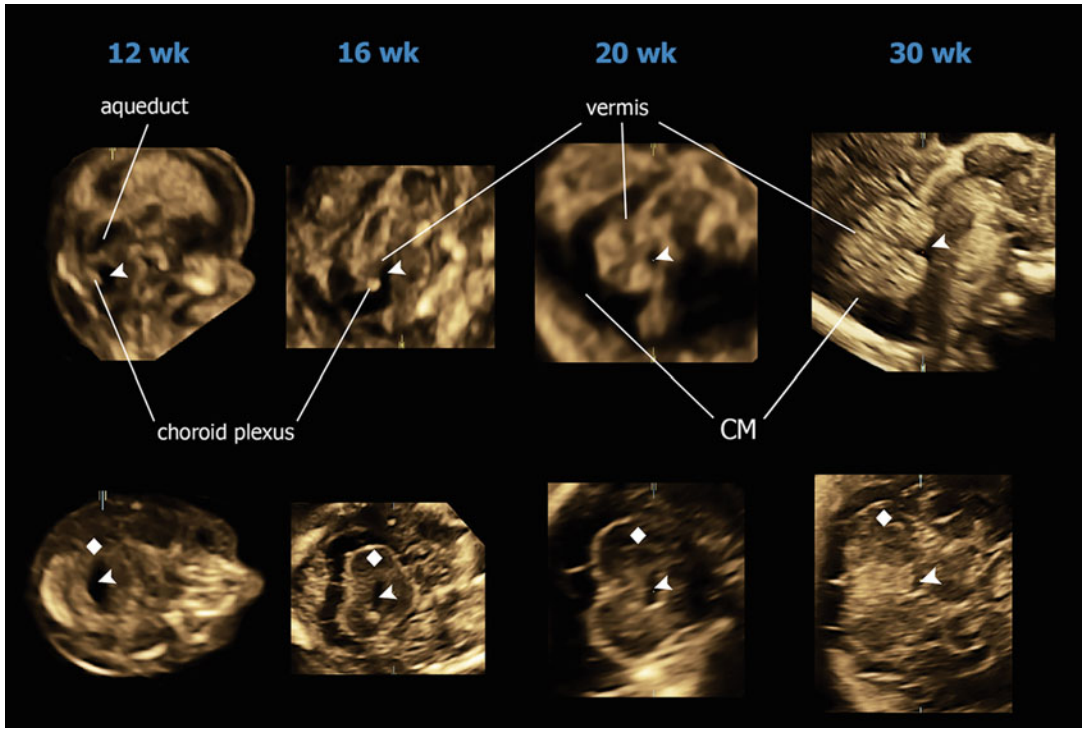

Fig. 12 Development of the 4th ventricle. The 4th ventricle (arrowhead) is visible from the early fetal period (12 weeks) until late in pregnancy. Its normal development is shown in this image on midsagittal views (upper row) and axial ones (lower row). On axial views, the cerebellum is identified with a white mark

dedicated section below. The latter approach – the diagnostic one – is required when a suspicion of CNS anomaly is raised at screening ultrasound and the patient is then referred for expert sonography. In this case, the task of the fetal medicine expert is to carry out a thorough sonographic evaluation of the fetal brain, the so-called neurosonography (ISUOG 2007; Monteagudo and Timor-Tritsch 2009; Timor-Tritsch and Monteagudo 1996). The different objectives of the two types of examinations dictate the scanning approach – transabdominal for screening and transvaginal for detailed neurosonography – unless a breech position of the fetus makes the transvaginal approach not feasible. For the readership not used to fetal ultrasound, it should be noted that transabdominal approach relies on the employment of lower emission frequency transducers which, in turn, increase the depth of insonation at the expense of the resolution. On the contrary, if the fetus is in vertex presentation, using transvaginal transducers warrants much higher resolution and, doing so, allows also subtle abnormal findings (e.g., subependymal heterotopias) to be detected. Another important concept regards the employment of three-dimensional ultrasound. These techniques allow not only to store whole volume dataset of fetal brains for future reassessment but enhance, at the same time, the accuracy of the evaluation, due to the possibility of multiplanar image correlation. Finally, color Doppler, or preferably, the more sensitive and less angle-dependent power Doppler, is used for detailed assessment of the fetal brain circulation, both in 2D and in 3D.

2. *The scanning windows and the scanning concept*. One of the challenges we encounter in exploring the fetal brain with ultrasound is

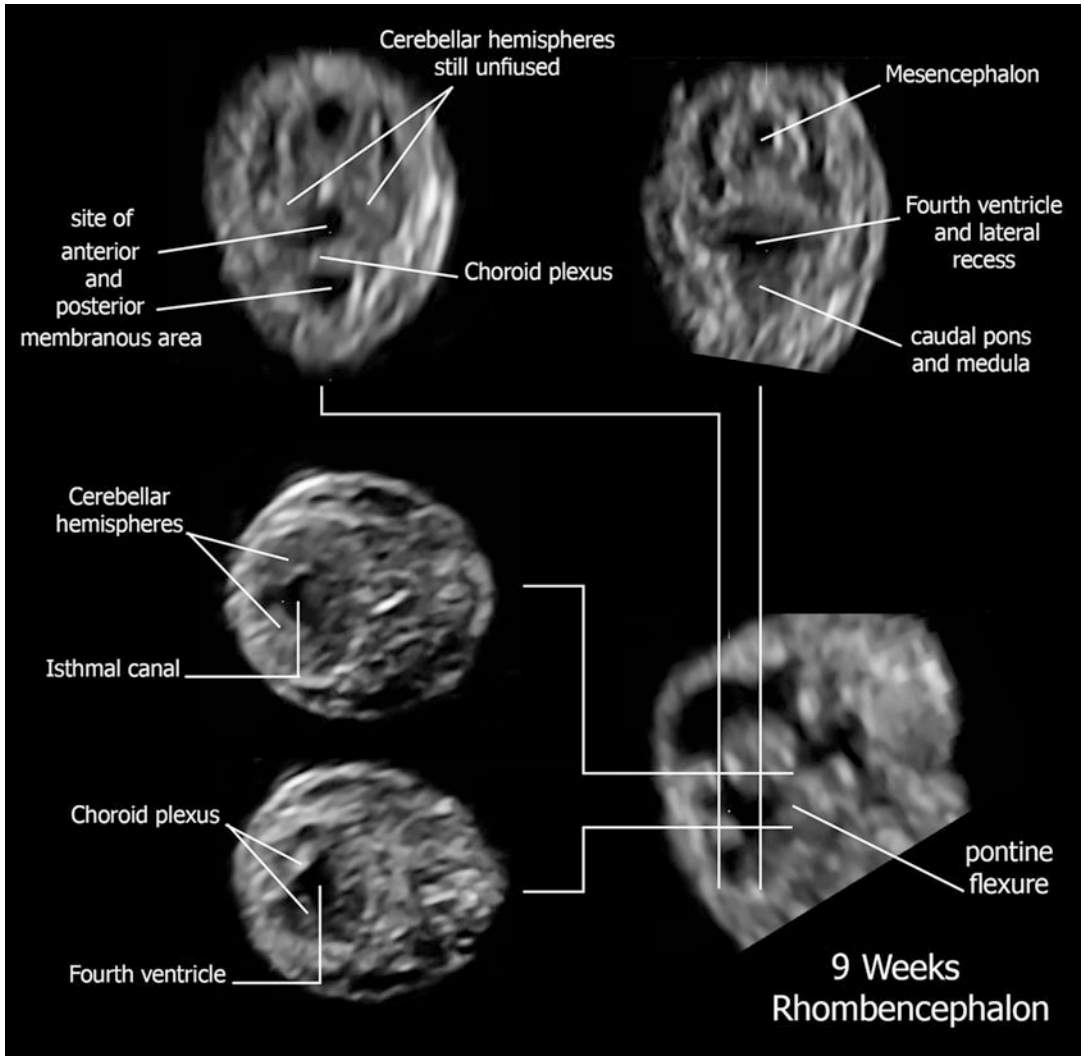

Fig. 13 Development of the rhombencephalon. Cross-sectional ultrasound imaging of the rhombencephalon in a 9-gestational-week-old fetus

represented by the calvarial bones, the mineralization of which hampers ultrasound waves' penetration. This is why we are bound to use the fontanelles and the still unsealed cranial sutures as ports of access to explore the fetal brain with ultrasound. In particular, the anterior and posterior fontanelles and the coronal suture are used in transvaginal ultrasound, whereas the coronal, mastoid, and parieto-occipital areas are employed in transabdominal ultrasound (Fig. 16). Considering what has been expressed above, especially about the restrictions imposed by the calvarial ossification to ultrasound beam penetration, it becomes clear why with transabdominal ultrasound mainly axial views can be obtained, with limited exceptions. These are also simpler to obtain for screening purposes. On the other hand, transvaginal neurosonography uses the fontanelles to literally penetrate with the tip of

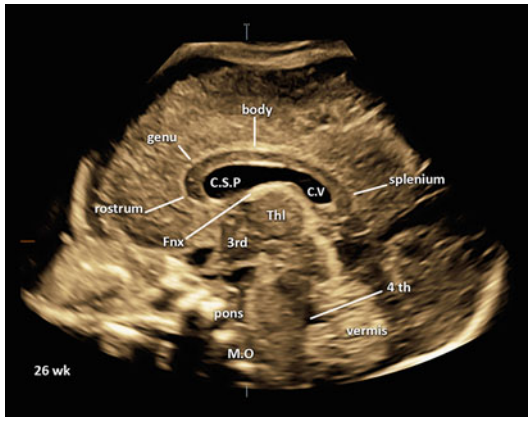

Fig. 14 Midsagittal view of the brain in 26-gestational-week-old fetus. The fully developed corpus callosum with its subsegments is labeled in this image. (3rd, third ventricle; 4th, fourth ventricle; CSP, cavum septi pellucidi; CV, cavum vergae; Fnx, fornix; MO, medulla oblongata; Thl, thalamus)

the transducer just beyond the bones allowing most of the brain to be seen. This approach leads to a series of images of the brain that can be oriented with a fanlike movement of the transducer on the coronal and the sagittal planes (Fig. 17).

3. *Normal anatomy*
   - *Key landmark appearance by gestational age*. In fetal CNS imaging, the operator should be aware of a series of developmental steps not to incur in basic diagnostic mistakes. As an example, the cavum septi pellucidi appears at about 15–16 gestational weeks to disappear after 34–35 weeks, becoming the septum pellucidum. Along the same lines, a developed cingulate gyrus cannot be visualized with ultrasound before 28 weeks of gestation.
   - *Twelve to 14 gestational weeks*:
     – Figure 18 shows a cross-sectional anatomy of a 12 GW brain on the axial plane view. The brain's subdivisions are distinguished, along with the following structures:
     – Butterfly-shape CPs of the lateral ventricles
     – Midline
     – Developing thalami (diencephalon) and midbrain (mesencephalon)
     – Aqueduct of Sylvius
     – Cerebellum
     – Fourth ventricle
   - *Nineteen to 22 gestational weeks*:
     – Figures 19 and 20 *show brain structures normally observed on the axial view at 20–22 GW. The main features include the following:*
     – Cerebral cortex visible
     – Cavum septi pellucidi and corpus callosum
     – Insula visible
     – Vermis and cerebellum visible with cisterna magna
     – Initial evidence of calcarine and parieto-occipital fissures
   - *Twenty-seven to 28 gestational weeks* (Figs. 21 and 22):
     – Operculization of insula
     – Deepening of calcarine and parieto-occipital fissures
     – Beginning of the cingulate gyrus
   - *>30 gestational weeks* (Figs. 21 and 22):
     – Cingulate gyrus evident
     – Convexity sulci visible
     – Further opercolization of insula
4. *Characterization of the ventricular system*

The appearance of the ventricular system in prenatal life is completely different from what is considered normalcy after birth. This is why there is a need to illustrate the differential features in detail.

Lateral ventricles. As a result of the progressive development of the anterior and temporal hemispheric poles, the corresponding anterior and temporal horns of the lateral ventricles evolve (Fig. 23). At approximately 11–12 GW, the posterior (occipital) horn begins to evaginate posteriorly. This gives rise to the following subdivisions of each lateral ventricle: the anterior horns, central part (body), and atrium, commonly termed the *trigone* (representing a triangular spatial junction between the anterior areas and the posterior and inferior, temporal horns). From the

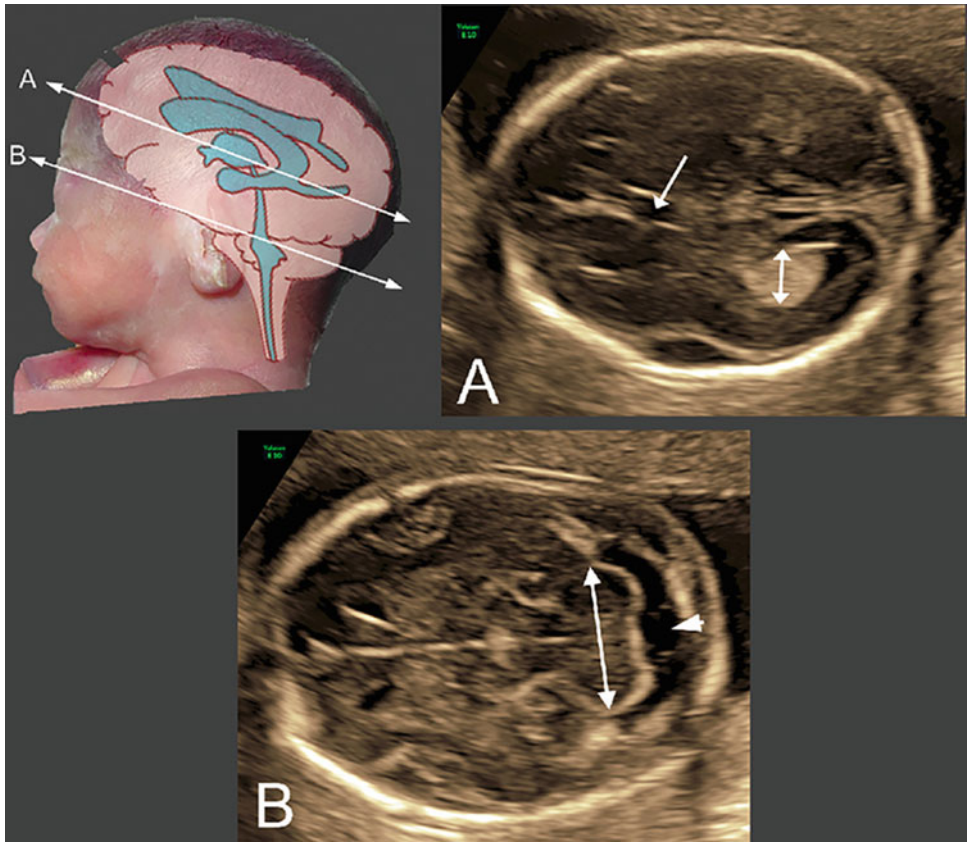

Fig. 15 Axial views of the fetal head routinely used for midtrimester ultrasound screening of central nervous system malformations in the fetus. The two planes pass through the lateral ventricle (**a**) and the cerebellum (**b**), as shown in the image on the left. The corresponding sonographic planes are illustrated in A and B, in a normal fetus at 21 weeks of gestation. (A) The axial transventricular plane, cutting through the lateral ventricles (double arrow), demonstrates absence of ventriculomegaly (atrial width less than 10 mm). On the same view, the presence of the cavum septi pellucidi (arrow) should be documented. If absent, it may be a sign of corpus callosum agenesis. (B) The axial trans-cerebellar view demonstrates a normal posterior fossa, with an unremarkable cerebellum (double arrow) and a normal amount of fluid in the cisterna magna (arrowhead). On this view, the trans-cerebellar diameter is measured

sonographic point of view, the ventricular system is best studied using the multiplanar approach, aimed at both measuring and examining the appearance of the entire ventricular lumen, its ependymal continuity, and the surrounding brain parenchyma. The CPs appear as echogenic structures located within the ventricular lumen. The part located at the atrium of the lateral ventricle is called the glomus of the CP, and from there it continues both anteriorly (toward the anterior horn and IVF) and inferiorly (toward the temporal horn), giving the CP its C-shape appearance (Fig. 24). As mentioned earlier, along development, the CPs become progressively small compared with the growing brain structures (Fig. 23). Under normal conditions, the CPs of the 3rd and 4th ventricles are not routinely visualized during the routine midpregnancy scan due to the small size of both the CP and the surrounding ventricular lumen.

By tilting the US transducer laterally, in a fanlike movement (Fig. 17), on a parasagittal plane, the entire lateral ventricle can be

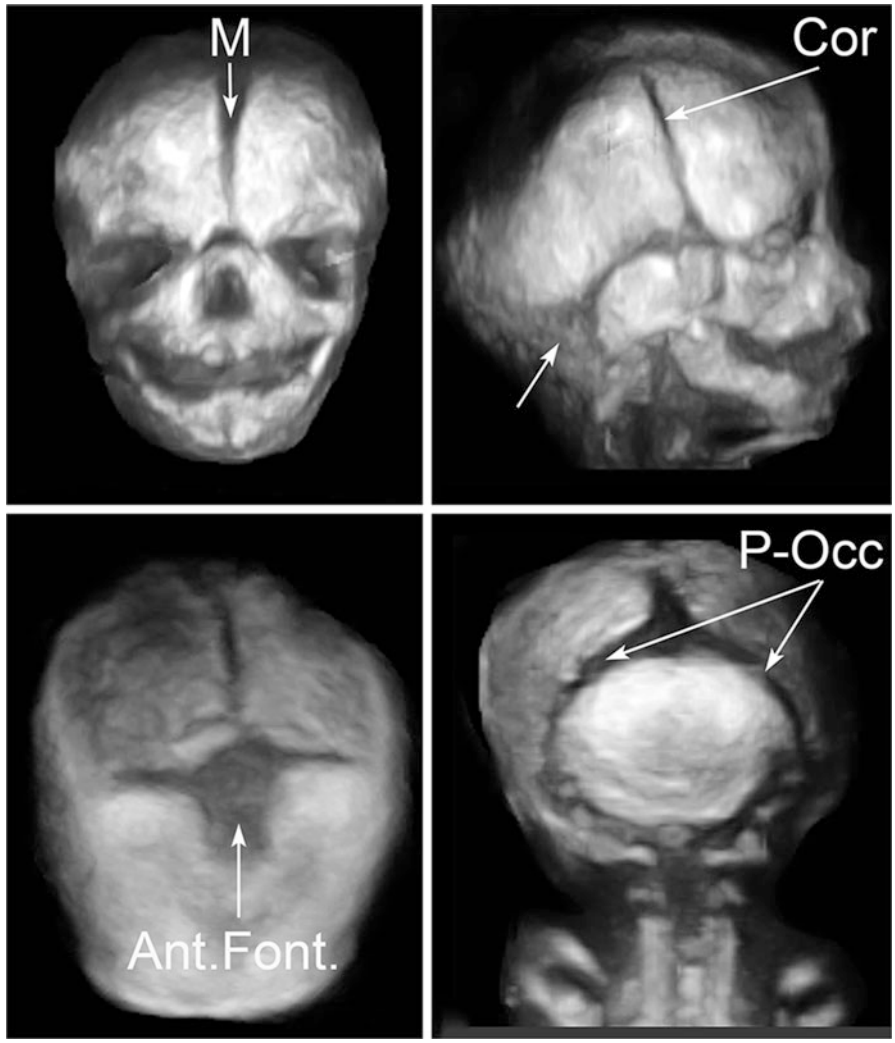

Fig. 16 Three-dimensional surface rendering of the fetal calvarium demonstrates the still unossified fontanelles and sutures that are used to insonate the fetal brain. The posterior fontanelle can be seen in the lower right image, between the parieto-occipital suture (P-Occ) and the sagittal one (Ant. font, anterior fontanelle; Cor, coronal suture; M, metopic suture)

examined (Fig. 24). Furthermore this plane allows the assessment of the temporal horns and their surrounding brain parenchyma. A coronal, posterior view of the occipital lobes allows to compare the size of the occipital horns of the ventricles (Fig. 25). The same plane can also be employed to assess the gyration process, evaluating the calcarine fissure.

The two anterior horns of the lateral ventricles are part of a more complex structure termed the *anterior complex,* observed in the frontal coronal plane. As demonstrated in Fig. 26, the anterior complex represents a unique configuration of integrated structures: the anterior horns laterally, the floor of which is formed by the head of the caudate nucleus bilaterally, and the medial walls by the septum pellucidum. Roofing over the cavum septi pellucidi (CSP) is a transverse section of the corpus callosum, and bordering ventrally are

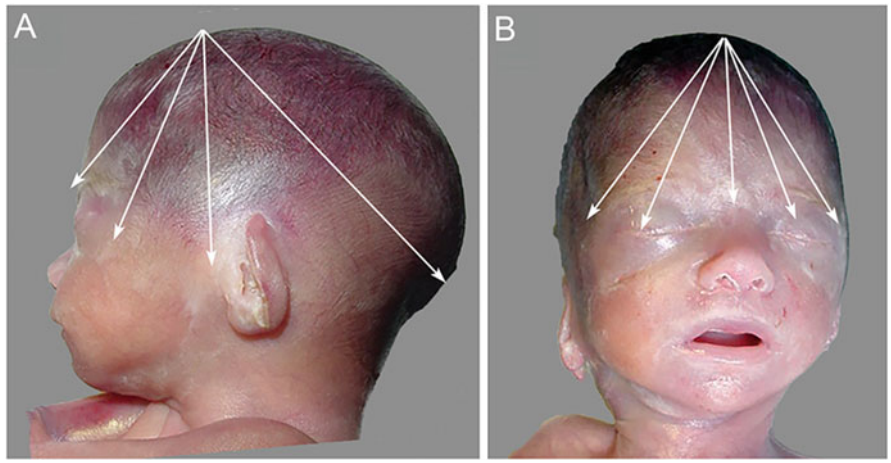

Fig. 17 The image shows the sonographic planes of the fetal brain that can be obtained with transvaginal ultrasound. Indenting the anterior fontanelle, four coronal and five sagittal/parasagittal planes can be displayed. (**a**) The four coronal planes correspond to a cut through the frontal lobes; the frontal horns of the ventricles and the cavum septi pellucidi; the basal ganglia; the posterior fossa with the occipital horns. (**b**) The five sagittal/parasagittal planes are the midsagittal; a slightly parasagittal plane on either side demonstrating the whole hemisphere and the lateral ventricle; a more lateral one on either side demonstrating the Sylvian fossa with the insula and the temporal horns

the two columns of the fornix, approaching each other at the midline, roofing over the area of the slit-like 3rd ventricle.

Third ventricle. A cross section of the 3rd ventricle can be seen on axial scans from the embryonic period, until the end of pregnancy (Hertzberg et al. 1997; Sari et al. 2005). On this plane, it appears as a small, round structure between the two thalami. A dated article describes the 3rd ventricle's width to be 1 mm wide in the second and 1.9 mm in the 3rd trimester (from 29 weeks onward), respectively (Hertzberg et al. 1997). Although additional ultrasound studies describing the aspect of the 3rd ventricle in the fetus have not been published, we believe that it can be visualized on the midsagittal view of the fetal brain, at least from the 2nd trimester onward. It shows the well-known triangular shape, with the apex reaching down to the hypothalamic area and the massa intermedia connecting the two thalami (Fig. 27).

The aqueduct of Sylvius. The Sylvian aqueduct is clearly visible during the embryonic and early fetal periods, until 12–13 weeks (Figs. 8 and 9). After this period, its lumen becomes virtual and can only be detected when partially obstructed or on MRI, when carried out in the second half of pregnancy. On rare occasions, the aqueduct can be seen on an axial plane passing through the midbrain, anterior to the tectum, and on the midsagittal view (Fig. 27).

Fourth ventricle. The 4th ventricle derives from the rhomboid-shaped lumen of the rhombencephalon. It is visible from the embryonic period until late in pregnancy (Figs. 6 and 9). Nevertheless, under normal conditions, as the brain develops beyond early fetal life, the sonographic appearance of the 4th ventricle is no longer rhomboid, and only the midline area, i.e., the *fastigium*, is visualized (Fig. 12).

5. *Cortical development – normal gyration and sulcation*

Using the three-dimensional multiplanar approach, normal cortical development with respect to the sequential appearance of fissures, sulci, and gyri can be assessed. At early stages, sulci appear as small "V"-shape indentations on the surface of the brain. As cortical development proceeds, the sulci become bright echogenic lines protruding internally from the

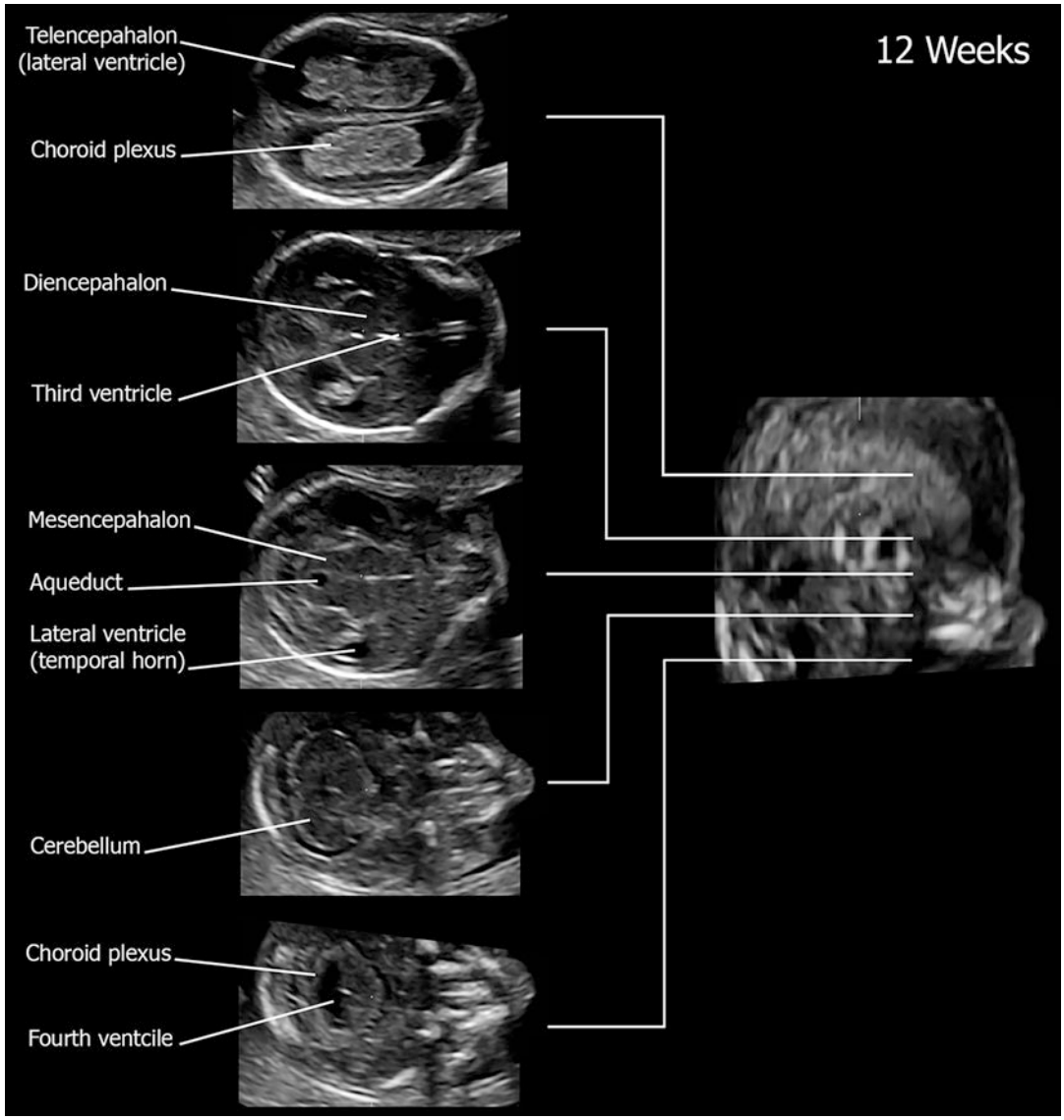

Fig. 18 Cross-sectional anatomy of a 12 gestational weeks' brain on the axial plane view. Note the thin 3rd ventricle and aqueduct passing through the developing brain structures

surface (representing two segments of cortex facing each other as the sulci get deeper). Figures 21, 22, and 28 show the sequential development of the cerebral cortex during gestation. As mentioned earlier in the embryology section, at 18–20 GW, the brain is almost completely smooth with only the following major fissures observed on US: the *interhemispheric fissure* (IHF), *Sylvian fissure* (also called the *lateral fissure*), and the *callosal sulcus*. The parieto-occipital fissure begins to appear at this developmental age. At 22 GW the beginning of the *calcarine fissure* is observed. At 26 GW, the *cingulate sulcus* and *gyrus* begin to appear, along with further deepening of the previously mentioned convolutions and a gradual closure of the *Sylvian fissure*. The *olfactory sulci* begin to appear at

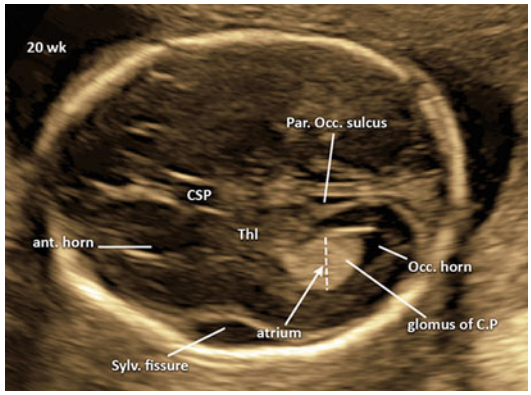

Fig. 19 Axial, transventricular plane of the fetal brain. This is one of the two views employed for screening of cerebral anomalies in the fetus (the other is the trans-cerebellar). On this view, it is possible to demonstrate the atrium of the lateral ventricle distal to the transducer (the proximal one is shadowed by the parietal bone). On this view, the atrial width (dotted line) should be measured positioning the calipers IN to IN, in order to detect ventriculomegaly (the commonly accepted cutoff for abnormalcy is >9.9 mm). The measurement should be taken at the level of the glomus of the choroid plexus. On the same plane, the following anatomical structures can be seen: the adjacent parieto-occipital sulcus, which deepens with advancing gestational age; anteriorly, the cavum septi pellucidi (visible from the 17th to the 35th week); the Sylvian fissure, which also deepens with advancing gestational age

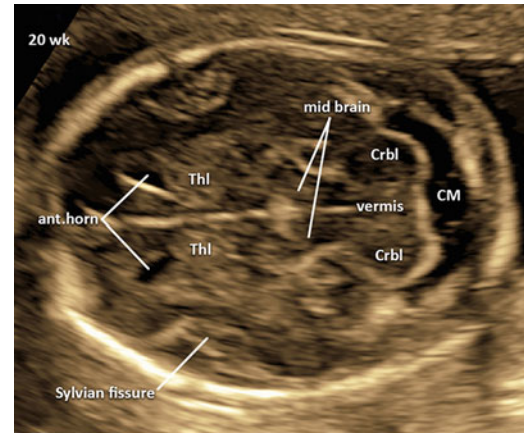

Fig. 20 Twenty-gestational-week-old fetus. Axial trans-cerebellar section of the brain showing the anatomical landmarks. This is one of the two views employed for screening of cerebral anomalies in the 2nd trimester (the other is the transventricular view; Fig. 19). This section is at the level of the cerebellum and midbrain. The contour of the two symmetrical cerebellar hemispheres is shown. Note the fluid-filled cisterna magna (ant, anterior; crbl, cerebellum; thl, thalamus)

26–28 GW and are confidently seen at 30 GW. *Operculization* of the insular cortex can be visualized both on the parasagittal and coronal views. On the former, the Sylvian fissure has an echogenic V-shape appearance, progressively closing from occipital to temporal direction (Fig. 22) (Cohen-Sacher et al. 2006; Monteagudo and Timor-Tritsch 1997; Toi et al. 2004).

6. *Screening for CNS lesions in the fetus*. Having demonstrated the normal sonographic anatomy in the former heading, we move here to illustrate how prenatal screening for CNS lesions is carried out. Since routine obstetric scans are carried out in most countries at 11–13, 18–22, and 28–32 gestational weeks, these are the timings in which a basic assessment of the fetal brain is carried out. At the end of the 1st trimester, only the most obvious and severe anomalies are detected, such as holoprosencephaly, anencephaly/exencephaly, and cephalocele (Fig. 29). The 2nd trimester, at 19–21 gestational weeks, is the time where screening ultrasound for all major anomalies detectable in utero is carried out. This is based on two axial scanning views, the trans-ventricular and trans-cerebellar views (ISUOG 2007) (Fig. 15). The former represents an axial view of the fetal head and brain passing through the occipital horns of the lateral ventricles (Fig. 19). On this view, the atrial width at the level of the glomus of the choroid plexus is measured, wall to wall (positioning the calipers IN to IN), in order to detect ventriculomegaly. In the fetus, ventriculomegaly is rated moderate if the atrial width is 10–15 mm and severe if it exceeds 15 mm (Fig. 19). Some authors also differentiate mild (10–12 mm) from moderate (13–15) ventriculomegaly, considering that feto–neonatal outcome may vary significantly in the two categories.

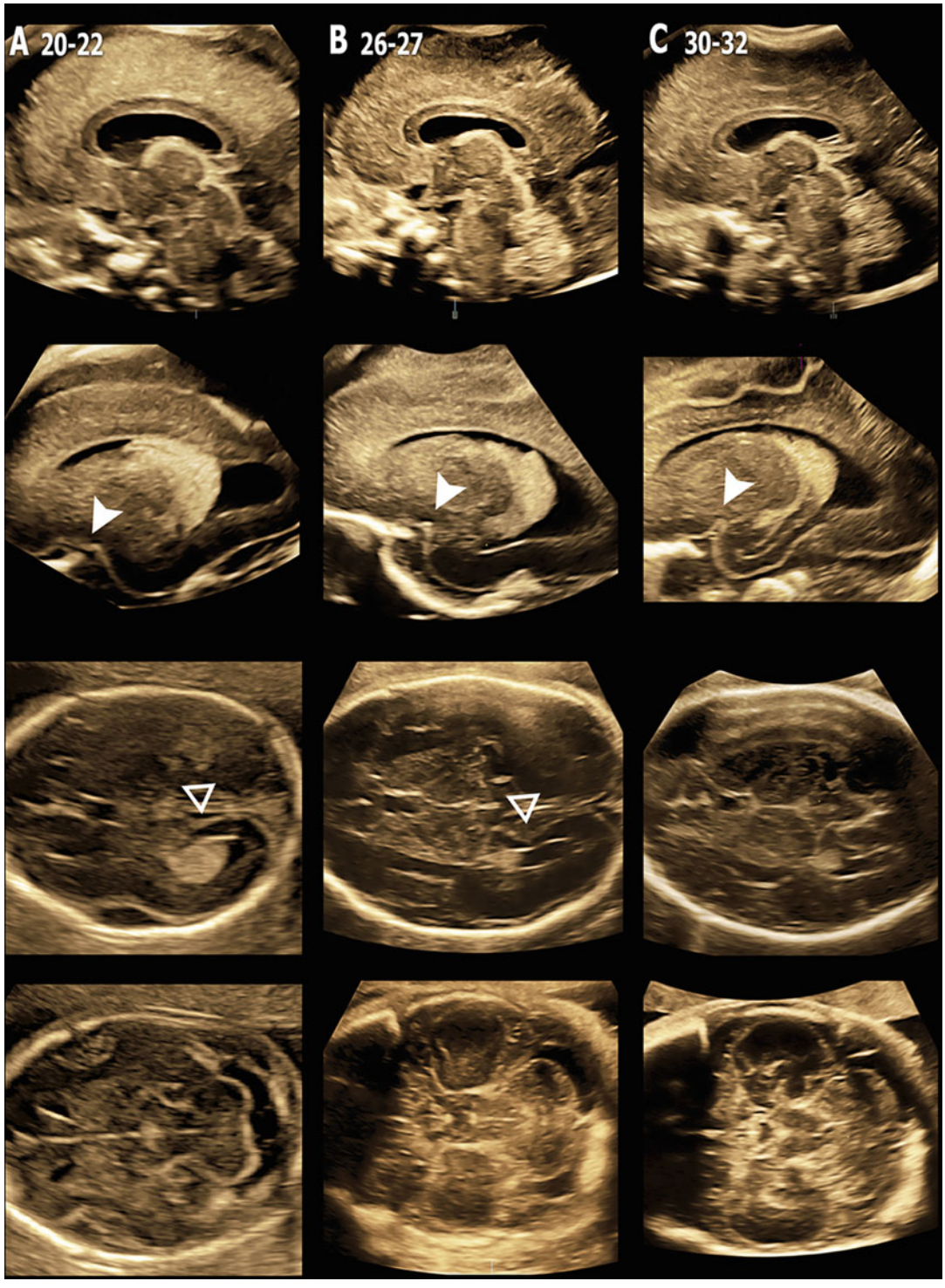

Fig. 21 (continued)

On the very same scanning plane, i.e., the transventricular view, also the cavum septi pellucidi is checked – according to most national and international guidelines (Fig. 19). This is recommended in order to reach an indirect diagnosis of agenesis of corpus callosum, being the CSP absent in all cases of complete agenesis and in a third of partial ones.

The other scanning view which has to be visualized during screening ultrasound in pregnancy is the trans-cerebellar one (Fig. 20). The visualization of this plane is recommended in order to diagnose abnormalities of the posterior fossa, mainly cystic vermian anomalies, such as Dandy-Walker malformation or vermian hypoplasia (Figs. 20 and 30).

Most of the anomalies are detected in the 2nd trimester of pregnancies thanks to the two scanning views described above. However, the brain is one of the organs whose development continues in the 3rd trimester of pregnancies, especially with neuronal migration and gyration. Hence, there are several malformations of the CNS that are *late-onset*, i.e., that can be detected *only* in the 3rd trimester of pregnancy because their signs are virtually absent or non-recognizable earlier. A partial list of these conditions is shown in Table 1.

7. *Diagnosis of CNS lesions in the fetus*. *Fetal neurosonography*. The above–described screening views are part of the 2nd trimester anomaly scan, the routine sonographic assessment of midpregnancy, the main objective of which is to screen for all congenital anomalies, including cerebral ones. Once the suspicion of a CNS anomaly is raised, the patient is referred to an expert. The experts perform then the diagnostic procedure which is called *fetal neurosonography*, i.e., a scan performed by an expert who is able to thoroughly assess the cerebral anatomy on ultrasound. The two main features of the *fetal neurosonography* are (1) that it includes not only axial planes, but sagittal and coronal ones, and (2) that, if the fetal presentation allows, the examination is performed transvaginally. In this way, higher emission frequency transducers allow a much higher spatial resolution than conventional transabdominal probes.

Normal anatomy of the fetal brain has already been described in the heading above. Hereafter, the reader will find a description of all pathologic conditions possibly associated with ventriculomegaly in the fetus. As already outlined in other parts of this chapter, a definite diagnosis of *primary, obstructive hydrocephalus* cannot be made with certainty in the fetus in most cases.

Ventriculomegaly and Hydrocephalus

Hydrocephalus is the correct term for pathologic dilatation of the brain's ventricular system from increased pressure, usually due to obstruction. Ventriculomegaly is the appropriate term when dilatation is due to other causes, such as brain dysgenesis or atrophy. Because ventricular pressure cannot be measured prenatally, the two terms are sometimes used synonymously when applied to the fetus. Most commonly, the term "ventriculomegaly" is used when the ventricles are mildly enlarged, and "hydrocephalus" is used when they measure >15 mm (Fig. 31). Considering also that in the fetus the Sylvian aqueduct cannot be visualized for most of the pregnancy, then the most common cause of obstructive hydrocephalus, i.e., aqueductal stenosis, cannot be diagnosed with certainty.

Fig. 21 Normal developmental changes in the sonographic appearance of the fetal brain from the midtrimester (20–22 weeks, left column) to the early 3rd (26–27 weeks, middle column) and full 3rd trimester (30–32 weeks, right column). The four rows correspond to midsagittal view, with the corpus callosum and the vermis in the posterior fossa; parasagittal view, showing the insula (arrowhead) and the cerebral mantle; axial, transventricular view, showing the lateral ventricle and the cavum septi pellucidi (arrowhead: parieto-occipital fissure); and axial, transcerebellar view, showing the posterior fossa and the cerebellum with the vermis. Note the dramatic changes occurring in 10 weeks (left vs. right column) at all levels

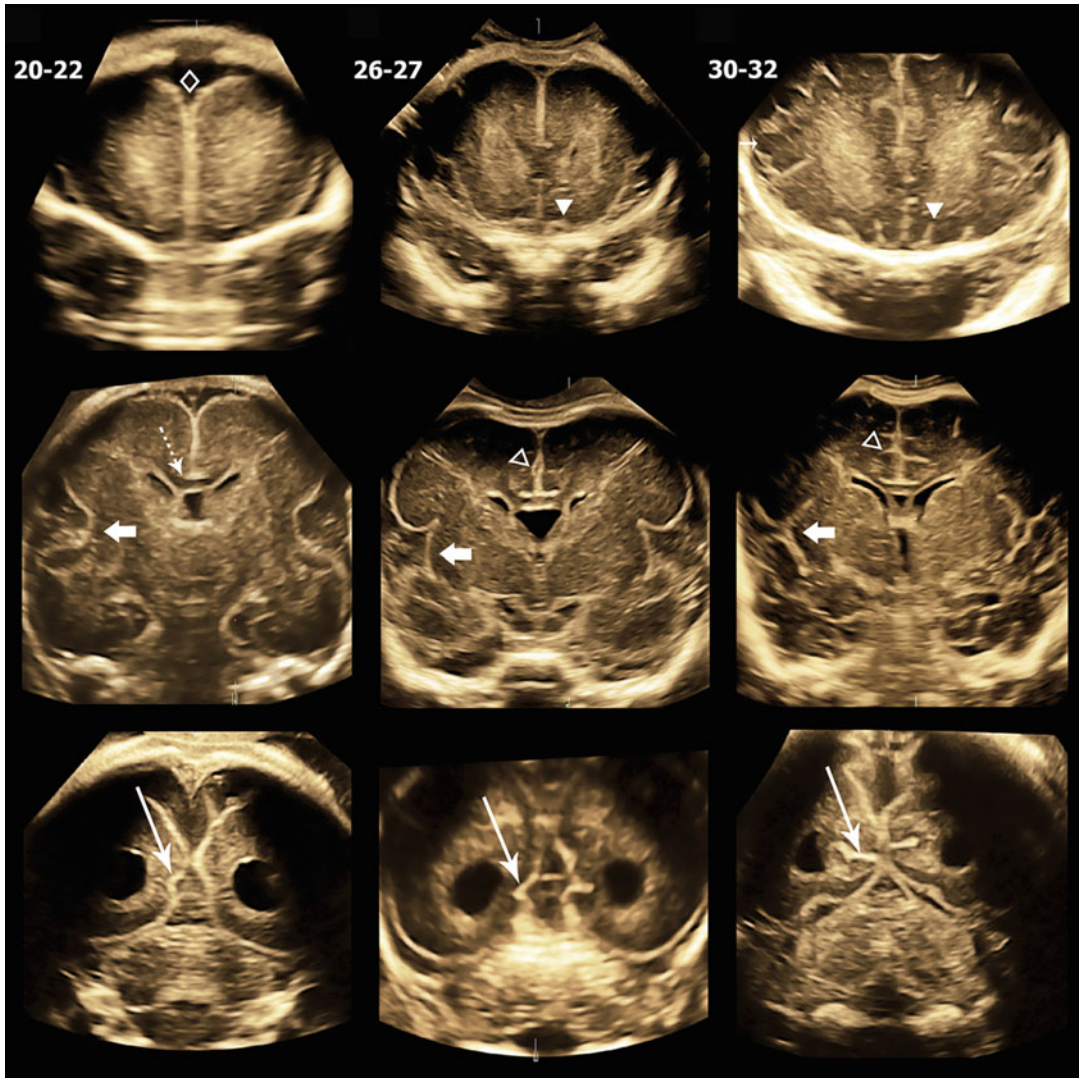

Fig. 22 Normal developmental changes in the sonographic appearance of the fetal brain from the midtrimester (20–22 weeks, left column) to the early 3rd (26–27 weeks, middle column) and full 3rd trimester (30–32 weeks, right column). The three rows correspond to trans-frontal plane, trans-caudate plane, and trans-occipital plane. On the trans-frontal plane, the development of the olfactory sulci (arrowhead) from absent (20–22 week) to fully developed (30–32 weeks) is evident; on the trans-caudate plane, the opercularization of the insula (arrow) is evident (arrowhead, cingulate sulcus; thin, dashed arrow, callosal sulcus); on the trans-occipital plane, the development of the calcarine fissures (arrow) is evident. The cerebellum is visible in the lower part, with the cisterna magna

As already mentioned, the lateral ventricle is measured at the level of the atrium. The atrium of the lateral ventricle is the portion where the body, posterior horn, and temporal (inferior) horn converge. Atrial diameter remains stable between 15 and 40 weeks of gestation (Cardoza et al. 1988). A number of studies have assessed the normal size of the fetal atria. Most of these studies are in agreement with the original study by Cardoza et al. (1988), who found that in the

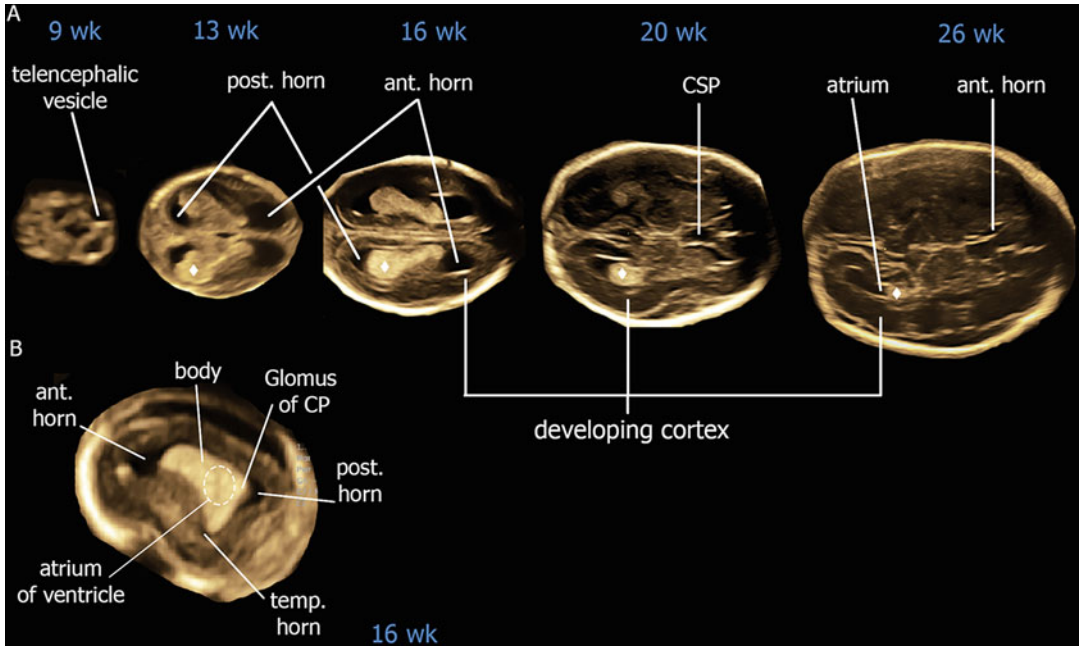

Fig. 23 Development of the ventricular system. (**a**) Axial transventricular view of the fetal brain across gestation. Note the progressive decrease in the representation of the choroid plexuses and the lateral ventricles in relation to the growing cortex; (**b**) parasagittal view of a 16 GW brain demonstrating the different segments of the lateral ventricle (ant. Horn, anterior horn; CSP, cavum septi pellucidi; CP, choroid plexus; post. Horn, posterior horn; temp. Horn, temporal horn)

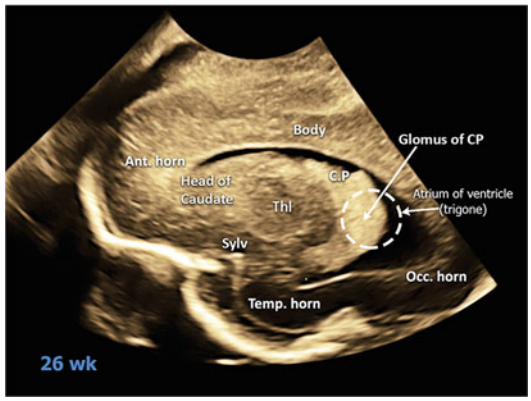

Fig. 24 Parasagittal view of the brain in a 27-gestational-week-old fetus. Anatomical landmarks. This plain cuts through most segments of the lateral ventricle. Note the atrium of the lateral ventricle, harboring the choroid plexus and connecting the anterior posterior and inferior luminal sections. Development of the Sylvian fissure can be studied using this plain

2nd trimester the mean ± SD measurement is 7.6 ± 0.6 mm and suggested a threshold of abnormality of 10 mm, corresponding to about four SD above the mean. In a pooled analysis of nine studies containing 8216 cases, Almog et al. (2003) showed no significant change in width between 20 and 40 weeks of gestation.

VM is defined as an atrial diameter ≥ 10 mm (ISUOG 2007). VM is generally considered mild if the atrial diameter is between 10 and 15 mm and severe if >15 mm, although some authors use the categories of mild (10–12 mm), moderate (13–15 mm), and severe (≥16 mm) (Bromley et al. 1991) (Fig. 31).

Ventriculomegaly is considered "isolated" when the fetus has no other anomalies, except those that are a direct result of the ventricular enlargement. By definition this is a provisional diagnosis of exclusion. Many cases that appear isolated prenatally are ultimately found to have other abnormalities, particularly when ventriculomegaly exceeds 15 mm. We will illustrate these abnormalities in the second part of this chapter.

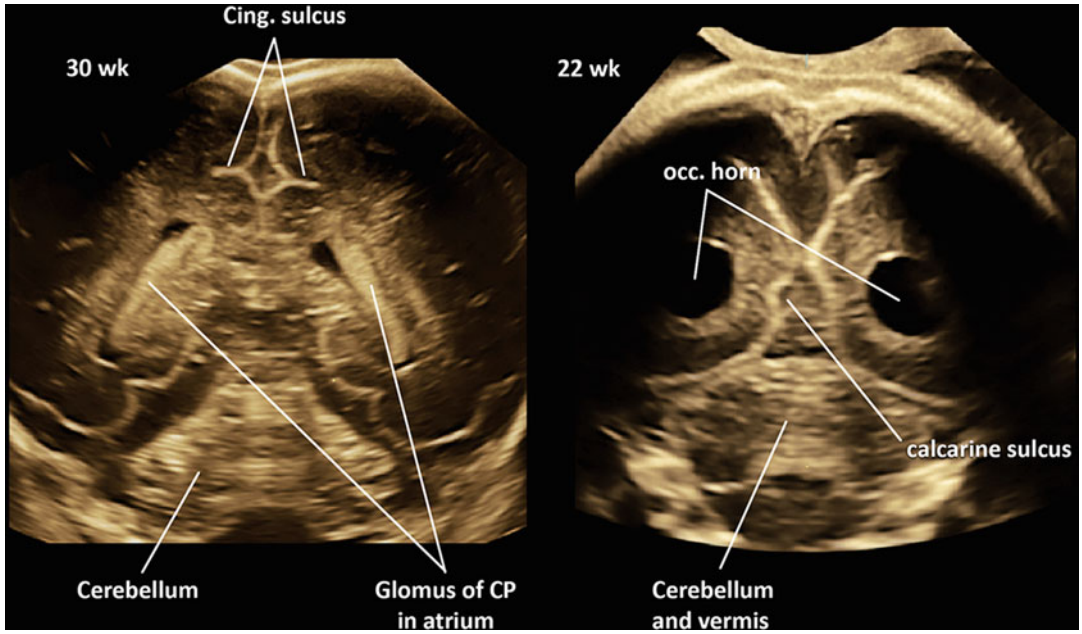

Fig. 25 Coronal section through the posterior brain. Left image: at the level of the glomus of the choroid plexus of a 30 gestational weeks' brain. Right image: at the level of the posterior horns of a 22 gestational weeks' brain. This plain enables a good comparison between the two occipital lobes and occipital horns of the lateral ventricles. The gestational-dependent differences in the gyration process are clearly evident comparing the two images (Cing. sulcus, cingulate sulcus; CP, choroid plexus; occ, occipital)

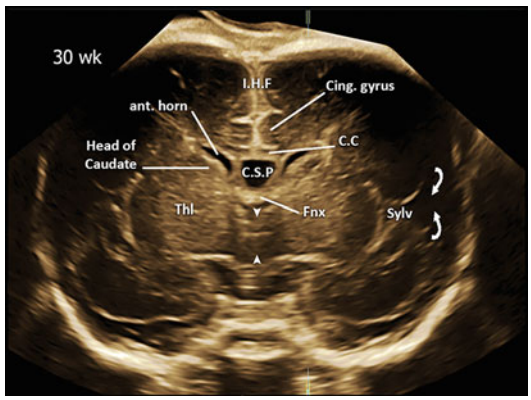

Fig. 26 Coronal section through a 30 gestational weeks' brain, anatomical landmarks. Structures of the anterior complex are labeled. Note the advanced operculization of the insular cortex and the insular fissure (ant, anterior; arrowheads, anatomical location of 3rd ventricle; CC, corpus callosum; cing. Gyrus, cingulate gyrus; CSP, cavum septi pellucidi; IHF, interhemispheric fissure; Fnx, fornix; Sylv, Sylvian fissure; Thl, thalamus)

Isolated Mild Ventriculomegaly

Isolated mild VM (atrial width 10–12 mm; Fig. 31b) represents a relatively common condition, complicating 1% of all pregnancies. It is a benign finding in most cases, but it may associated with a wide range of completely different etiologies, from infections to chromosomal anomalies, from cerebral clastic conditions to migration abnormalities. As such, considering also its common occurrence, the diagnostic management of mild VM (called until recently *borderline VM*) and the prenatal counseling for it have been the topic of several articles. Recently, an elegant meta-analysis (Melchiorre et al. 2009) summarized the pertinent literature. As far as the *diagnostic management* is concerned, should the suspicion of mild ventriculomegaly be raised at midtrimester screening ultrasound, this should undergo transvaginal neurosonography, fetal echocardiography,

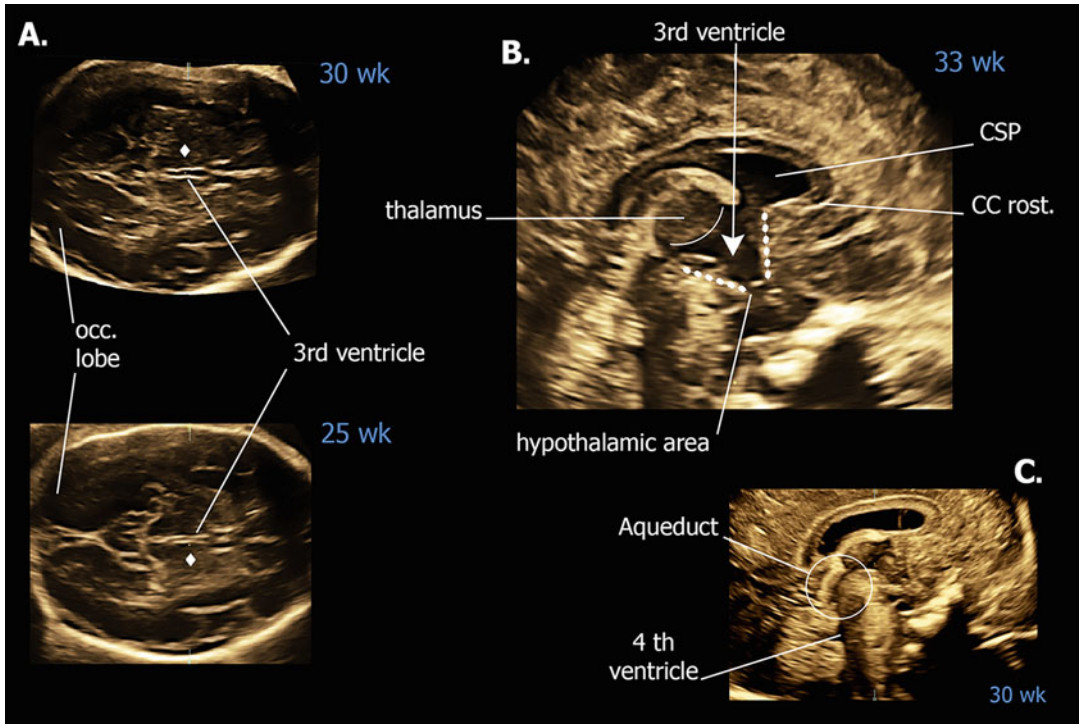

Fig. 27 Sonographic evidence of the 3rd ventricle and Sylvian aqueduct. The 3rd ventricle can be appreciated in most cases both on axial planes and on the midsagittal one: (**a**) on axial views, the 3rd ventricle is visible as a slit-like structure on the midline, between the thalami (mark) and cerebral peduncles. (**b**) On a midsagittal view, its roughly triangular shape becomes evident, with the downward tip pointing toward the hypothalamus (dotted lines: outline of the 3rd ventricle); (**c**) on the contrary, sonographic visualization of the Sylvian aqueduct is challenging, probably also due to its physiology (see text). On rare occasions, it can be demonstrated as a hypoechoic line joining the posterior aspect of the 3rd ventricle with the 4th one (CSP, cavum septi pellucidi; CC rost, corpus callosum, rostral part; Occ. lobe, occipital lobe)

and detailed anatomic assessment in order to exclude or diagnose concurrent malformations. The *employment of MRI* as an adjunctive diagnostic procedure is controversial. On one hand, the literature seem to demonstrate that when MRI is performed in case of apparently isolated mild ventriculomegaly, it detects 5–9% of significant CNS abnormalities that have a significant impact on the prognosis (Ouahba et al. 2006; Salomon et al. 2006). However, with the exception of cortical malformations, which may be a challenging diagnosis on ultrasound, the anomalies detected at MRI and not at ultrasound in these studies include malformations that *should* have been diagnosed at transvaginal neurosonography, such as vermian hypoplasia or partial agenesis of the corpus callosum. Therefore, the evidence is such that the decision to perform an MRI in case of apparently isolated mild ventriculomegaly depends on the experience of the expert performing fetal ultrasound and on the local resource allocation. However, should an MRI deemed advisable, this should be carried out not before 28 gestational weeks, to be able to evaluate cortical development. Another issue is the *infectious disease workup*. All the infections that are known to be teratogenic for the fetus – rubella, CMV, and toxoplasmosis – may be responsible for mild ventriculomegaly. In most of the cases in which these infections reach

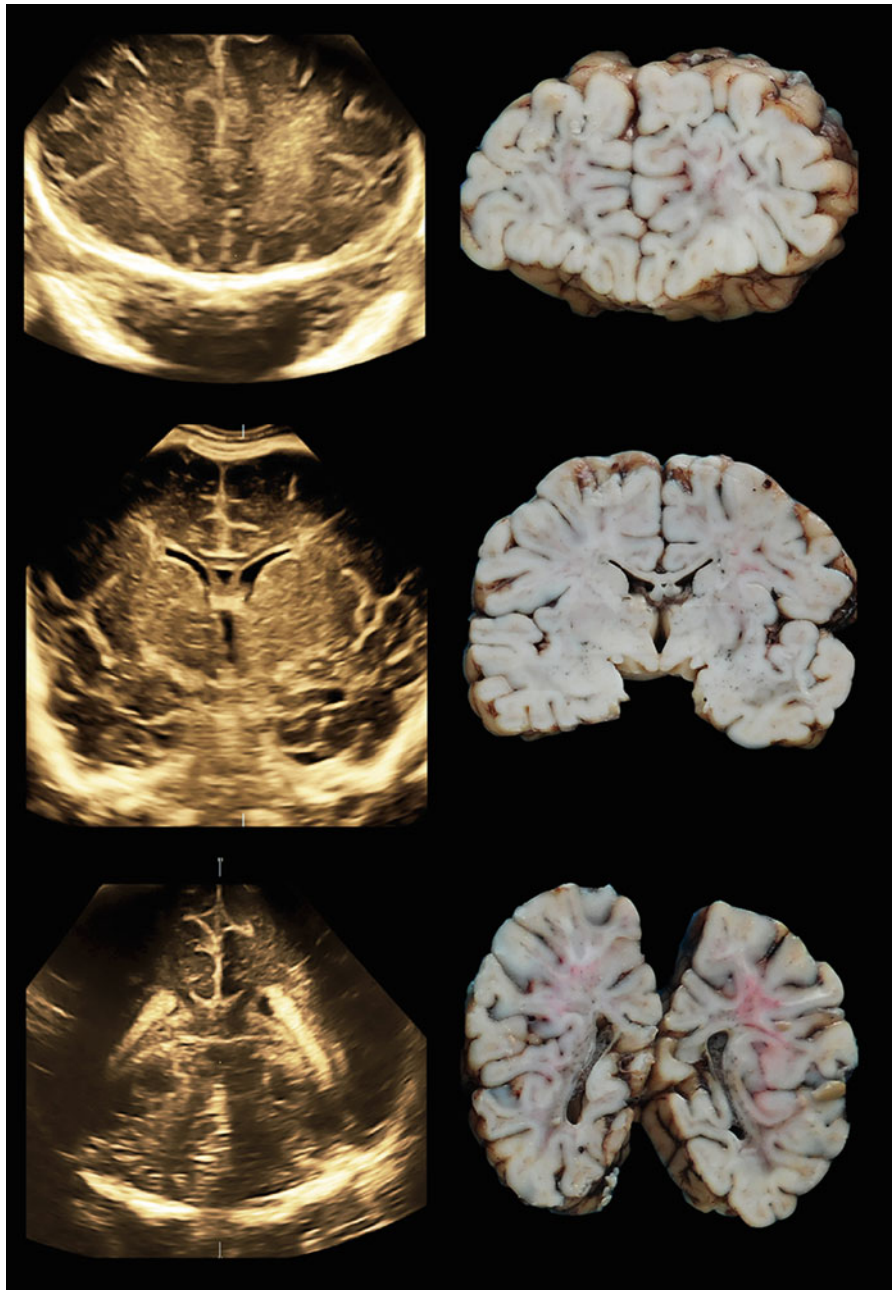

Fig. 28 Echo-anatomic correlation of the three main coronal planes of the fetal brain obtainable through the anterior fontanelle (see also Fig. 17), in a 30-week-old fetus and corresponding specimen. (**a**) trans-frontal plane, cutting at the level of the frontal lobes. Note the olfactory sulci (arrowheads), just above the bone, and all the sulci of the convexity; (**b**) trans-caudate plane. This represents one of the most important coronal planes. At this gestational age, the cingulate gyrus (arrow), the frontal horns (fh), the slit-like 3rd ventricle (arrow), and the operculization of the insula (in) are evident; (**c**) trans-occipital plane. This plane cuts through the occipital lobes. The occipital horns of the lateral ventricles are visible, with the hyperechoic choroid plexuses. The vermis is visible on the sonographic image, but the infratentorial compartment has been removed on the specimen

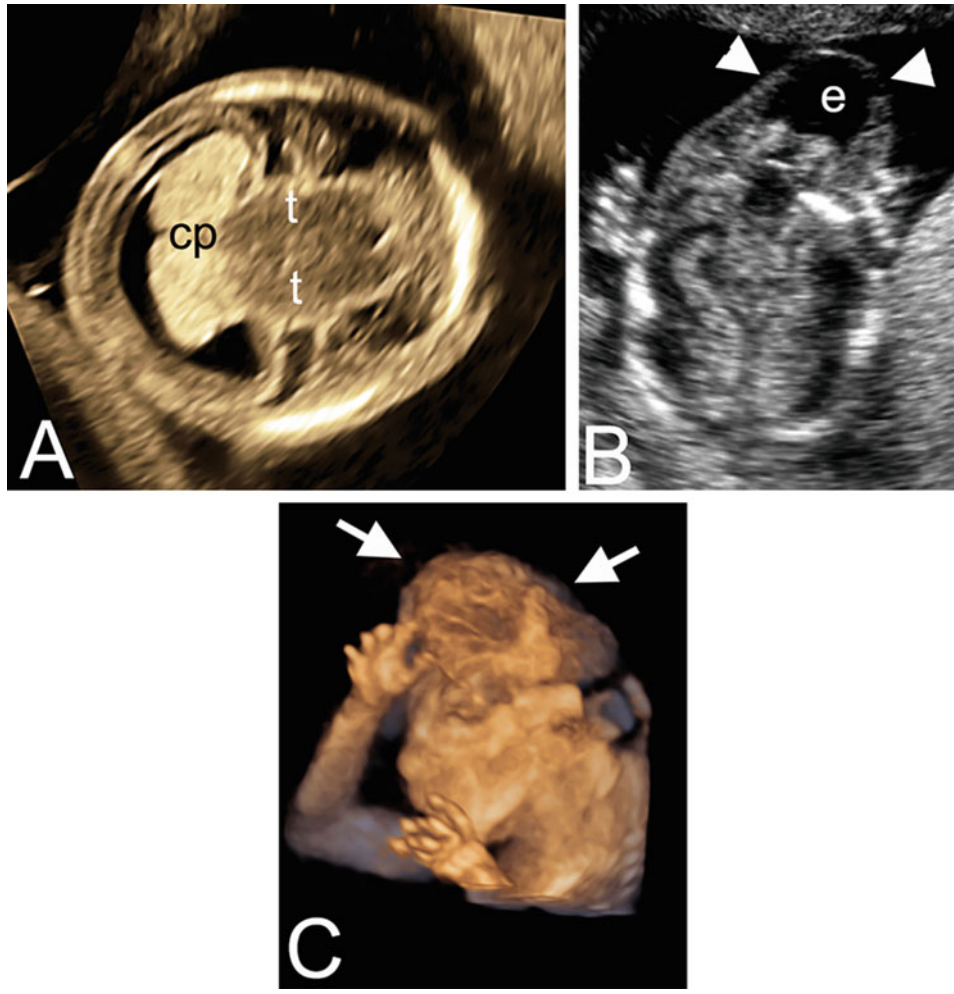

Fig. 29 Severe congenital anomalies of the fetal brain that can be diagnosed by the end of the 1st trimester include (**a**) alobar and semilobar holoprosencephaly (cp, single choroid plexus within a single ventricular cavity; t, fused thalami) and (**b**) cephalocele. The protruding occipital cephalocele (e) with the meninges (arrowheads) and the cerebellum outside the calvarium can be seen; (**c**) anencephaly/exencephaly. The first stage of the lesion is exencephaly, which is shown here. The calvarium is absent, and the brain (arrows) can be observed directly on three-dimensional ultrasound. The second stage – anencephaly – develops later in gestation and is due to the complete destruction of the brain parenchyma because of trauma against the uterine wall and the contact with the amniotic fluid. Therefore, eventually the brain melts away, and only the basal ganglia are visible (not shown)

the feus, there will be other CNS and/or non-CNS signs of infection in addition to ventriculomegaly. However, 0–5% of foetuses with mild ventriculomegaly will eventually result infected with CMV. Therefore, it is a general recommendation that maternal serology should be checked for CMV and *Toxoplasma gondii*. Next comes *karyotyping*: older articles report an association rate for mild ventriculomegaly up to 10%. However, the currently available early screening tests for aneuploidies (combined test [nuchal translucency + biochemistry] and cell-free DNA in maternal blood) ensure a 90–99.5% detection rate for Down syndrome, respectively. Therefore, the prevalence of trisomy 21 among 2nd trimester fetuses with VM will highly depend on

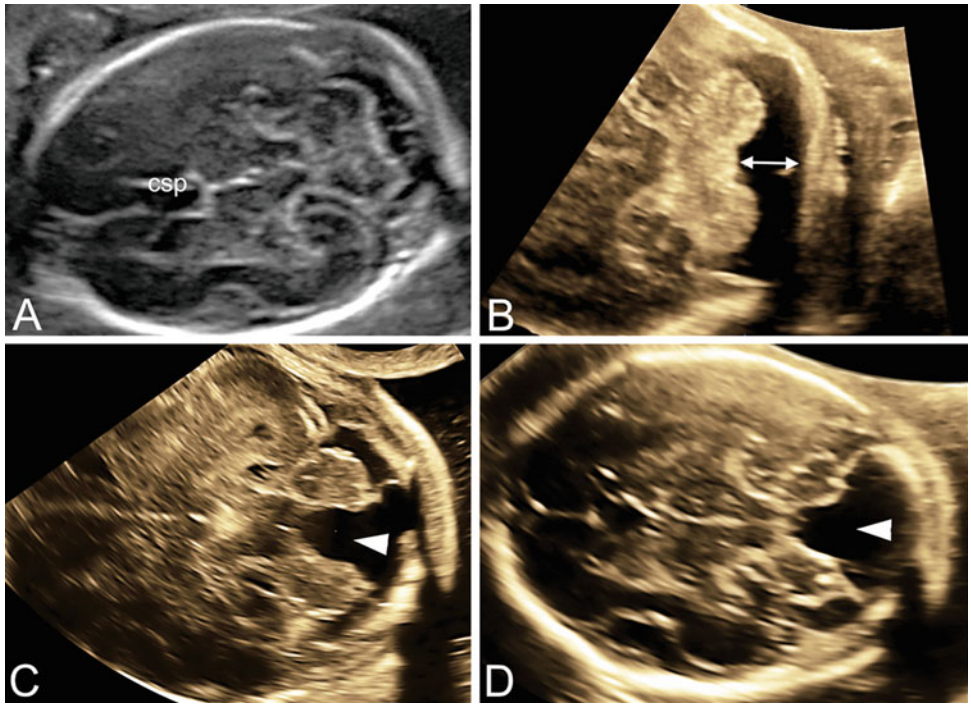

Fig. 30 Trans-cerebellar view of the fetal head. (**a**) Normal appearance of the cerebellum, vermis, and cisterna magna; (**b**) Megacisterna magna. This condition is diagnosed when the distance between the vermian edge and the occipital bone (double arrow) is ≥10 mm. Note that also visually the amount of fluid in the posterior fossa is increased, also around the cerebellar hemispheres; (**c**) *keyhole sign* (arrowhead): the two cerebellar hemispheres are normal, but the vermis cannot be seen, on the midline. The amount of fluid in the posterior fossa is normal to slightly increased. When this sonographic sign is seen, neurosonography is needed to differentiate between the two conditions that share this very same aspect on the axial view and that have significantly different outcome: Blake's pouch cyst (normal outcome in most cases) and vermian hypoplasia (possibly associated with significant neurodevelopmental delay in a variable percentage of cases according to the literature; see text); (**d**) Dandy-Walker malformation. The wedge in between the two cerebellar hemispheres is deeper and wider, and the two hemispheres are splayed apart. The collection of fluid is significantly increased (csp, cavum septi pellucidi)

the extent of the population coverage with those screening tests. In most developed countries, the overwhelming majority of the pregnant population undergoes one or the other test, according to their moral and religious background. Therefore, currently the prevalence of fetuses with Down syndrome in the 2nd trimester of pregnancy has significantly decreased, due to termination of pregnancy. Consequently, the risk of association of mild ventriculomegaly with aneuploidy has dropped and is now considered to be around 2–3%. Considering the relative incidence of Down syndrome and mild ventriculomegaly in the fetus, the likelihood ratio for Down syndrome has been estimated to be 9. Hence, investigation for aneuploidy in the presence of this finding may therefore be appropriate, depending on the prior risk (Van den Hof et al. 2005).

Table 1 Late-onset anomalies of the fetal brain

Congenital
• *Hydrocephalus*
• *Malformation of cortical gyration*
• *Microcephaly*
• *Arachnoid cyst*
Acquired
• *Hemorrhage*
• *Tumors*
• *Destructive lesions from infections*
• *Arteriovenous malformations*

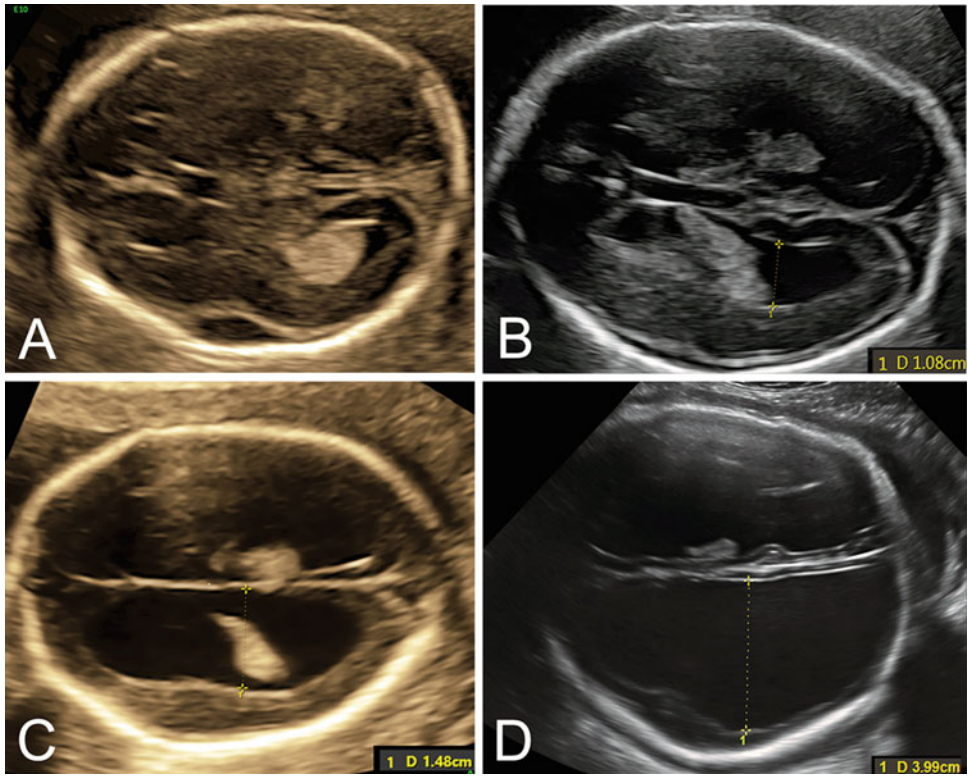

Fig. 31 Transventricular view of the fetal head. (**a**) Normal appearance and normal atrial width (<10 mm); (**b**) moderate ventriculomegaly, with atrial width <12 mm; (**c**) moderate ventriculomegaly, with atrial width >12 mm; (**d**) severe ventriculomegaly, with atrial width >15 mm. Larger is the width of the atrium, worse is, in general, the neonatal outcome (see text)

The last issue regards the neurological outcome of fetuses with a diagnosis of mild ventriculomegaly. Several studies have addressed the issue of neurodevelopmental delay, with controversial data. However, pooled data seem to lead to consider a figure of 10% (confidence interval, 6.1–18.1%) as a reliable estimate for this risk (Melchiorre et al. 2009).

Factors that have been found to be irrelevant for the outcome include gestational age at diagnosis, gender, laterality (uni- or bilateral), and asymmetry.

In utero progression from mild to severe ventriculomegaly occurs in about 16% of the cases, and in this subset of fetuses, the prognosis deteriorates, with an incidence of *adverse outcome* of 44%.

Severe Ventriculomegaly

In the fetus, a diagnosis of severe ventriculomegaly is made when the atrial width is >15 mm (Fig. 31d). In general, severe ventriculomegaly is bilateral, though some degree of asymmetry may be seen. However, in selected cases, unilateral severe ventriculomegaly can be found. Again, a wide range of conditions may represent the ultimate cause of the ventriculomegaly. In bilateral ventriculomegaly, aqueductal stenosis or severe developmental malformations may be present. In unilateral severe ventriculomegaly, the etiology is more often acquired, considering that the pathogenesis of the ventriculomegaly is in this case obstruction

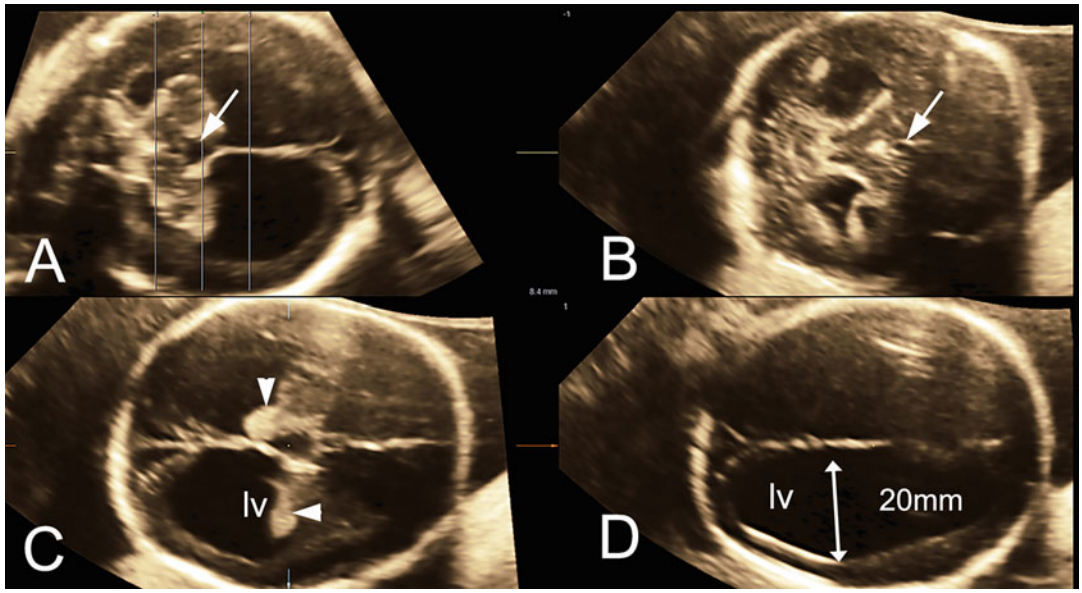

Fig. 32 Aqueductal stenosis, 21 weeks of gestation. Three-dimensional tomographic imaging of the fetal head. (**a**) In this coronal image, the levels of the other three images are shown (lines); the dilated 3rd ventricle (arrow) is also visible; (**b**) on the most caudal axial plane, the slightly dilated 3rd ventricle is shown; (**c**) severe ventriculomegaly with dangling choroid plexuses (arrowhead) is evident (lv, lateral ventricles); (**d**) the atrial width is 20 mm, which corresponds to severe ventriculomegaly (lv, lateral ventricle)

of the foramen of Monro. This may be due to hemorrhage, tumor, or arachnoid cysts which all have a mass effect on the foramen of Monro.

Severe ventriculomegaly may or may not be accompanied by macrocephaly (i.e., head circumference greater than two standard deviations above the mean). In general, macrocephaly is detected from the 26–28 weeks of gestation onward, with only a limited number of cases showing macrocephaly in the 2nd trimester of pregnancy.

When severe ventriculomegaly is detected, a first diagnostic effort to make regards the distinction of primary obstructive ventriculomegaly (i.e., hydrocephalus) from ventriculomegaly secondary to other CNS severe malformations, such as diencephalosynapsis or Dandy-Walker malformation. This distinction has important prognostic significance because severe neurodevelopmental delay is expected in the overwhelming majority of secondary hydrocephalus, while the outcome may be better in case of obstructive hydrocephalus due to aqueductal stenosis. In most industrialized countries, with obvious differences due to religious and moral background, couples who receive such a diagnosis for their fetus tend to opt for termination of pregnancy, especially in case of severe ventriculomegaly associated with other major cerebral malformations. This is why the spectrum of diseases that can be seen in the fetus is completely different from that seen after birth.

Aqueductal Stenosis in the Fetus

From what has been said so far, it becomes clear how a clear-cut diagnosis of aqueductal stenosis cannot be made in prenatal life. However, there are some signs and hints that may lead to suspect such a diagnosis; in any case, the final diagnosis will only be confirmed by postnatal MRI.

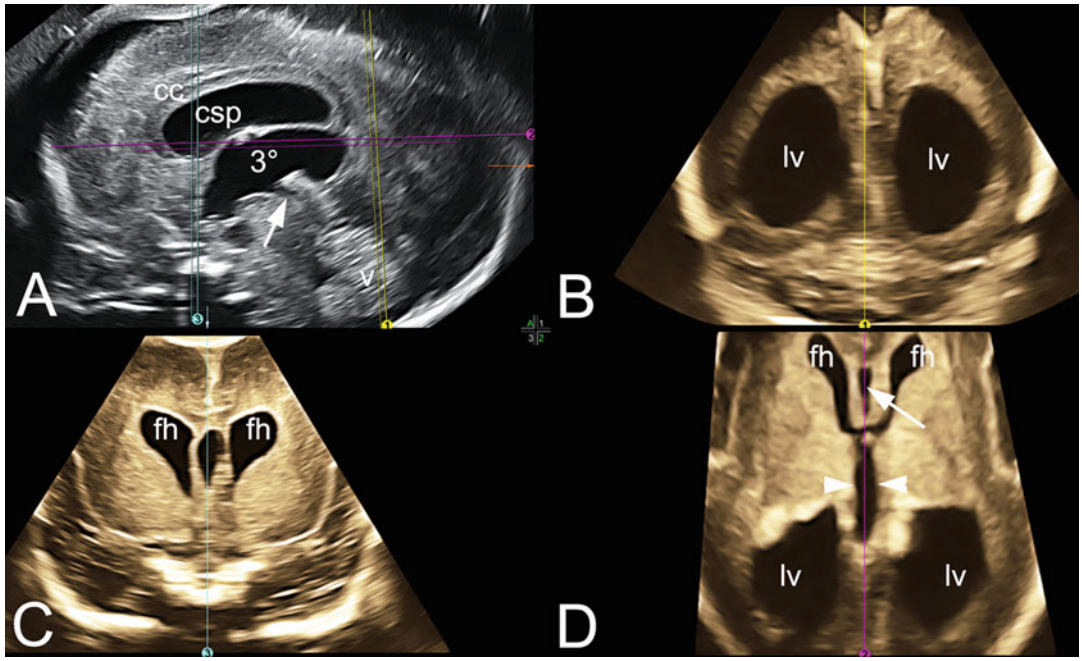

Fig. 33 Aqueductal stenosis, 25 weeks of gestation. (**a**) The midsagittal view demonstrates the dilated 3rd ventricle and an enlarged cavum septi pellucidi (csp). The very initial tract of the aqueduct is also visible (arrow). (cc, corpus callosum; v, cerebellar vermis). The three colored lines (light blue, yellow, purple) correspond to the planes shown in B, C, and D, respectively. (**b**) On the coronal view of the occipital horns of the ventricles, bilateral moderately severe ventriculomegaly is evident; (**c**) on this coronal view clear dilatation of the frontal horns is also evident; (**d**) on the reconstructed axial plane, it can be appreciated that the dilatation involves the lateral ventricles (fh, frontal horns; lv, lateral ventricles), the 3rd ventricle (double arrowhead), and the cavum septi pellucidi (single arrow). The dangling choroid plexuses are also visible in the lateral ventricles

The sonographic and MR signs that seem to indicate the likely presence of aqueductal stenosis are as follows (Emery et al. 2005) (Figs. 32 and 33):

1. Severe ventriculomegaly (atrial width >15 mm)
2. Symmetrical parenchymal thinning
3. Dangling choroid plexuses
4. Dilated 3rd ventricle (>2 mm)
5. Normal posterior fossa
6. Loss of peri-cerebral spaces (on MRI)
7. No evidence of an aqueduct distal to the 3rd ventricle (on MRI)

The authors who proposed these criteria were apparently able to correctly diagnose six out of six cases of aqueductal stenosis in fetuses (Emery et al. 2005). However, to the best of our knowledge, this is the only article appeared so far in which a prospective diagnosis of aqueductal stenosis was reported to be feasible in the fetus. With this exception, most authors have considered such a diagnosis an exclusion diagnosis: when no other CNS abnormalities are seen in association with (severe) ventriculomegaly, the underlying occurrence of aqueductal stenosis is hypothesized. It should be noted that a significant amount of information can be gathered only from the end of the 2nd trimester onward, both on neurosonography and MRI. This is due to the fact that the brain changes completely appearance in the 3rd trimester due to migration and gyrification. Hence, all migration-related abnormalities – and these may also be associated with ventriculomegaly – represent *late-onset*

malformations that can be diagnosed not before the end of the 2nd trimester in most cases. In fact, fetal brain MRI provides much better results if performed >26 weeks of gestation (Paladini et al. 2014). Considering that most cases of ventriculomegaly are diagnosed in the 2nd trimester, it can be easily understood how the diagnosis of aqueductal stenosis is a putative one. In the 3rd trimester, an associated malformation will be discovered in a significant number of cases of ventriculomegaly, reducing the number of case in which a diagnosis of aqueductal stenosis is maintained until delivery. Final confirmation will be provided by postnatal MRI.

Hydranencephaly

Hydranencephaly is characterized by a complete or almost complete absence of the cerebral cortex, with the normal brain tissue being replaced by a large fluid collection covered by leptomeninges and dura. The presence of the falx and of the cranial nerves demonstrates that the hemispheres have developed but have subsequently been destroyed. The most accepted hypothesis for explaining such a huge destructive process is an early vascular disruption process involving both carotid arteries. This process may be triggered by maternal (severe hypoxia, abdominal trauma) or fetal (CMV infection, coagulation deficits, twin-to-twin transfusion syndrome, especially when one fetus dies in utero) conditions (Figs. 34 and 35).

Ventriculomegaly and Associated Genetic Conditions

In this heading, we summarize a limited number of severe genetic conditions that: (1) feature hydrocephalus/ventriculomegaly as one of the main signs and (2) can be – and have been – diagnosed in the fetus.

– *Walker-Warburg syndrome (WWS)*. WWS is a dystroglycanopathy, being due to an abnormal O-glycosylation of alpha-dystroglycan. This condition shows genetic heterogeneity, and, hence, a direct molecular diagnosis is not feasible in all cases, especially prenatally; only fetuses of families with known mutations can undergo CVS for diagnostic purposes. However, in families at risk, the detection of ventriculomegaly and/or associated CNS and eye anomalies, such as cataract (Fig. 36), may lead to the diagnosis in the 2nd trimester. The classic *cobblestone lissencephaly* develops often only in the 3rd trimester and can therefore be diagnosed only >27–28 gestational weeks in most cases on transvaginal neurosonography and MRI.

  WWS represents the most severe form of congenital muscular dystrophy, leading almost invariably to death by the age of 3–4 years.

– *L1 syndrome (MASA – CRASH)*. L1 syndrome is a mild to severe congenital X-linked developmental disorder characterized by hydrocephalus of varying degrees of severity, intellectual deficit, spasticity of the legs, and adducted thumbs. The syndrome represents a spectrum of disorders including: X-linked hydrocephalus with stenosis of the aqueduct of Sylvius (HSAS), MASA syndrome, X-linked complicated hereditary spastic paraplegia type 1, and X-linked complicated corpus callosum agenesis. L1 syndrome is caused by mutations in the L1CAM gene (Xq28) encoding the L1 cell adhesion molecule that is expressed mainly in the developing nervous system. Prenatal diagnosis through chorionic villous sampling or amniocentesis can be performed in pregnant female carriers if an L1CAM disease-causing mutation has been identified in a family member. In this case, the known mutation can be searched in the fetal DNA. The acronyms MASA (Mental retardation, Aphasia, Shuffling gait, Adducted thumbs) and CRASH (Corpus callosum hypoplasia, Retardation, Adducted thumbs, Spasticity, Hydrocephalus) had been used in the past to identify conditions that eventually were included in the L1 syndrome, sharing the same mutations of the L1CAM gene on Xq28.

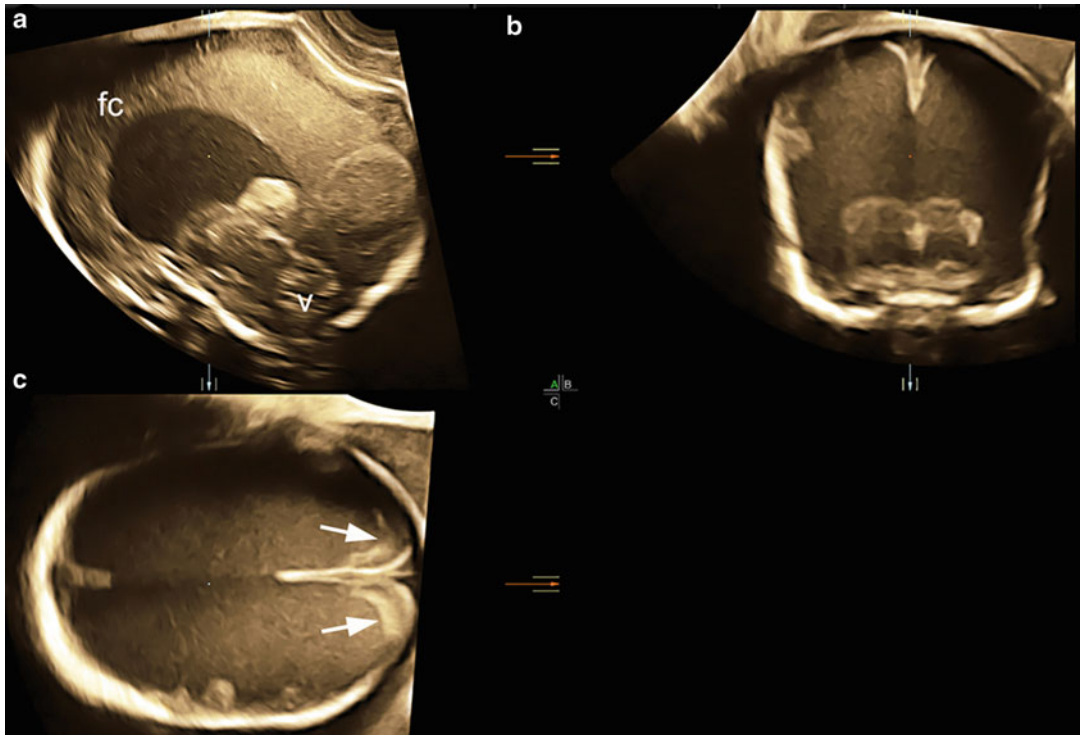

Fig. 34 Hydranencephaly at 21 weeks of gestation. Three-dimensional multiplanar imaging. (**a**) On the midsagittal view, the cerebral falx (fc) is evident, together with the cerebellar vermis (v); (**b**) on the coronal view, it is demonstrated that only the basal ganglia and very limited remnants of the cortex are visible. Both hemispheres are completely replaced with cerebrospinal fluid; (**c**) on the axial plane, the extent of parenchymal destruction is more evident. The whole cavity is filled with cerebrospinal fluid with the exception of a small portion of the occipital lobes (arrows)

Fig. 35 Hydranencephaly at 21 weeks of gestation. On the midsagittal view of the fetal head, complete absence of the supratentorial brain is found. The basal ganglia and infratentorial components (bs, brainstem; v, cerebellar vermis) are still visible and normal

On prenatal ultrasound, the most common lesion is agenesis of the corpus callosum, while ventriculomegaly is less common (Fig. 37). On some occasions, the adducted thumbs may be displayed with three-dimensional ultrasound.

In families with positive history, both hydrocephalus and more often – at least in the fetus – corpus callosum agenesis (partial or complete) can be diagnosed from mid-gestation. Alternatively, as mentioned, the L1 gene can be analyzed on fetal DNA samples. In Fig. 37a, a case of prenatal diagnosis of L1 syndrome is shown. In this case, there was partial agenesis of the corpus callosum but not hydrocephaly in all affected members of the family including two fetuses.

– *Megalencephaly, polymicrogyria, polydactyly, hydrocephalus (MMPH) syndrome*. All the

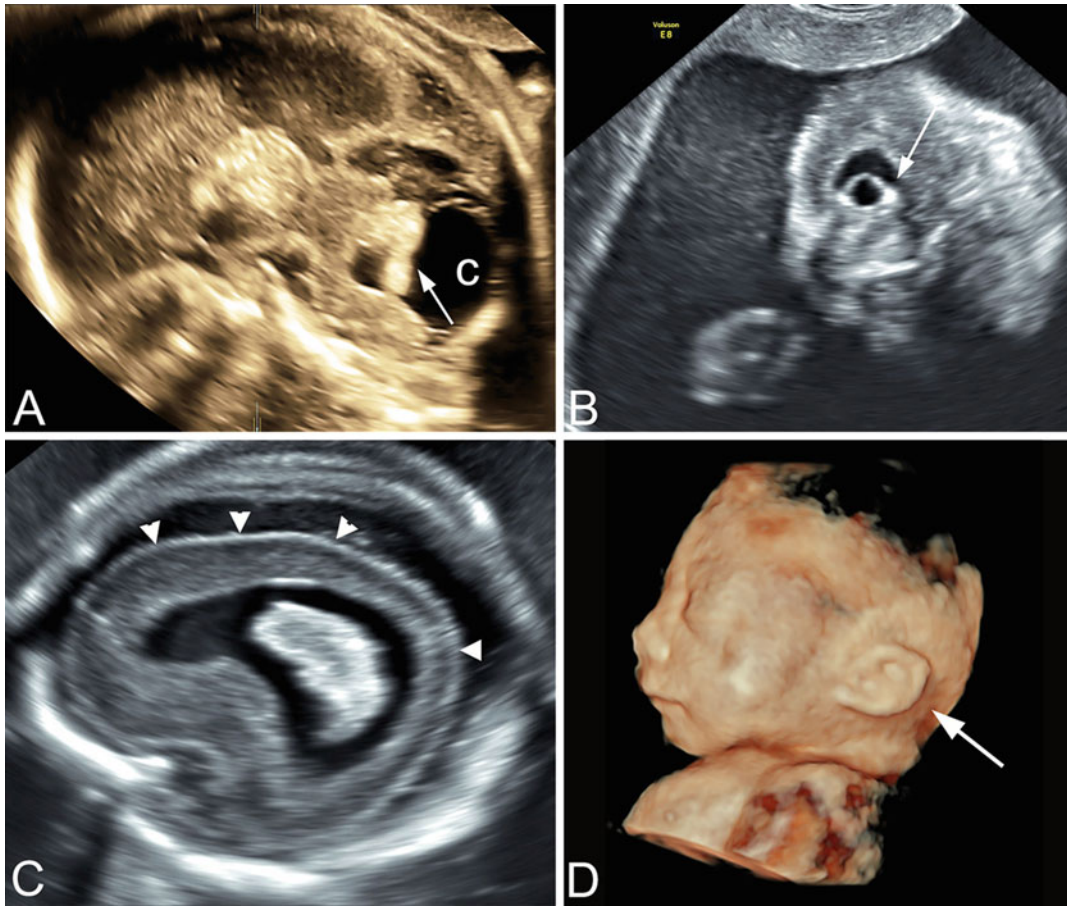

Fig. 36 Walker-Warburg syndrome at 21 weeks of gestation. (**a**) On the midsagittal view, the associated vermian hypoplasia (arrow) and a cystic component (c) in the cisterna magna are visible; (**b**) lens opacity is visible on examination of the fetal eye; (**c**) an abnormally smooth cortex (arrowheads) is visible on parasagittal view of the brain. Note also the ventriculomegaly and the prevalent subdural spaces; (**d**) three-dimensional surface rendering of the fetal face shows low-set ears (arrow)

CNS abnormalities present in this genetic condition – megalencephaly (and macrocrania), polymicrogyria, and ventriculomegaly – can be detected in the fetus (De Keersmaecker et al. 2013). MRI is needed to characterize the cortical malformation, but neurosonography can effectively detect megalencephaly and ventriculomegaly. All these are late-onset abnormalities and can, therefore, be diagnosed only in the 3rd trimester. The only feature which might be recognized as early as the 1st trimester is the postaxial polydactyly.

Ventriculomegaly Secondary to Other CNS Malformations

This represents an extensive chapter in fetal neurology. In fact, the spectrum of possible cerebral malformations that can be associated with ventriculomegaly is rather wide. We will try to approach this topic systematically, dealing with the various groups of developmental anomalies that may be responsible for ventriculomegaly. From the diagnostic standpoint, the extent of ventriculomegaly (bi-, tri-, or

tetraventricular) may suggest where the obstruction is. As an example, Dandy-Walker malformation is associated with tetraventricular hydrocephalus, whereas hemorrhage or aqueductal stenosis may determine triventricular hydrocephalus. However, again this concept has to be adjusted taking also gestational age at diagnosis into account; in fact, in Dandy-Walker malformation, the onset of ventriculomegaly is between the end of the 2nd and the beginning of 3rd trimester of pregnancy, with the lateral ventricles being unremarkable up to 22–25 weeks of gestation in a significant percentage of cases.

– *Holoprosencephaly.* This malformation is one of the first to be determined in the cerebral organogenesis, occurring at 28–40 days of development. The term "holoprosencephaly" refers to a group of complex abnormalities of the forebrain deriving from a failed cleavage of the prosencephalon that yields an incomplete division of the cerebral hemispheres and of the telencephalon from the diencephalon. Three main subtypes (alobar, semilobar, and lobar) have been recognized, but this anomaly represents a spectrum of malformations, so intermediate forms may occur. A robust genetic base has been found in several cases, with trisomy 13 being the most common occurrence. However, the etiology comprises microdeletions, duplications, single-gene mutations, and environmental factors (retinoic acid or alcohol exposure, rubella, CMV infections, nonchromosomal syndromic conditions [Smith-Lemli-Opitz syndrome], etc.) which have been found in several cases.

The diagnosis can be made very early in pregnancy, because the absence of the falx and the fused cerebral hemispheres are evident from the 1st trimester of pregnancy (Figs.1a and 38). The distinctive feature is the single ventricle. The amount of cerebrospinal fluid is only slightly increased. The cerebrospinal fluid increases later in pregnancy, but this event is seldom seen because in developed countries the overwhelming majority of women opt for termination of pregnancy. In the rare instance of late diagnosis or if the couple elects to continue the pregnancy, single-ventricle ventriculomegaly may ensue (Fig. 38c). A long series of midline facial anomalies may be associated

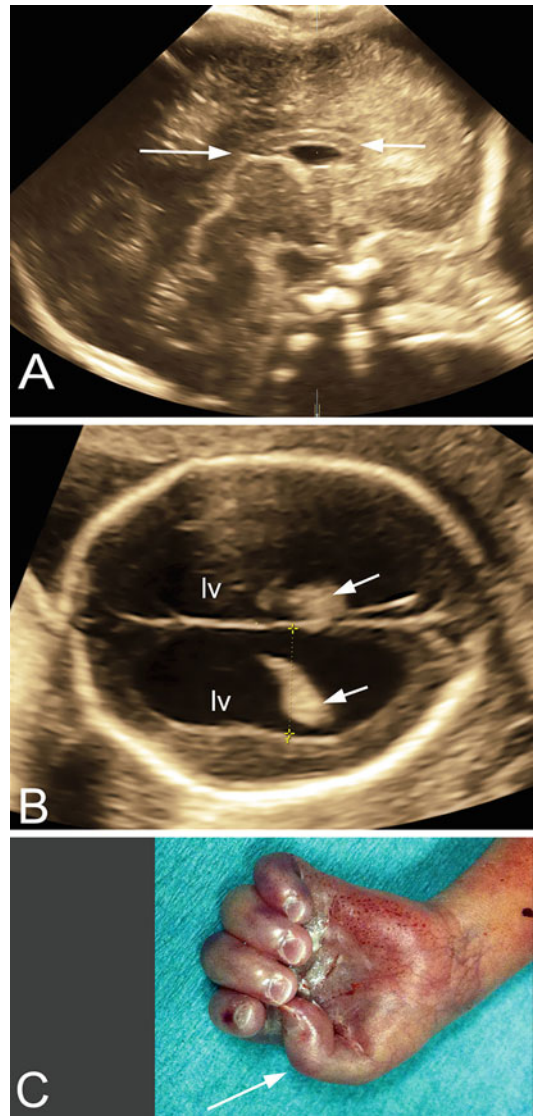

Fig. 37 L1 syndrome (MASA; CRASH, see text). (**a**) Twenty-eight-week-old fetus with partial agenesis of the corpus callosum (arrows). The family had positive history and genetic characterization of the mutation of the L1CAM gene responsible for the disease (see text); (**b**) another case in a family with positive history. At 21 weeks, there is typical bilateral ventriculomegaly (lv: lateral ventricles), with dangling choroid plexuses (arrows); (**c**) the typical adducted thumb on autopsy of the fetus shown in B after termination of pregnancy

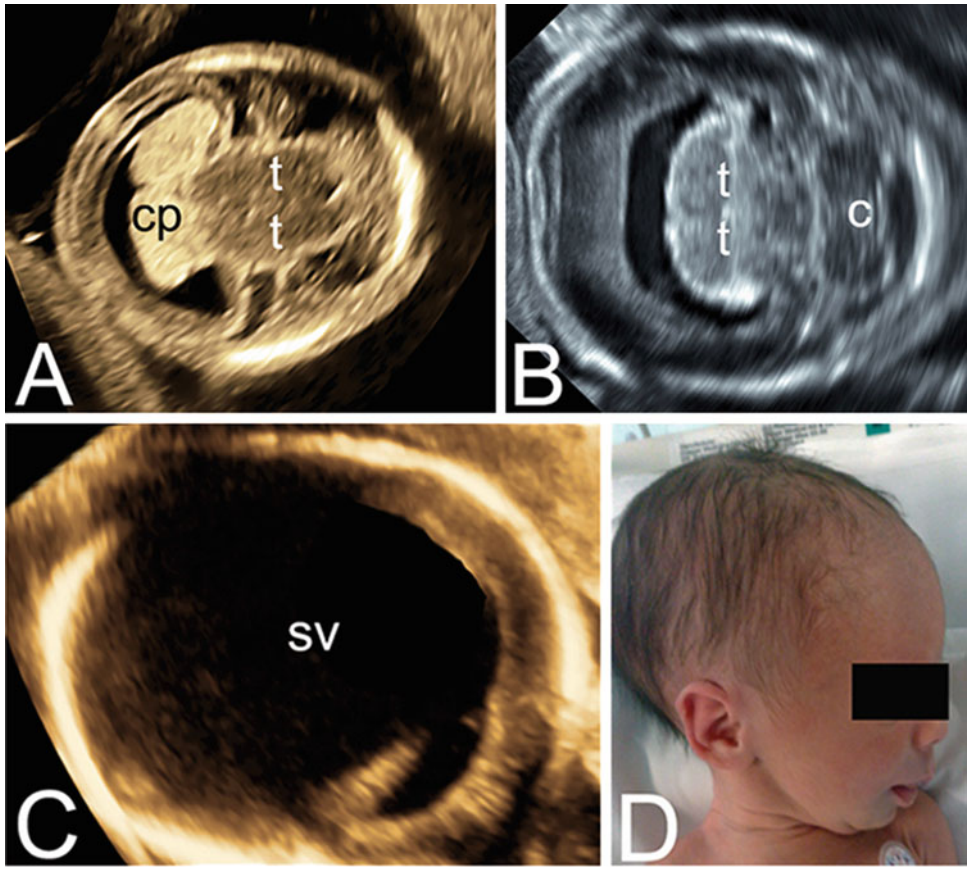

Fig. 38 Alobar holoprosencephaly. Note the single ventricular cavity in all cases. (**a**) Diagnosis at 13 gestational weeks (cp, single choroid plexus; t, thalami); (**b**) diagnosis at 19 gestational weeks (c, cerebellum; t, thalami); (**c**) a rare case seen at 29 gestational weeks (sv, single ventricle); (**d**) the neonate of the case C at birth. Note the macrocrania due to the large amount of cerebrospinal fluid in the single cavity

(Fig. 39). The most frequent facial anomalies are usually classified into the following types: cyclopia, with a single midline orbit or absent eyes; arhinia, with or without a proboscis; ethmocephaly, with evident ocular hypotelorism and a proboscis located between the eyes; cebocephaly, with less pronounced ocular hypotelorism and a nose with a single nostril; and a median cleft lip and palate, with premaxillary agenesis (Fig. 39).

Prenatal management includes amniocentesis for karyotyping and, if possible, cGH-Array, considering the wide range of microdeletions, duplications, and single-gene disorders that may be responsible for holoprosencephaly. Brain MRI has a limited role, considering the fact that, due to the severity of the prognosis, most couple opt for termination of pregnancy.

– *Agenesis of the corpus callosum*. The formation of the CC starts with the development of the genu; the body and splenium develop at a later stage. Due to this developmental sequence, in case of partial agenesis of the corpus callosum, usually the posterior portion is affected. On the other hand, if the CC is missing due to clastic events, such as CMV infection or tumors, any part of the commissure can be involved.

The etiology of ACC is very heterogeneous. Identified causes are chromosomal, monogenic, and teratogenic. Chromosomal abnormalities are present in 20% of cases,

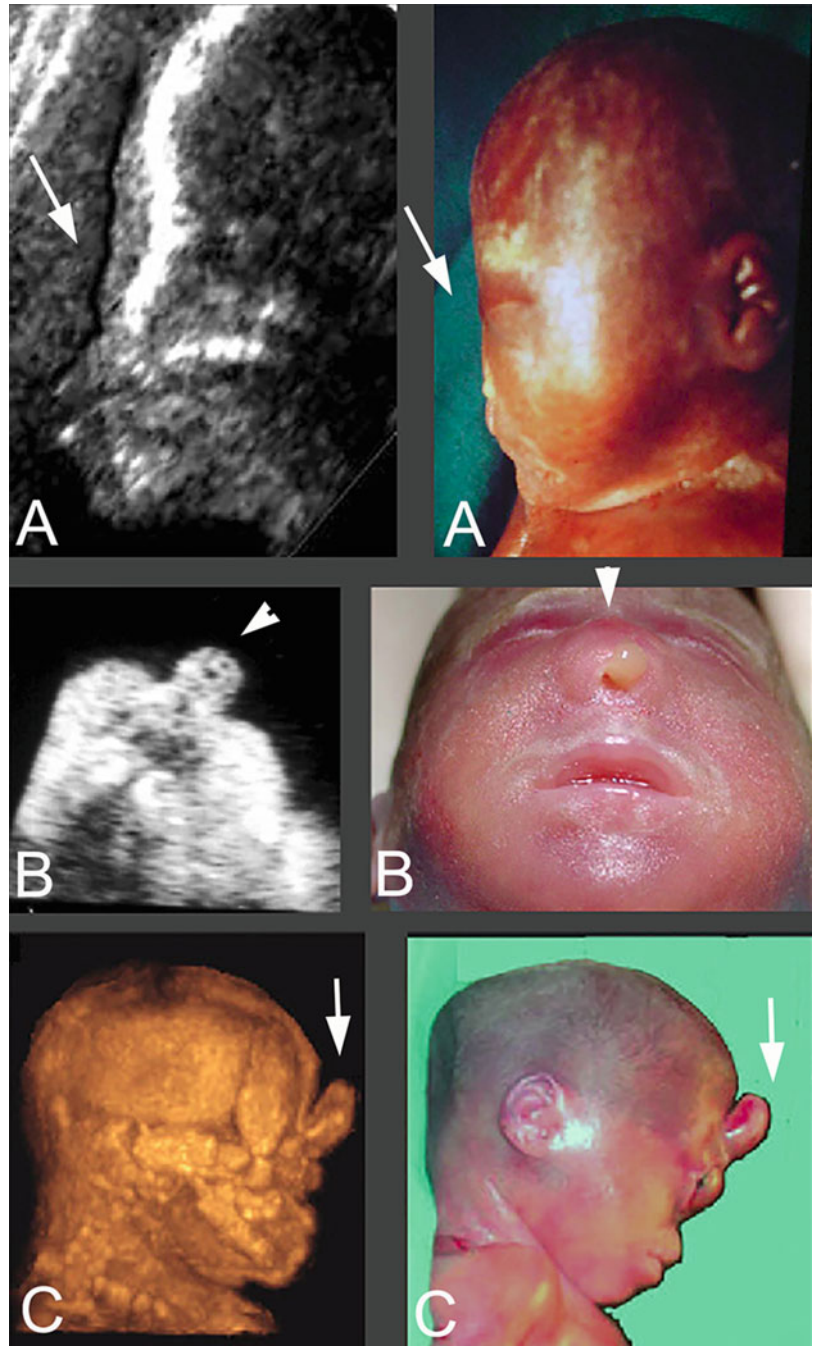

Fig. 39 Midline facial malformations in holoprosencephaly. (**a**) Ethmocephaly. Complete arrhythmia (arrow) at 22 gestational weeks, with necropsy confirmation; (**b**) cebocephaly. A single nostril (arrowhead) and very flat nose are evident. Note also the severe hypotelorism (specimen, on the right); (**c**) proboscis with arrhythmia and cyclopia (not evident due to the lateral view of the head) at 22 gestational weeks

especially trisomies 18 and 13. However, >100 syndromes involving ACC have been reported in the literature.

A pathogenetic classification of ACC takes into account the presence/absence of the so-called Probst bundles. Probst bundles are the misrouted callosal axons that run parallel to the interhemispheric fissure and do not cross the midline. ACC can then be basically classified into four categories: (1) ACC may be the result of earlier forebrain abnormalities blocking its development, e.g., holoprosencephaly or frontal

cephalocele; (2) ACC without Probst bundles, wherein this group includes those cases in which the overall neuronal population is decreased and, therefore, the Probst bundles cannot form, and it includes conditions such as cobblestone lissencephaly and Walker-Warburg syndrome; (3) ACC with Probst bundles, which is the typical and more common subtype of ACC; and (4) clastic ACC (Barkovich et al. 2009).

The suspicion of corpus callosum agenesis is raised commonly at the midtrimester scan due to non-visualization of the cavum septi pellucidi on the transventricular view (see above) and colpocephaly. Then, neurosonography is carried out, and the direct signs of ACC are detected. These include non-visualization of the CC on the midsagittal view of the fetal brain (Fig. 40a), abnormal shape of the frontal horns, and cranial displacement of the 3rd ventricle on the coronal view (Fig. 40b). An associated interhemispheric cyst may or may not be present (Fig. 40a, d). As far as secondary ventriculomegaly and colpocephaly, we have demonstrated that the teardrop dilatation of the occipital horns is often evident from 20 weeks but with near-normal atrial width; the atria becomes abnormally enlarged only by the end of the 2nd trimester in most cases, usually >24 gestational weeks (Paladini et al. 2013), with the degree of ventriculomegaly that may vary significantly. However, if severe ventriculomegaly is found in association with ACC, then the occurrence of other CNS malformations and/or syndromic conditions should be carefully evaluated (Fig. 41).

Associated CNS malformations are found relatively often, the most common of which are Dandy-Walker malformation (Fig. 40b), cortical malformations, and heterotopias.

– *Prenatal management* includes also in this case amniocentesis for karyotyping and, if possible, cGH-Array. In case of ACC, the latter is of overwhelming importance, considering that, on one hand, truly isolated ACC is associated with a good prognosis in the majority of cases (Mangione et al. 2011) while, on the other, several cases result eventually associated with microdeletions, duplications, and single-gene disorders (such as the L1 syndrome; see above). ACC represents one of the main indication to perform fetal brain MRI, because of the association, among other CNS defects, with gyration abnormalities that may escape, especially if involving the convexity of the hemispheres, sonographic diagnosis. As underlined in the dedicated section, fetal CNS MRI is recommended to be carried out >25 gestational weeks, ideally at 28–30 weeks, when its diagnostic performance is optimal, in comparison with earlier gestational ages (Paladini et al. 2014).

– *Dandy-Walker malformation (DWM)*. This anomaly represents the more obvious cystic malformation of the cerebellar vermis. In the fetus, the anatomic criteria to diagnose DWM are (1) complete or partial agenesis of the vermis, (2) cystic dilatation of the 4th ventricle that fills the posterior fossa and extends into the cisterna magna, (3) enlarged posterior fossa with upward displacement of the tentorium, and (4) upward rotation of the partial agenetic vermis (Barkovich and Kjos 1989).

The diagnosis of DWM and other cystic abnormalities of the posterior fossa cannot be made in the 1st trimester of pregnancy, due to the fact that the cerebellar vermis is still physiologically incomplete at that gestational age (see "Early Organization" subheading). In fact, the only evidence we have of posterior fossa and vermian abnormalities at 12–13 weeks of gestation is represented by a *cystic posterior fossa* (Fig. 42; Volpe et al. 2015). However, until now, the early sonographic differentiation of benign (e.g., Blake's pouch cyst) and less benign (DWM, vermian hypoplasia) conditions is impossible at that gestational age. From 16 weeks onward, there is the possibility to make a putative diagnosis; at 20–22 weeks, the differential diagnosis among the various conditions (DWM, vermian hypoplasia, Blake's pouch cyst, mega cisterna magna) can be reliably made in most of the cases (Figs. 43 and 44). The sonographic criteria for a differential diagnosis among the various entities are reported in Table 2 (Paladini et al. 2012;

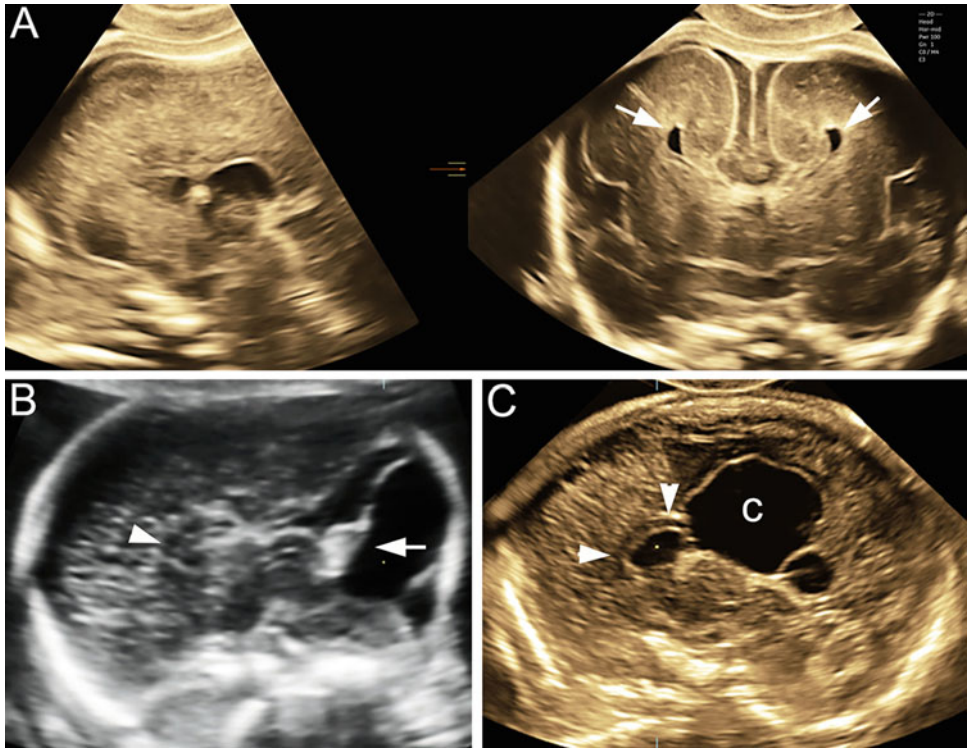

Fig. 40 Agenesis of the corpus callosum. (**a**) On the midsagittal view, the corpus callosum cannot be demonstrated; a dorsal cyst may be present, as in this case; (**b**) on the coronal view, the two frontal horns (arrows) are distorted (resembling *bullhorns* or a *bicycle handlebar*), and the cross section of the corpus callosum is not visible; (**c**) other CNS abnormalities can be associated with agenesis of corpus callosum. In this case, partial agenesis of the corpus callosum (arrowhead) was associated with Dandy-Walker malformation (arrow); (**d**) on other occasions, the dorsal cyst may be rather large, as in this case of partial agenesis (arrowheads point to the anterior portion of the corpus callosum which was present)

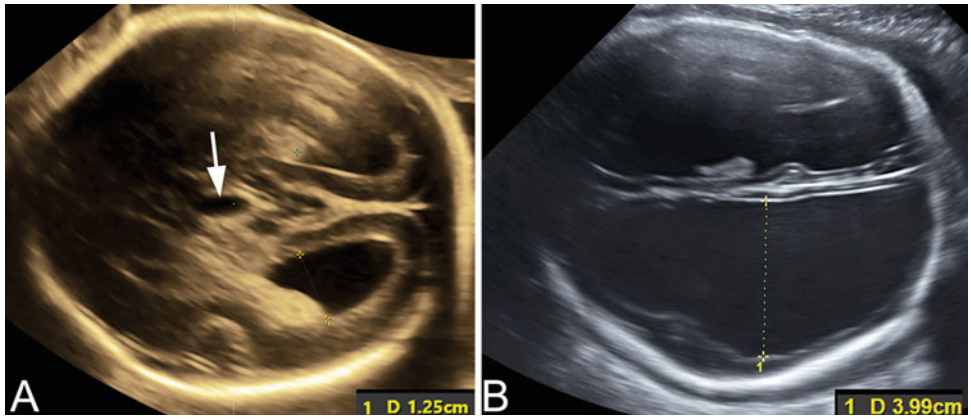

Fig. 41 Complete agenesis of the corpus callosum. (**a**) Colpocephaly with moderate ventriculomegaly progresses with advancing gestational age. In this case at 24 weeks, the atrial width was 12.5 mm. Note the 3rd ventricle (arrow) which is displaced upward due to the absence of the corpus callosum; (**b**) if the degree of ventriculomegaly is severe, then other anomalies should be present. In this case, the huge dilatation (39.9 mm) was due to the association with aqueductal stenosis

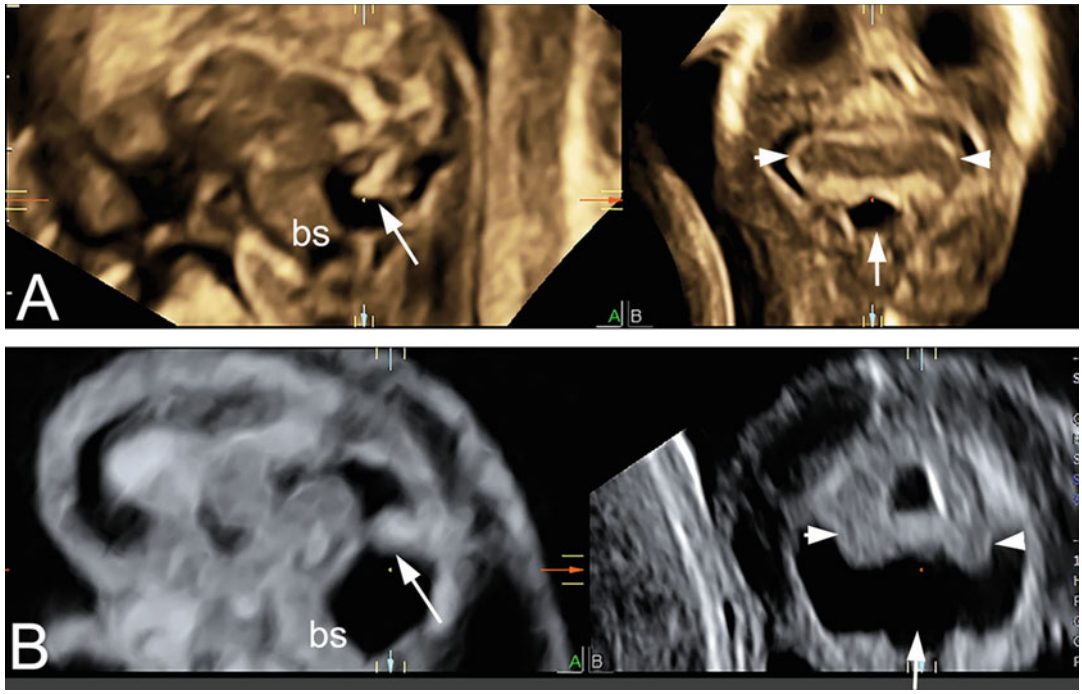

Fig. 42 The differential diagnosis of the cystic abnormalities of the cerebellar vermis cannot be carried out in the 1st trimester. In fact, at 12–13 weeks, only a larger posterior fossa can be detected. (**a**) Normal aspect at 13 weeks of gestation. On the left, the midsagittal view shows the brainstem (bs) and the small (normal) developing vermis (arrow). The amount of fluid in the cisterna magna is limited. On the corresponding coronal view, on the right, the cerebellum (arrowheads) and the 4th ventricle (arrow) are visible. (**b**) In case of "cystic posterior fossa," as evident both on the midsagittal plane (left) and on the coronal one (right), there is an increase in the amount of the fluid, but there is no way to differentiate between benign conditions (such as Blake's pouch cyst) and more severe ones (Dandy-Walker malformation or vermian hypoplasia) (coronal view, both cases, arrowheads, cerebellum; arrow, cisterna magna)

Paladini and Volpe 2006). As evident, obstructive ventriculomegaly may complicate some of these malformations. By definition, being the obstruction at the level of the 4th ventricle, in all these cases ventriculomegaly is tetraventricular (Fig. 43b).

DWM may be associated with chromosomal anomalies (mainly trisomy 18 and 13), other CNS, and extra-CNS malformations. Therefore, *prenatal management* includes also in this case amniocentesis for karyotyping and, if possible, cGH-Array. Prenatal MRI is rarely needed to confirm a diagnosis of DWM. However, in some cases in which there is a diagnostic doubt about vermian hypoplasia and Blake's pouch cyst, it may help, provided that it is carried out in the 3rd trimester, when the performance of MRI in the characterization of fetal CNS anomalies is highest (Paladini et al. 2014).

– *Blake's pouch cyst* (BPC or persistence). This entity has been described in the pediatric literature only 20 years ago (Tortori-Donati et al. 1996). Several years have passed before the same entity was recognized in the fetus (Paladini et al. 2012). In prenatal life, the diagnostic triad to diagnose BPC is (Fig. 45) (1) vermis has normal size; (2) there is anticlockwise rotation of variable degree; and (3) there is a cystic structure in communication with the 4th ventricle, which occupies the posterior fossa. In most cases, the cyst wall and the differential echogenicity of the cyst content (anechoic) versus the cisterna magna fluid (hypoechoic) is also evident. Interestingly, there is a striking difference among the two populations: in

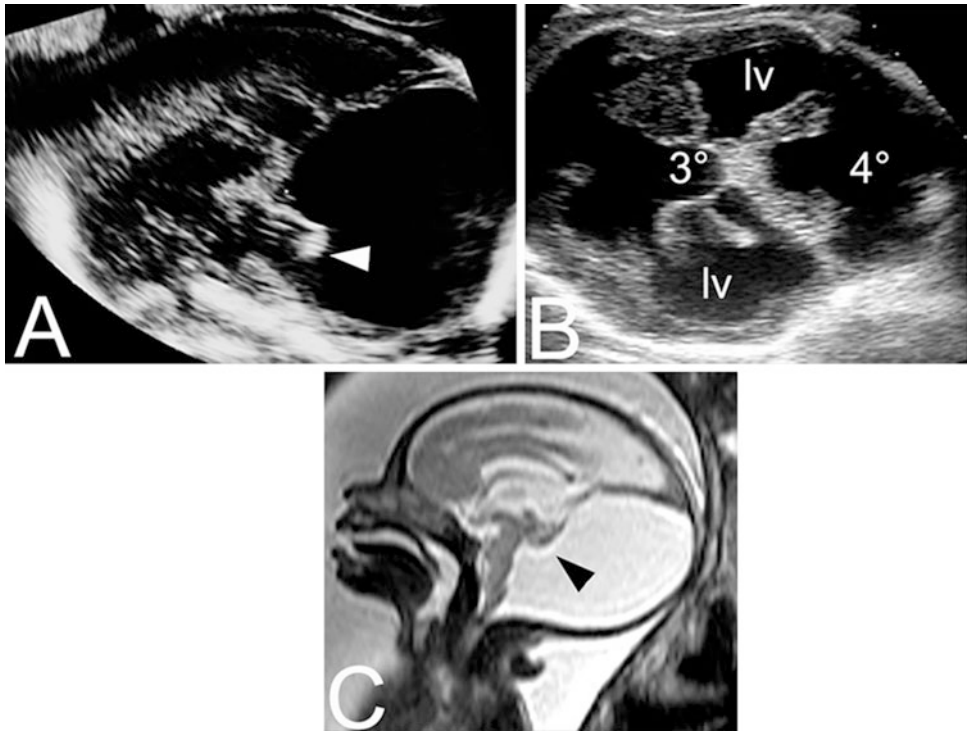

Fig. 43 Dandy-Walker malformation. (**a**) On the midsagittal plane, the extremely severe vermian hypoplasia is evident (arrowhead) as well as the pronounced anticlockwise rotation; also, there is a huge collection of fluid in the posterior fossa and the insertion of the tentorium is elevated; (**b**) in the 3rd trimester, obstructive tetraventricular hydrocephalus ensues in most cases. The image represents an axial plane showing the dilatation of the lateral ventricles (lv), the 3rd and 4th ventricles (3°; 4°); (**c**) MRI midsagittal T2 image confirming all the features shown in A on ultrasound. (Courtesy M. Quarantelli); in particular, the anticlockwise rotation and the vermian hypoplasia (arrowhead) are particularly evident

neonates and infants, BPC seems almost invariably associated with obstructive hydrocephalus (Tortori-Donati et al. 1996), whereas this is not happening in fetuses with such a diagnosis. Our perception is that after birth, only those cases resulting in obstructive hydrocephalus are referred and, hence, recognized as having a BPC, whereas the overwhelming majority in which there is an uncomplicated, asymptomatic BPC remain undiagnosed – at least before prenatal diagnosis was described. An interesting concept regards the patency of the Magendie and Luschka foramina and the timing of their opening. In fact, BPC may regress or disappear in the fetus at about 26 weeks of gestation (Paladini et al. 2012; Pinto et al. 2016), and this is the time of gestation when the Luschka foramina have been described to open (Brocklehurst 1969). We may speculate that if the BPC persists until birth, it can represent an unstable steady state which may be altered for whatever insult responsible for an increase in CSF production, such as inflammation or hemorrhage. In this case, the BPC might become responsible for obstructive hydrocephalus. In the remaining majority of cases, BPC remains silent and unknown if not for those cases with a prenatal diagnosis (Paladini et al. 2012; Pinto et al. 2016).

– *Rhomboencephalosynapsis (RES)*. In this rare pathological entity, the cerebellar vermis is

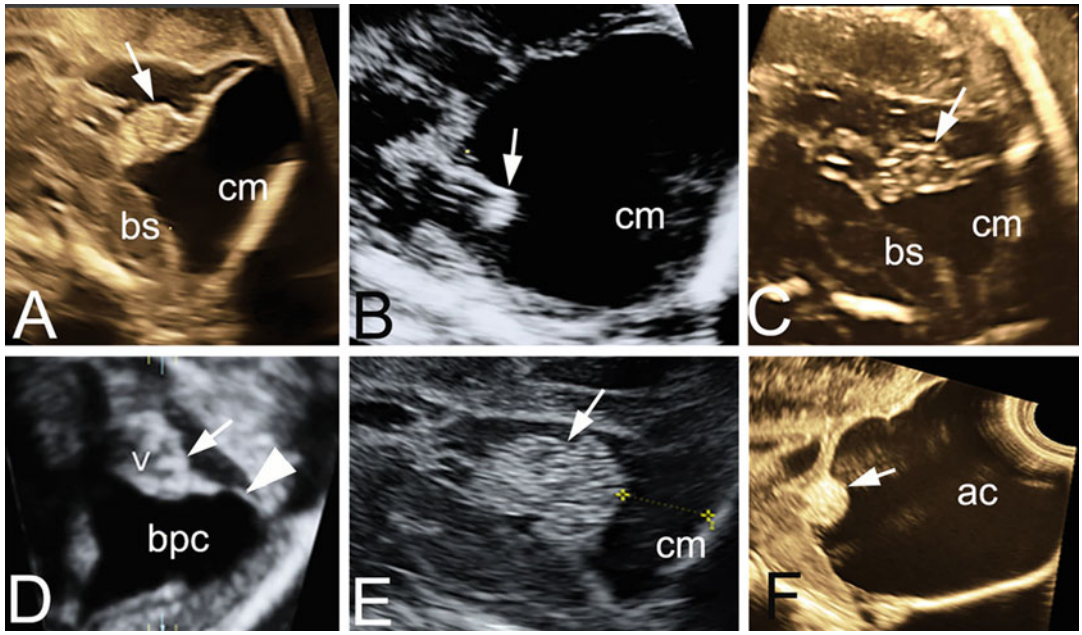

Fig. 44 Cystic abnormalities of the posterior fossa in the fetus. (**a**) Dandy-Walker malformation, 21 gestational weeks. The rotation and hypoplasia of the vermis (arrow) are evident; the cystic fluid collection in the cisterna magna (cm) is evident as well. Note also the high insertion of the tentorium and the wall of the cyst just behind the vermis; (**b**) another case of Dandy-Walker malformation, 29 gestational weeks. Note the differential aspect in relation to the same anomaly detected earlier in pregnancy (cfr with **a**); (**c**) vermian hypoplasia, 21 gestational weeks. In this case, the tentorium is normally inserted; the fluid collection and the anticlockwise rotation are less pronounced than in Dandy-Walker malformation (bs, brainstem; cm, cisterna magna). The key features are that the size of the vermis is smaller than normal, and the fastigium cannot be seen; (**d**) Blake's pouch cyst, 21 gestational weeks. In this case the anatomy as well as the size of the vermis (v) are normal (note the normal lobulation, arrow). The wall of the Blake's pouch cyst (bpc) is evident behind the vermis (arrowhead). Also in this pathological entity, there is a variable degree of anticlockwise rotation; (**e**) megacisterna magna, 27 gestational weeks. In this case, there is on rotation of the vermis. The only feature is an increase in the amount of fluid in the cisterna magna (>10 mm), with no apparent compression on the vermis (arrow, primary fissure). (**f**) Arachnoid cyst of the posterior fossa. In this case, unlike in megacisterna magna, there is evident compression on the cerebellar vermis (arrow). The cyst (ac) is also indenting the occipital bone posteriorly

completely absent, and there is fusion of the two cerebellar hemispheres on the midline. Kinking of the brainstem is often found in association. On prenatal ultrasound, the complete absence of the midline vermis is relatively easy to recognize (Fig. 46). In particular, at ultrasound, the cerebellar hemispheres are hypoechoic, while the vermis is hyperechoic, which leads to an easy differentiation between the two anatomical structures on an axial scan (Fig. 46c). At the same time, the absence of the vermis determines a pathological reduction in the transverse cerebellar diameter, which represents one of the basic measurements in obstetric screening ultrasound (Fig. 46c). On transvaginal neurosonography, the employment of higher-frequency transducers leads to a clearer demonstration of the anomaly (Fig. 46b). In case of RES, the occurrence of severe hydrocephalus is common and early onset and leads to referral also in those cases in which the actual infratentorial anomaly has not yet been recognized (Fig. 46c).

In the fetus, RES should be differentiated from cerebellar hypoplasia. In the former,

Table 2 Sonographic criteria for a differential diagnosis of posterior fossa cystic abnormalities in the fetus

Entity	Tentorium	Vermian size	ACW rotation	Ventriculomegaly
DWM	Elevated[a]	Severe hypoplasia	Pronounced	From 3rd trimester in 50% of the cases
Vermian hypoplasia	Normal	From moderate to severe hypoplasia	From moderate to pronounced	Absent
Blake's pouch cyst	Normal	Normal[b]	Usually moderate but may also be pronounced	Absent[c]
Mega cisterna magna	Normal	Normal	Absent	Absent
Arachnoid cyst	Normal	Normal[d]	Absent	Absent[e]

[a]Based on US criteria, occipital muscles' insertion cannot be assessed
[b]Sometimes, compression from the cyst may lead to suspicion of vermian hypoplasia
[c]Absent in all prenatal cases reported so far; in postnatal life, it is described as common occurrence
[d]Sometimes, compression from the cyst may lead to suspicion of vermian hypoplasia
[e]Ventriculomegaly may develop due obstruction in case of large cysts

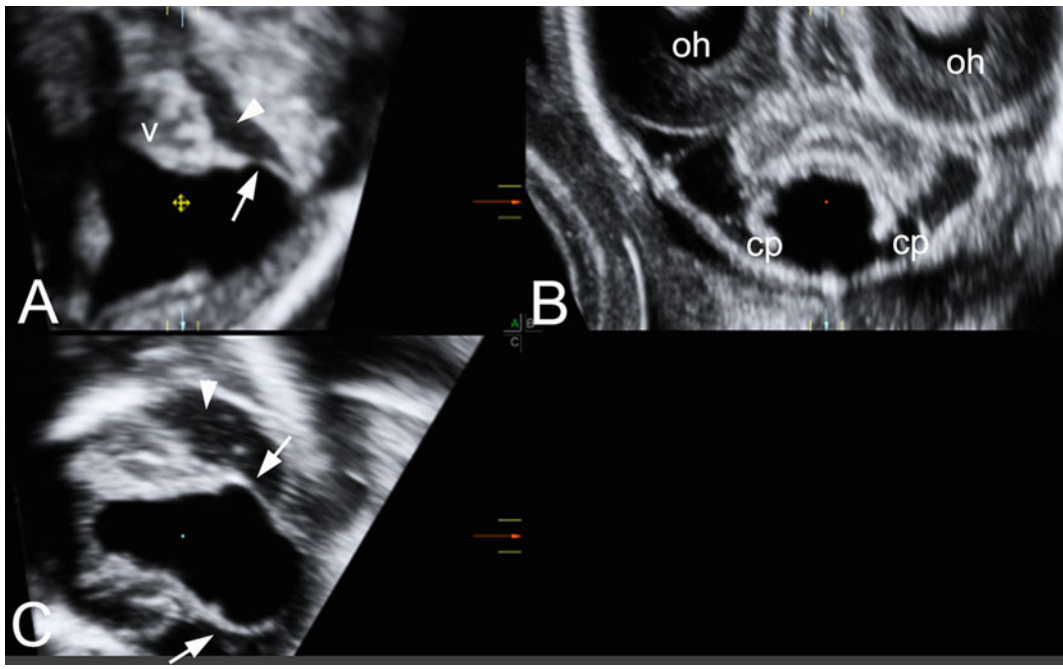

Fig. 45 Blake's pouch cyst (persistence), 22 gestational weeks. The diagnostic features are (**a**) normal vermis size, (**b**) variable anticlockwise rotation of the vermis, and (**c**) presence of a cystic structure in communication with the 4th ventricle, which occupies the posterior fossa. In most cases, the cyst wall and the differential echogenicity of the cyst content (anechoic) versus the cisterna magna fluid (hypoechoic) are also evident (arrows, cyst walls; arrowheads, hypoechoic content of the cisterna magna; cp, choroid plexus of the 4th ventricle; oh, occipital horns; v, cerebellar vermis)

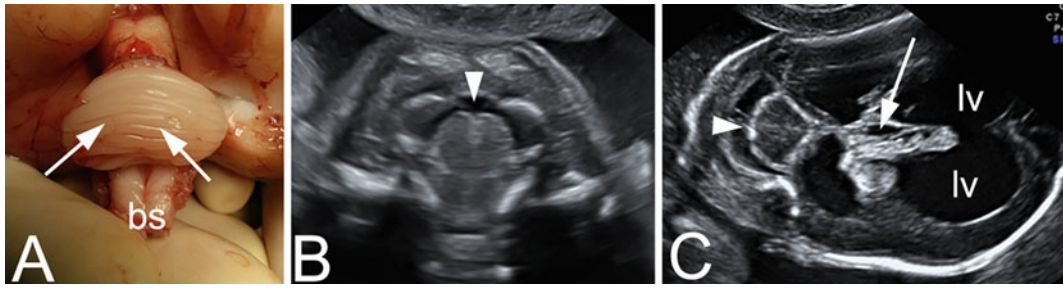

Fig. 46 Rhomboencephalosynapsis. (**a**) Twenty gestational weeks' specimen showing fusion of the cerebellar hemispheres and complete absence of the vermis in the middle (arrows) (bs, brainstem). (**b**) On transvaginal high-resolution imaging, the midline fusion (arrowhead) of the two hypoechoic hemispheres with no evidence of the hyperechoic vermis is easy to demonstrate; (**c**) on the transabdominal axial trans-cerebellar plane, the small diameter of the cerebellum, its abnormal shape (arrowhead), and the obstructive hydrocephalus often associated are shown (arrow, dilatation of the 3rd ventricle; lv, lateral ventricles)

the vermis is absent, and, often, the cerebellum shows a triangular shape; in the latter (cerebellar hypoplasia), the sonographic appearance of the cerebellum is not modified, but the whole organ is significantly hypoplastic.

– *Diencephalosynapsis*. This is an extremely rare anomaly, in which there is failure of diencephalic cleavage; in particular, it is characterized by partial or complete fusion of the thalami associated with third-ventricle atresia (Cagneaux et al. 2013). In most cases, this condition is associated with severe cerebellar hypoplasia or, in some cases, RES. This is due to the fact that the mechanism behind the failed diencephalic cleavage extends to the mesencephalon, leading to mesencephalosynapsis. In this case, by definition, there is obstructive triventricular hydrocephalus, which is early onset and associated, in several cases, with early-onset macrocephaly. At ultrasound, the striking features are represented by cerebellar hypoplasia and early-onset severe ventriculomegaly (Fig. 47). Even if the cerebellar anomaly is overlooked at screening, the latter always triggers referral to experts because of the severity of the ventricular enlargement.
– *Malformations of cortical development*. This covers a wide spectrum of developmental and genetic anomalies. In pregnancy, the two main features are that they are *late-onset* anomalies, because they are in general virtually unrecognizable in the 2nd trimester of pregnancy, and that mild ventriculomegaly may be associated. It is thought that in this type of malformation, ventriculomegaly represents a passive filling of volumes that are not filled with neurons.

Ventriculomegaly Secondary to Acquired CNS Lesions

Ventriculomegaly – as well as obstructive hydrocephalus – may also develop as a complication of brain insults occurred during gestation. There are two pathogenetic mechanisms that may lead to ventriculomegaly in acquired lesions: either obstruction of the ventricular system (e.g., hemorrhage, tumors) or destruction of brain parenchyma close to the ventricular system followed by cavitation and filling with CSF (e.g., porencephaly, schizencephaly). Space-occupying lesions, such as arachnoid cysts, tumors, but also hemorrhage, and all those conditions associated with significant distortion of the brain anatomy are those in which fetal MRI is more helpful in reaching the final diagnosis, in comparison with neurosonography (Paladini et al. 2014). In this study, 773 cases of fetal brain malformations underwent neurosonography, and an MRI was requested as second diagnostic step in 126 (16.3%). In this subgroup of cases, MRI

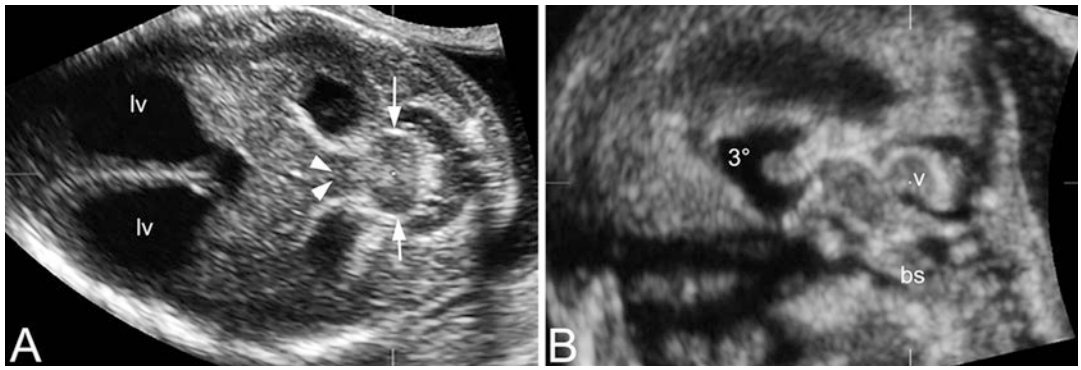

Fig. 47 Diencephalosynapsis. In this exceedingly rare malformation complex, there is severe cerebellar hypoplasia and atresia of the Sylvian aqueduct. (**a**) 18 weeks fetus. On the axial plane, severe cerebellar hypoplasia (arrows), fusion of the diencephalon with aqueductal atresia (arrowheads), and severe early-onset obstructive hydrocephalus (lv, lateral ventricles) are visible; (**b**) on the midsagittal view, the dilatation of the 3rd ventricle (3°) and the hypoplasia of the vermis (v) and the brainstem (bs) can be seen

provided additional clinically relevant information in three of seven space-occupying lesion undergoing both neurosonography and MRI. This finding demonstrates that when the degree of brain anatomy distortion is high, MRI performs better than neurosonography, especially if MRI is performed in the 3rd trimester.

– *Cerebral hemorrhage*. This event may occur spontaneously or be due to underlying causes that make the vessels bleed. The most common etiology is *fetomaternal alloimmune thrombocytopenia* (FMAIT), which is the prenatal counterpart of the neonatal alloimmune thrombocytopenia. FMAIT is due to the maternal production of antibodies against paternal antigens (usually HPA-1a, less frequently HPA-1b – Paladini et al. 2005) present on fetal platelets that are not recognized by the maternal immune system. Maternal exposure to these antigens during pregnancy can lead to the production of various classes of immunoglobulins: the IgG antibodies are small enough to cross the placental barrier and enter the fetal circulation, causing severe thrombocytopenia. Unlike hemolytic disease of the newborn, FMAIT can also occur in the first pregnancy, if there is parental incompatibility. The importance of recognizing this etiology of fetal cerebral hemorrhage lies in the fact that it can be effectively treated, if disclosed prior to the hemorrhagic episode, with intravenous immunoglobulins and intrauterine transfusion of compatible platelets. More rarely, cerebral hemorrhage may be due to vascular malformations (e.g., vein of Galen aneurysm) or infection (e.g., CMV).

The severity of the hemorrhage is classified into four grades (Garel 2004): *Grade 1* (Fig. 48a), the hemorrhage is limited to the germinal matrix; *Grade 2*, the hemorrhage diffuses from the matrix into the ventricle, which fills up with blood without distension; *Grade 3* (Fig. 48b–d), the hemorrhage distends the ventricles; and *Grade 4* (Fig. 48e), there is extension of the hemorrhage to the parenchyma. In this case, when the necrotic areas clear up, they fill with CSF becoming porencephalic cysts (Fig. 48f). These are in communication with the ventricular system through disrupture of the ependymal lining. In Grades 2–4, the obstruction of the Sylvian aqueduct by debris and clots may lead to obstructive bi- or triventricular hydrocephalus (Fig. 48b–d). On rare occasions, posthemorrhagic membranes may obstruct selectively of one of the Monro foramina leading to progressive and severe unilateral ventriculomegaly (Fig. 49). Sonographic follow-up should be warranted, in order to assess the progression of the hemorrhage and the onset of complications. In fact, both progression of the same bleeding and

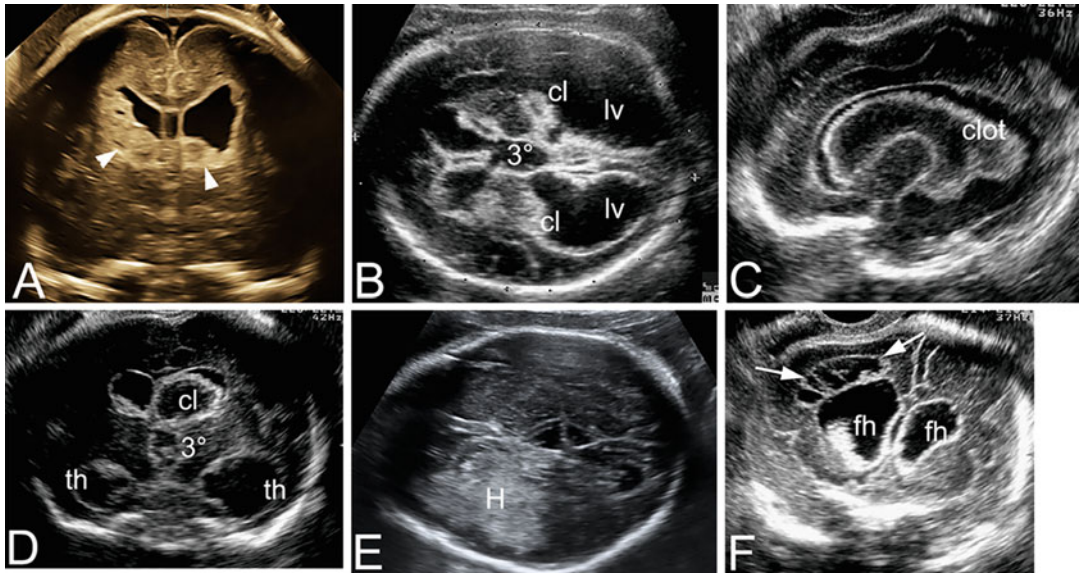

Fig. 48 Cerebral hemorrhage. (**a**) Grade I, involvement of the germinal matrix only (arrowheads). Coronal view, 28 weeks of gestation; (**b**) grade III, axial view showing dilated lateral ventricles (lv), with a clot visible (cl) and of the 3rd ventricle (3°). Debris is evident along the ependymal lining. Axial view, 30 gestational weeks; (**c**) same case as **b**. The parasagittal view shows the cast-like clot in the lateral ventricle; (**d**) grade III: another case showing a large clot in the lateral ventricle and the 3rd ventricle (th temporal horns). Coronal view, 31 gestational weeks; (**e**) grade IV: intraparenchymal hemorrhage (H), evident on an axial view at 32 gestational weeks; (**f**) porencephalic cyst (arrows), developing after the intraparenchymal clot liquefies. Note the residual strands of fibrin/clot in the cyst, which is in communication with the ventricular system (fh: frontal horns)

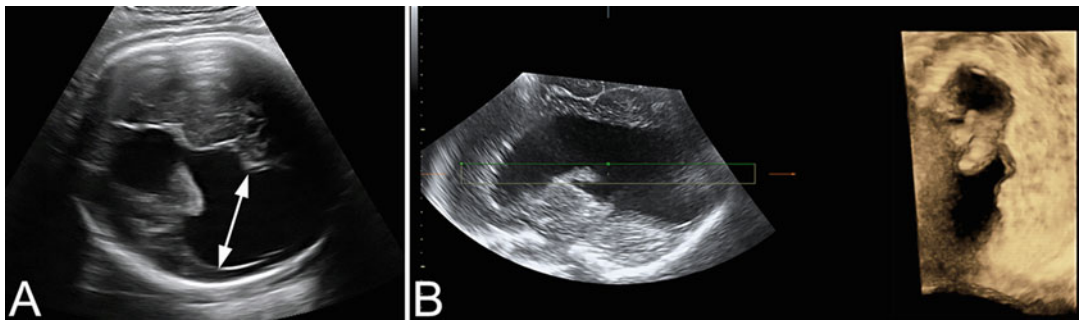

Fig. 49 Cerebral hemorrhage. In rare cases, after the initial hemorrhagic event, the clot seals selectively one foramen of Monro only. In this case, ventriculomegaly is unilateral, as demonstrated in this case at 35 weeks. (**a**) On the axial transventricular view, unilateral severe ventriculomegaly is evident (double arrow), with apparently no residual debris or clot in the ventricle; (**b**) on three-dimensional surface reconstruction, the dilatation of the ventricle and the dangling choroid plexus are demonstrated

recurrent bleedings have been documented, and these events are unpredictable. This is why in case of fetal cerebral hemorrhage, scans should be arranged at 3–4 days' intervals for the first week after the initial diagnosis and then biweekly. Only in this way, it will be possible to keep track of the progression of the lesion. The final prognosis will depend on the cause, the extent, and the location of the hemorrhage.

Hemorrhages from CMV infection have a typical parenchymal location, because they are

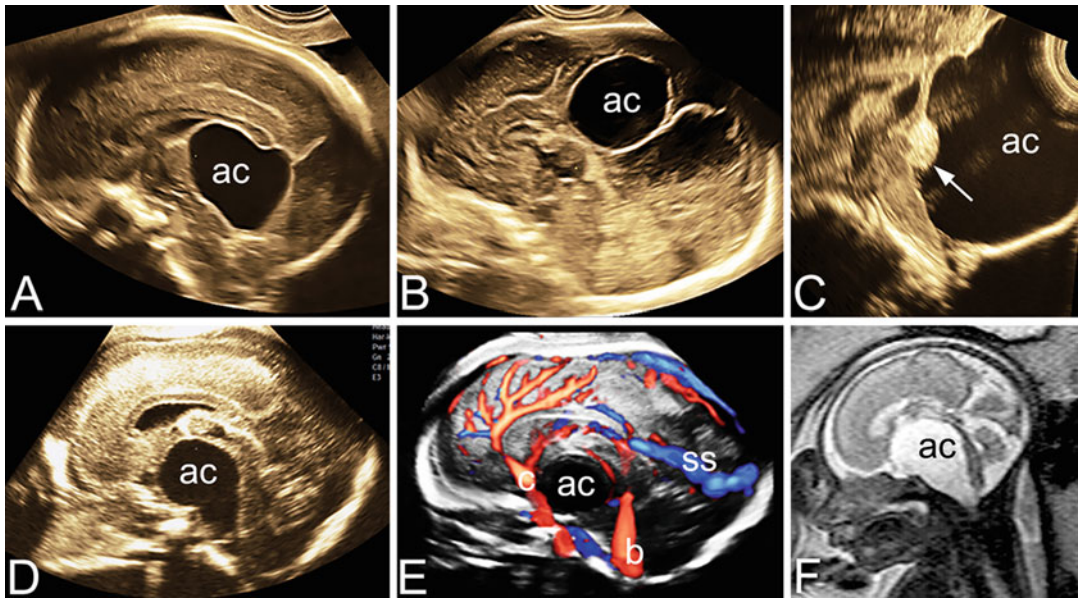

Fig. 50 Arachnoid cysts (ac) can occur in various sites. (**a**) Quadrigeminal plate. This is the one of the most likely to be obstructive because it can compress the Sylvian aqueduct, located just below the cyst; (**b**) interhemispheric; (**c**) posterior fossa; (**d**) supra-pontine; (**e**) same as **d**, with three-dimensional demonstration of the circulation (b, basilar artery; c, internal carotid artery; SS, straight sinus). Note also the pericallosal artery and the superior sagittal subdural sinus; (**f**) same case as E–F: MRI confirmation. (Courtesy M. Quarantelli)

probably due to vasculitis which may lead to local endothelial necrosis everywhere in the brain. Most common locations are parietal and cerebellar.

– *Arachnoid cyst*. Also arachnoid cysts are *late-onset* lesions in most of the cases. They can be responsible for parenchymal compression but also for compression on the ventricular system which leads to obstructive hydrocephalus (Fig. 50). Those located on the quadrigeminal plate or in the posterior fossa are more likely to obstruct the ventricular system leading to hydrocephalus. However, in rarer instances, arachnoid cysts may be found in severe syndromic conditions, such as Seckel syndrome. In this case, the arachnoid cysts are associated with other severe CNS malformations, such as ACC or gyration abnormalities, microcephaly, short limbs, and a typical facial appearance which is named *bird-headed dwarfism* (Fig. 51; Napolitano et al. 2009).
– *Cerebral arteriovenous malformations (including the vein of Galen)*. Also these lesions are in most of the cases appearing only in the 3rd trimester, with a limited number of them being diagnosed at the 20-week anomaly scan (Fig. 52). Even though the vein of Galen aneurysmal malformations account for <1% of all intracranial arteriovenous malformation, they represent the most common arteriovenous malformations detected prenatally. VGAM results from an arteriovenous connection between the primitive choroidal vessels and the median prosencephalic vein of Markowski, occurring between the 6th and 11th weeks of gestation. This leads to abnormal flow, preventing involution of the embryonic vein and subsequent development of the aneurysmatic dilatation of the vein of Galen. Prenatal diagnosis is usually made during the 3rd trimester, with color Doppler ultrasonography demonstrating turbulent arterial and venous flow within a hypoechogenic structure located in the midline of the posterior part of the 3rd ventricle (Deloison et al. 2012). On transvaginal neurosonography, the whole architecture of the vascular malformation can be studied

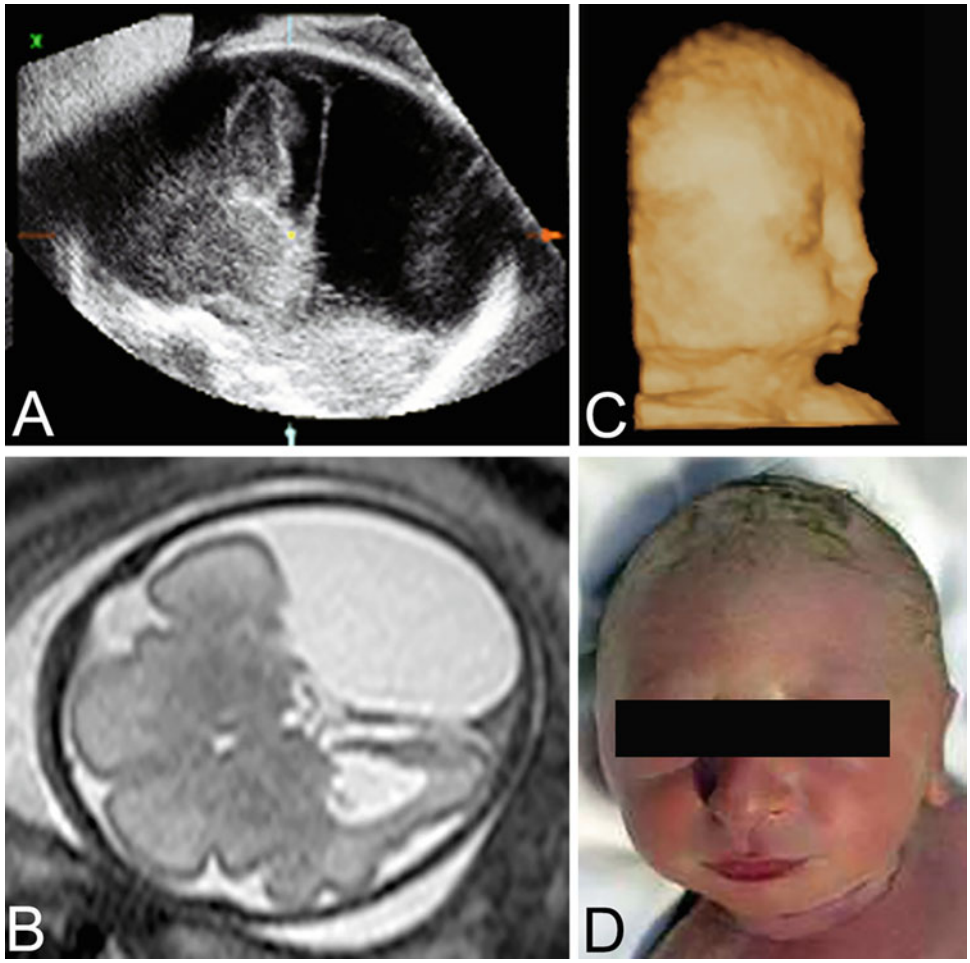

Fig. 51 Seckel syndrome. An arachnoid cyst may also be found in rare syndromic conditions. In Seckel syndrome, huge arachnoid cysts ((**a**) midsagittal sonographic view; (**b**) axial MRI view – courtesy M. Quarantelli) are associated with gyration anomalies (**b**), micrognathia (**c**), and a small head and face (**c**, **d**), which justifies the misnomer of *bird-headed dwarfism* given to this condition

with three-dimensional color/power Doppler (Figs. 52 and 53); at the same time, associated anomalies, such as ventriculomegaly, hemorrhage, or parenchymal necrosis, can be diagnosed, in order to make a prognostic evaluation (Fig. 54). MRI represents a must in this assessment, because it is able to detect better than ultrasound ischemic necrotic lesions also in the initial stage, unlike ultrasound. In fact, the perinatal mortality for this anomaly is high. Causes of death are cardiac decompensation from high-output cardiac failure (due to the arteriovenous fistula) and secondary brain lesions, including hemorrhage, necrosis, etc. A study reporting the largest number of fetal cases of VGAM which is going to be published shortly has shown that the most important poor prognostic signs are represented by severe tricuspid regurgitation and an aneurysmal volume $\geq$ 20 ml. In this setting, ventriculomegaly may be caused by obstruction or hemorrhage. In the former instance, it can regress after endovascular treatment of the VGAM; if due to hemorrhage, it obviously requires a surgical approach for treatment.

– *Tumors*. Also cerebral tumors represent *late-onset* lesions in most cases. It is quite rare to see brain tumors arising in the 2nd trimester (Fig. 55). In most cases, they appear in the 3rd trimester and, if malignant or locally invasive, progress rapidly, with secondary obstructive ventriculomegaly, parenchymal destruction, and macrocrania (Fig. 56). In this case, the prognosis is dictated by histology of the tumor and its location (Vassallo et al. 2012).
– *Schizencephaly* is characterized by the presence of abnormal clefts in the areas of the cerebral mantle that separate the lateral ventricles from the subarachnoid spaces. Clefts are lined by dysplastic gray matter, so that a loss of substance due to acquired causes, such as encephaloclastic porencephaly, can be ruled out. Schizencephaly can be uni- or bilateral, symmetric or asymmetric. Up to 50% of cases are bilateral; when bilateral, 60% are "open lipped" on both sides. Of the two types of schizencephaly, "closed-lip" schizencephaly shows very thin clefts (fused clefts), while open-lip schizencephaly has clefts filled with CSF and is often associated with ventriculomegaly. Schizencephaly is a malformation secondary to abnormal postmigrational development and is thought to be related to a vascular disruption process; in fact, in a significant proportion of cases, other non-CNS anomalies possibly related to a vascular insult have been found (e.g., gastroschisis, bowel atresia).

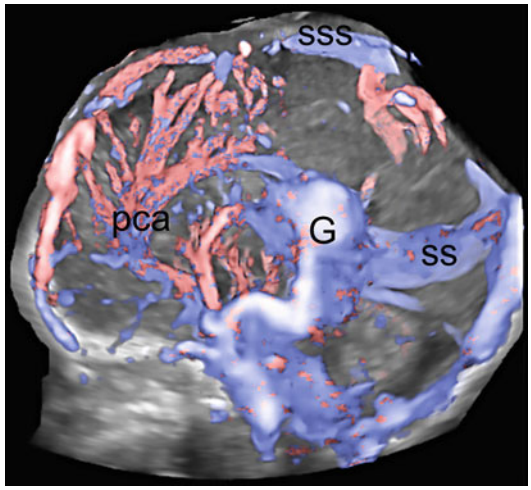

Fig. 52 Vein of Galen malformation. On rare occasions, the aneurysmal malformation is already present at mid-gestation, as in this 21-week-old fetus. Three-dimensional power Doppler, midsagittal plane. The aneurysm of the vein of Galen (G) is evident, as is the dilatation of the straight (ss) and superior sagittal sinuses (sss). The arterial feeder arteries are from the pericallosal (pca) group

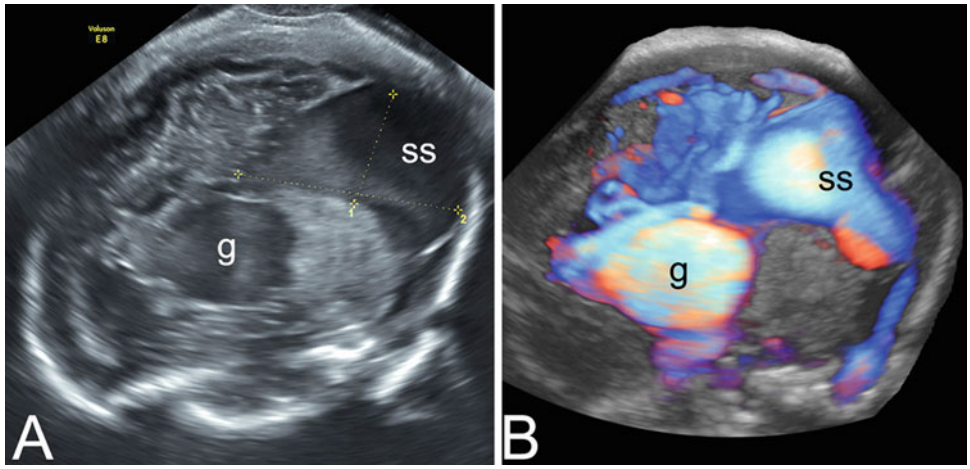

Fig. 53 Vein of Galen malformation. Classic onset is in the 3rd trimester, as in this 32-week-old fetus. (**a**) On transvaginal ultrasound, the midsagittal view shows the severe dilatation of the ampulla (G) and, especially, of the straight sinus (ss); (**b**) on three-dimensional power Doppler, the same findings are more clearly visible (g, Galen ampulla; ss, straight sinus)

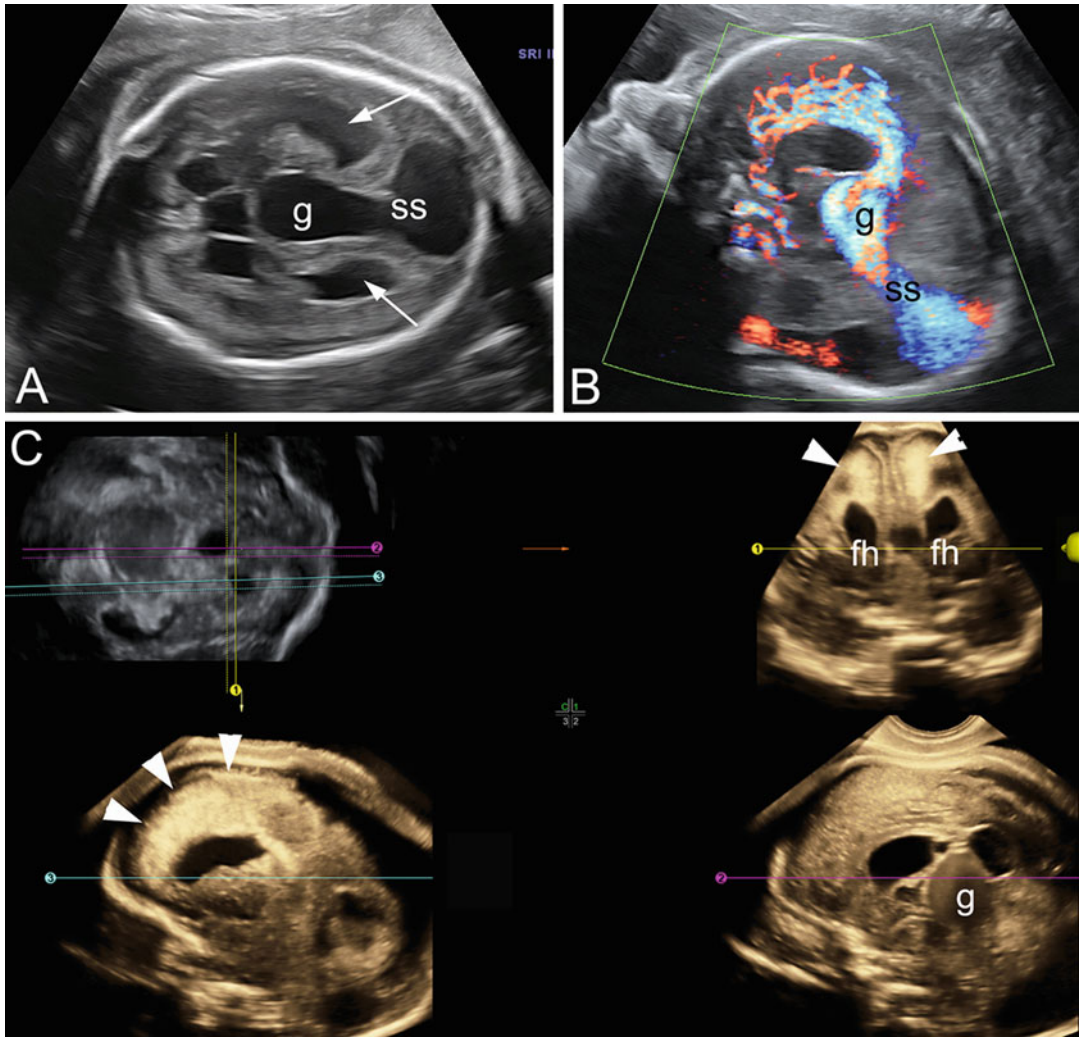

Fig. 54 Vein of Galen malformation. Associated lesions which represent poor prognostic signs include (**a**) ventriculomegaly (arrows, bilateral ventriculomegaly, from compression; g, Galen aneurysm; ss, dilatation of the straight sinus); (**b**) power Doppler midsagittal view demonstrating the vascular lesion already shown in **a**; and (**c**) multiplanar image correlation, showing severe necrotic (hyperechoic) lesions (arrowheads) at the level of the frontal and temporal lobes (fh, frontal horns; g, aneurysm of the vein of Galen)

On ultrasound, only the open-lipped form of schizencephaly can be diagnosed. The diagnosis is made when a CSF-filled cleft of one or both cerebral hemispheres that extends from the subarachnoid spaces to the lateral ventricles is found (Figs. 57 and 58). The lateral ventricles are often dilated and clearly visible on the transventricular plane. Schizencephaly involves more commonly the Sylvian fissure, and in this case it is often associated with septo-optic dysplasia. In the fetus, the most difficult differential diagnosis is with a large porencephalic cyst of the Sylvian fissure (Fig. 59). The aspect and the shape of the cystic lesion might in some cases lead to the correct diagnosis: schizencephaly is wedge-shaped or triangular, whereas poroencephalic cysts tend to be rounder.

On ultrasound, the diagnosis of schizencephaly is very simple: there is a huge

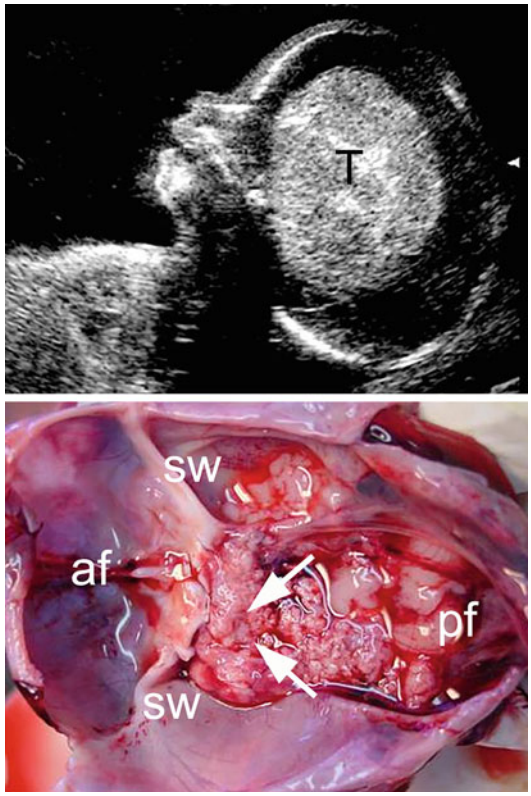

Fig. 55 Craniopharyngioma. Cerebral tumors generally arise in the 3rd trimester. On very rare occasions, they can present already at 22 weeks. This is a case of an aggressive craniopharyngioma detected at 22 gestational weeks. Ultrasound shows the huge mass which occupies most of the brain. On necropsy, the origin of the tumor from the Rathke's pouch (arrows) was confirmed (af, anterior cranial fossa; pf, posterior cranial fossa; sw, sphenoidal wing)

collection of CSF filling virtually the whole cranial cavity, with no recognizable cortex. The falx is usually present, though it may be eccentrically positioned; the thalami, basal ganglia, brainstem, and cerebellum may be normal, because the vascular insult usually involves the telencephalic portion of the brain (Figs. 57 and 58). In most cases, there is significant macrocrania.

– *Porencephaly.* The term "porencephaly" includes every type of lesion with cavitary character, that is, a fluid-filled area within the brain that usually communicates with the ventricles and, on very rare occasions, with subarachnoid spaces or both. It involves destruction of previously developed brain tissue, with subsequent cavity formation. It may be isolated or associated with ventriculomegaly. It is usually classified in two subtypes: *type I* is due to parenchymal damage followed by liquefaction/reabsorption (encephaloclastic porencephaly), resulting from an insult (ischemia, hemorrhage, etc.); *type II* (schizencephalic porencephaly) is completely cystic with a smooth wall. It is the less frequent type.

On ultrasound, porencephaly appears as a unilateral cystic lesion, usually communicating with the ipsilateral ventricle and/or the subarachnoid space. Due to destruction of brain tissue, it does not cause any mass effect. If the cyst is the result of a former parenchymal hemorrhage, debris from the clot liquefaction can be seen along the walls of the cyst (Fig. 48f). The final prognosis will obviously depend on the underlying etiology, the extent, and the site of the parenchymal destruction.

Ventriculomegaly Secondary to Open Spinal Dysraphisms

The prenatal sonographic approach to the examination of the normal and abnormal fetal spine has been thoroughly reported in another textbook (Paladini 2008). The reader interested in this type of defect and its evidence in the fetus may refer to that publication. Here, we report a brief summary of the basic and advanced evaluation of the fetal spine, in relation to the diagnosis of spinal dysraphisms, the related Chiari II malformation, and ventriculomegaly.

Until a few decades ago, the prenatal detection rate of spina bifida was relatively low and was based mainly on serum screening (alpha-fetoprotein). The low detection rate for spina bifida on screening ultrasound was due to the fact that it is often difficult or impossible to obtain a diagnostic view of the fetal spine

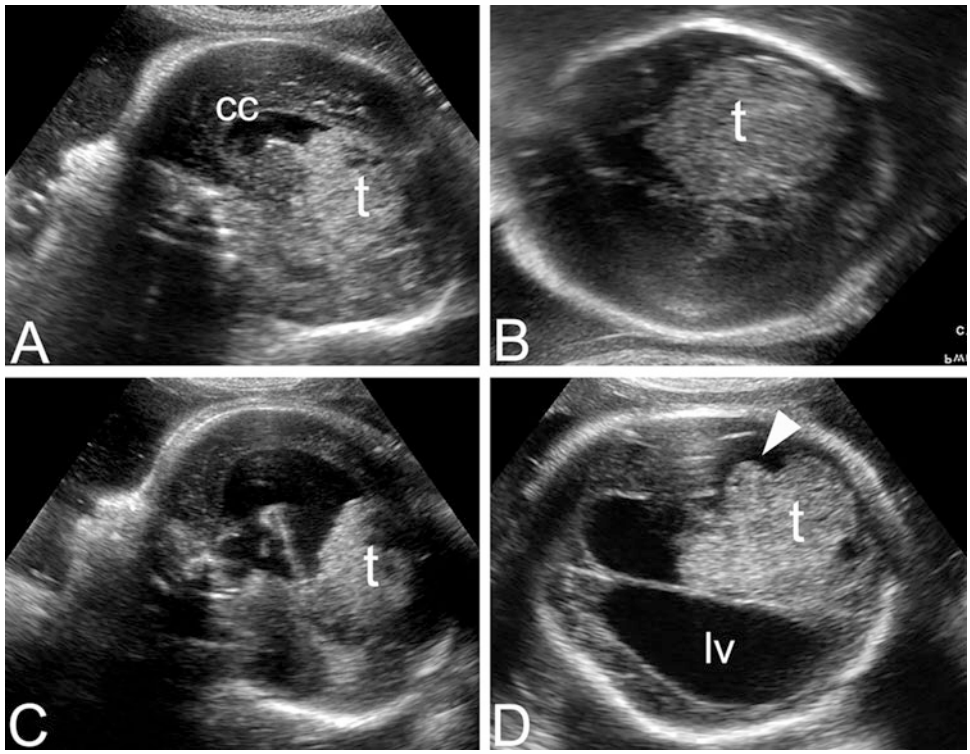

Fig. 56 Papillocarcinoma. The lesion was detected at 35 weeks. (**a**) On the midsagittal view, the large infiltrating tumor (t) is visible. At the same time, the corpus callosum (cc) and the cavum septi pellucidi show a normal appearance; (**b**) on the axial view, the large mass (t) is seen, with no overt ventriculomegaly; (**c**) 10 days after the initial evaluation, at 37 weeks, frank obstructive hydrocephalus is seen. Note the dilatation of the lateral ventricle which displays the midline (t: tumor); (**d**) on the axial view, the fast progression of the ventriculomegaly is evident. Also, the ventricular dilatation demonstrates that, indeed, the tumor (t) is located within the ventricle (arrowhead, papillocarcinoma) (lv: lateral ventricle) (Vassallo et al. 2012)

because the fetus often lies with its back along the uterine wall and this makes a detailed assessment of the fetal spine challenging or impossible. Only after the recognition that indirect endocranial signs were present in >97% of cases of open spina bifida did the detection rates increased significantly (Bahlmann et al. 2015; Nicolaides et al. 1986). The *indirect signs* of spina bifida are those related to the Chiari II malformation. This malformation is characterized by a small posterior fossa associated with downward displacement of a dysmorphic vermis, the brainstem, and the 4th ventricle into the foramen magnum or even into the cervical spinal canal. The ultrasound diagnosis of the Chiari II malformation is based upon the recognition of a series of signs including (Fig. 60): obliteration of the cisterna magna; dysmorphic and dysplastic cerebellum featuring an abnormal anterior curvature (banana sign); frontal scalloping, which is responsible for the lemon sign; and moderate-to-severe ventriculomegaly. The frontal bossing (lemon sign) develops early, is inconstantly present (50% of the cases), and is lost in most cases by 22–24 weeks. On the contrary, obliteration of the cisterna magna and the cerebellar banana sign are the most sensitive features, with the percentage of false positives being <3% (Bahlmann

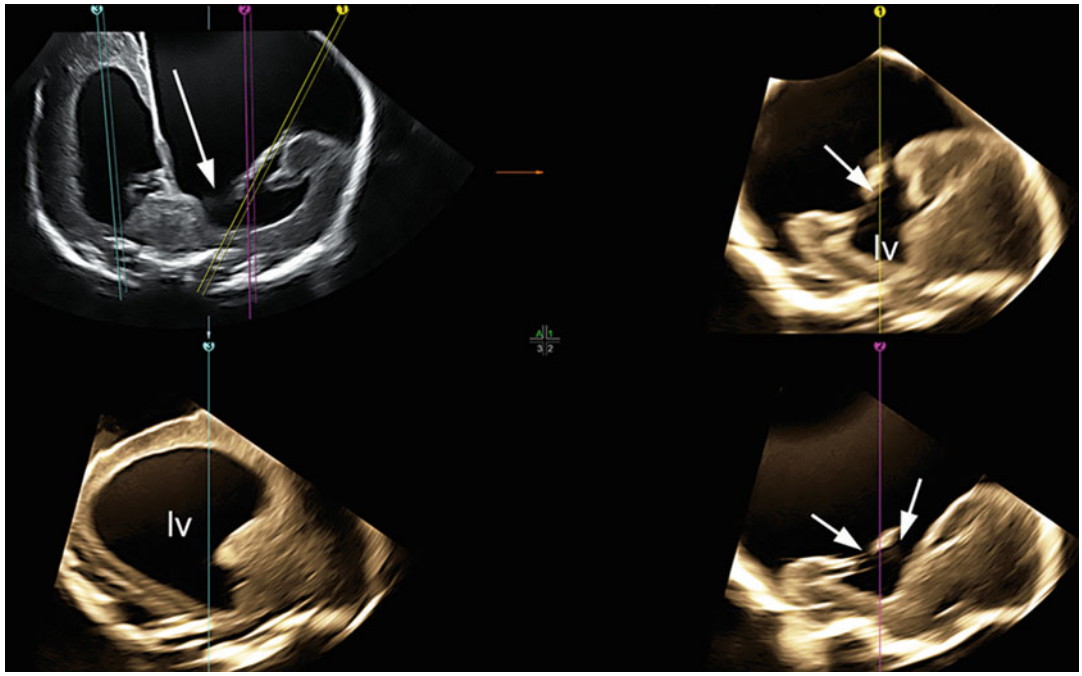

Fig. 57 Schizencephaly. 23 weeks of gestation. Three-dimensional multiplanar imaging demonstrates all the features of the anomaly. Top left, reference coronal view, showing the cleft in the cortex (arrow) and the planes corresponding to the other images; top right, the parasagittal cut demonstrates open-lip schizencephaly and part of the choroid plexus outside the ventricle (arrow) (lv, lateral ventricle); bottom left, the contralateral parasagittal cut shows severe ventriculomegaly (lv, lateral ventricle); bottom right, another demonstration of the cortex interruption (arrows)

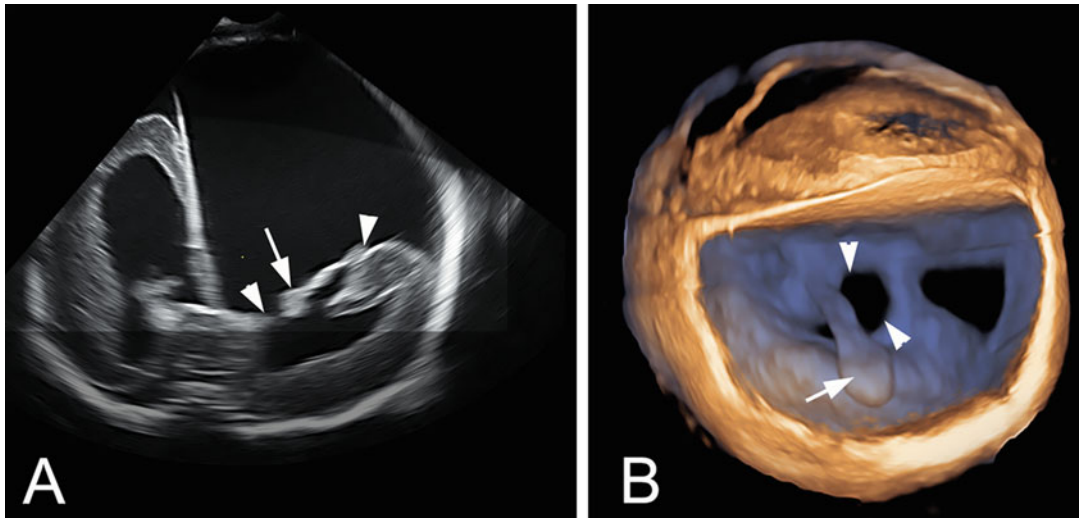

Fig. 58 Schizencephaly. In the same case of Fig.57, the surface-rendering technique (**b**) shows the choroid plexus (arrow) herniated through the gap in the cortex (arrowheads). The rendering is clearer than the two-dimensional coronal view in **a**

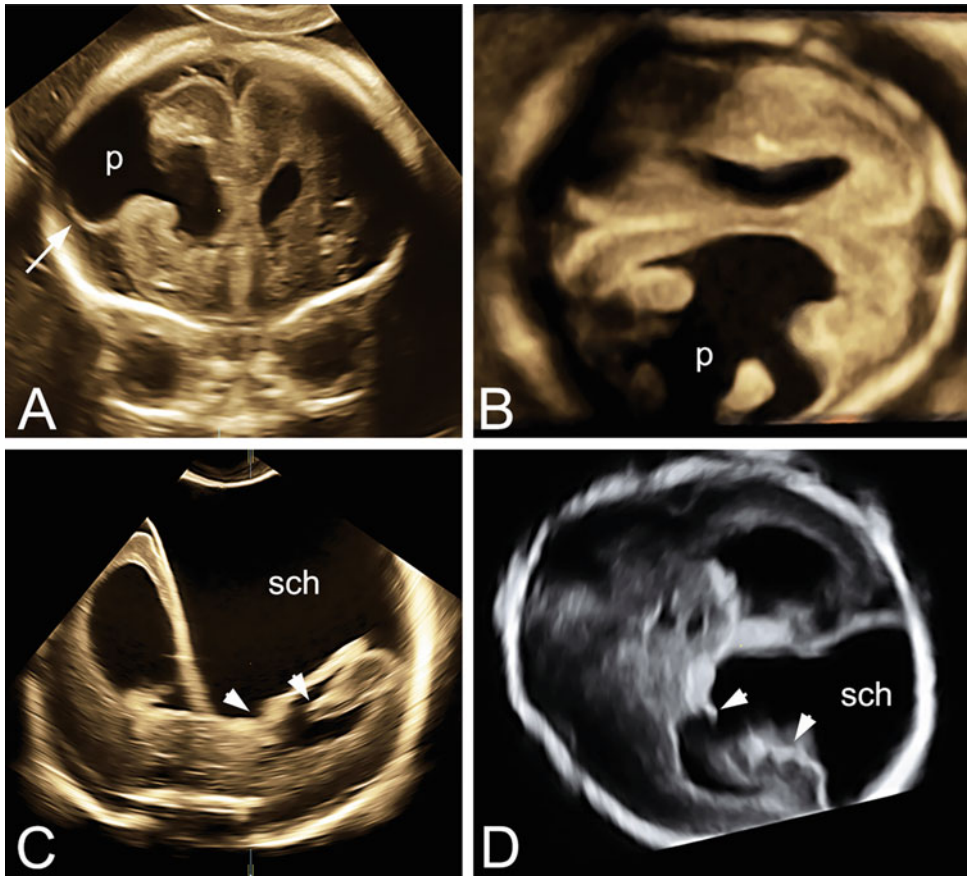

Fig. 59 The differential diagnosis between porencephaly and schizencephaly may be challenging. (**a**–**b**) Porencephaly (p) is characterized by a rounder aspect and sometimes a clear thin wall (arrow) can be recognized; (**c**–**d**) in schizencephaly, the cystic area is more triangular, with acute angles. Ventriculomegaly is often found in both lesions, as evident in all images

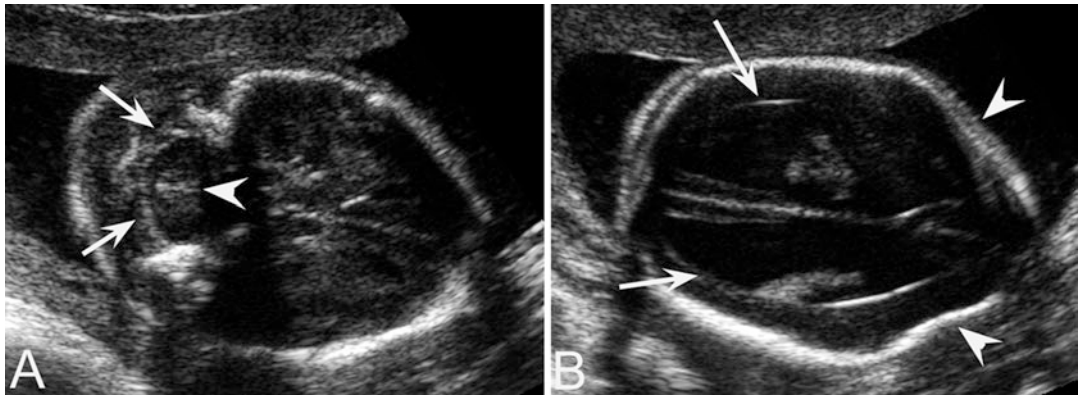

Fig. 60 Open spina bifida – indirect, cranial signs (Chiari II malformation). (**a**) On the trans-cerebellar view, it is possible to detect the annulment of the cisterna magna (arrows) and the banana-shaped hypoplastic cerebellum (arrowheads), which characterize the Chiari II malformation; (**b**) scalloping of the frontal bones (lemon sign – arrowheads) and moderately severe secondary ventriculomegaly (arrows)

et al. 2015). These signs can be found from 16 weeks of gestation until term. Ventriculomegaly is a relatively late-onset sign, and its features will be described separately below; it is found in 57% of the cases. Sonographic assessment of the fetal spine is rather difficult even today, being strongly dependent upon the fetal life. Direct sonographic recognition of the spinal defect requires systematic examination of each neural arch, from the cervical to the sacral ones, in the axial and midsagittal planes. In particular, the midsagittal plane can be used for an adequate evaluation of the cranio-caudal extension of the defect and to assess the dimensions of the myelomeningocele (Fig. 61). On axial views, it is possible to detect the interruption of the cutaneous contour at the level of the affected vertebrae, which will therefore show a "C" or "U" configuration, due to the absence of the dorsal arches (Fig. 61b). The coronal planes will demonstrate splaying of the lateral processes (Fig. 61c). The three aspects just mentioned can advantageously be demonstrated on the same panel of images using the multiplanar display allowed by three-dimensional ultrasound (Fig. 61a–c). It should be underlined that the direct recognition of the defect is not always so straightforward; in a significant number of cases, the spinal lesion is missed on initial evaluation – especially in case of myelocele or small sacral defects (Fig. 62) – and is diagnosed only because the operator has detected the previously described indirect signs at the level of the fetal head. Fortunately, even small lesions of the spine

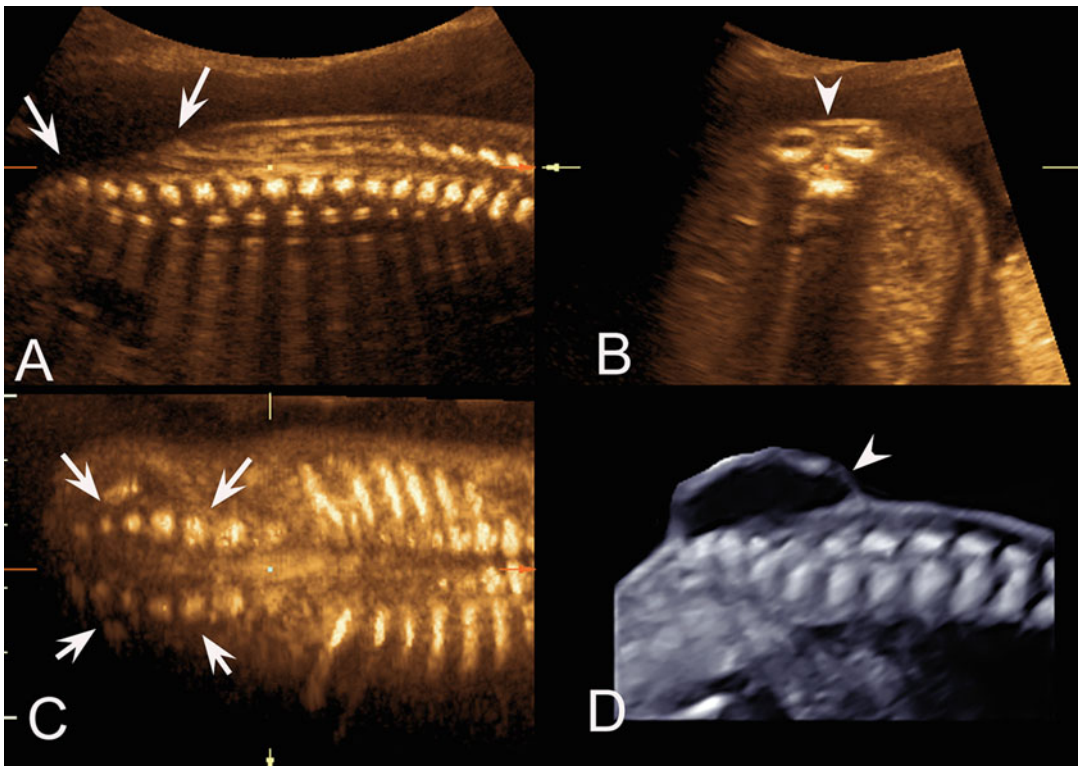

Fig. 61 Open spina bifida, direct spinal signs. Multiplanar imaging demonstrates: (**a**) Myelocele. Sagittal view showing the absence of the posterior processes (arrows); (**b**) axial view showing the U sign, with the vertebral canal open posteriorly (arrowhead); (**c**) coronal view, showing splaying of the lateral processes (arrows); (**d**) another case with a dorsal sac – myelomeningocele (arrowhead)

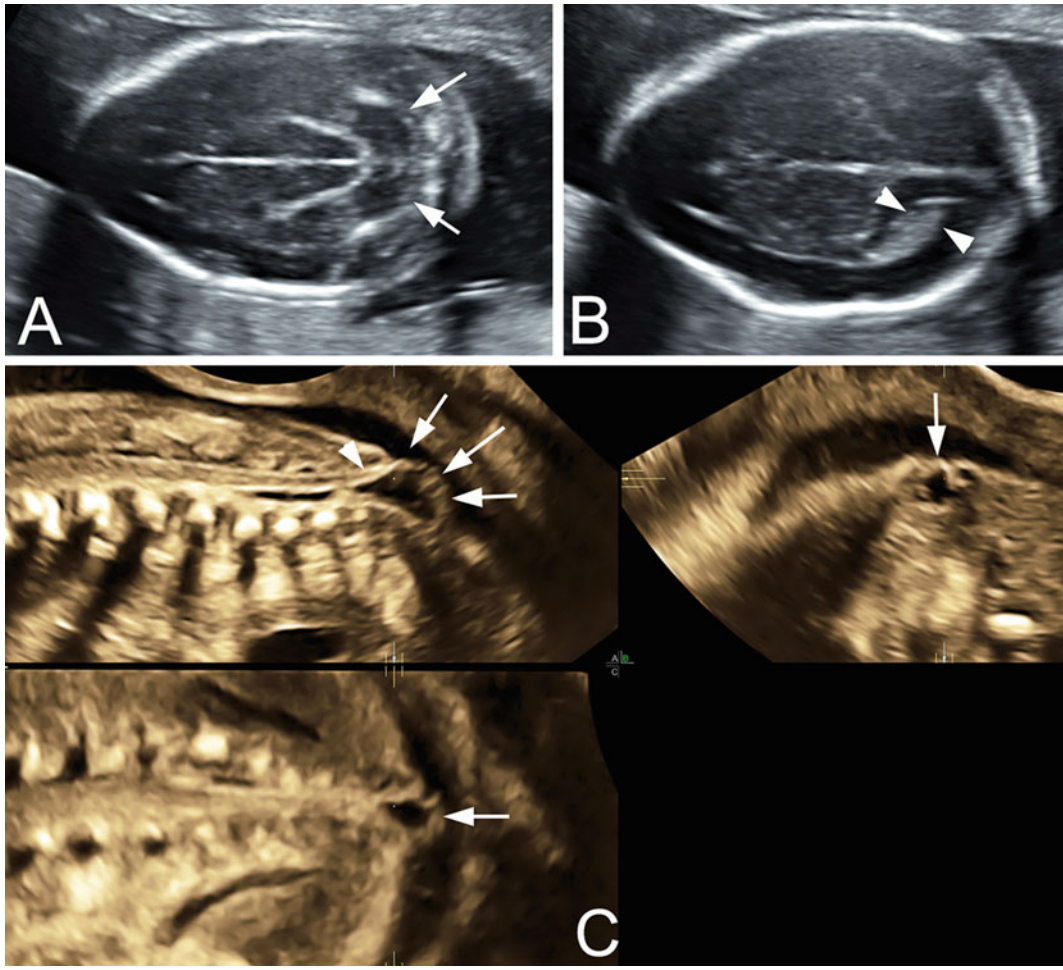

Fig. 62 Small sacral myelomeningocele at 21 gestational weeks. On assessment of the fetal head: (**a**) the Chiari II malformation (arrows, banana sign, with nulled cisterna magna and dysmorphic cerebellum) is found; (**b**) there is no associated ventriculomegaly (arrowheads, trigone). (**c**) Direct transvaginal assessment of the spine (three-dimensional multiplanar imaging) demonstrates a very small sacral myelomeningocele (arrows) associated with a tethered cord (arrowhead). The lesion would have been easily missed if not for cranial signs

are associated with these secondary cerebral abnormalities, provided that the spinal defect is an open one. In particular, it has been demonstrated that indirect cranial signs are associated with open spinal defects in more than 97% of the cases (Bahlmann et al. 2015). Conversely, closed spinal dysraphisms are never associated with cranial signs and can only be recognized on direct inspection of the spine and only in few instances. In some cases, open spina bifida is complicated by the presence of severe abnormalities of the affected segment. In particular, the lumbosacral tract of the spine may be severely distorted, showing acute posterior convexity (Fig. 63). It should be underlined that it is possible, by two- and three-dimensional ultrasound, to recognize the level and the extent of the spinal defect very accurately, and this information is

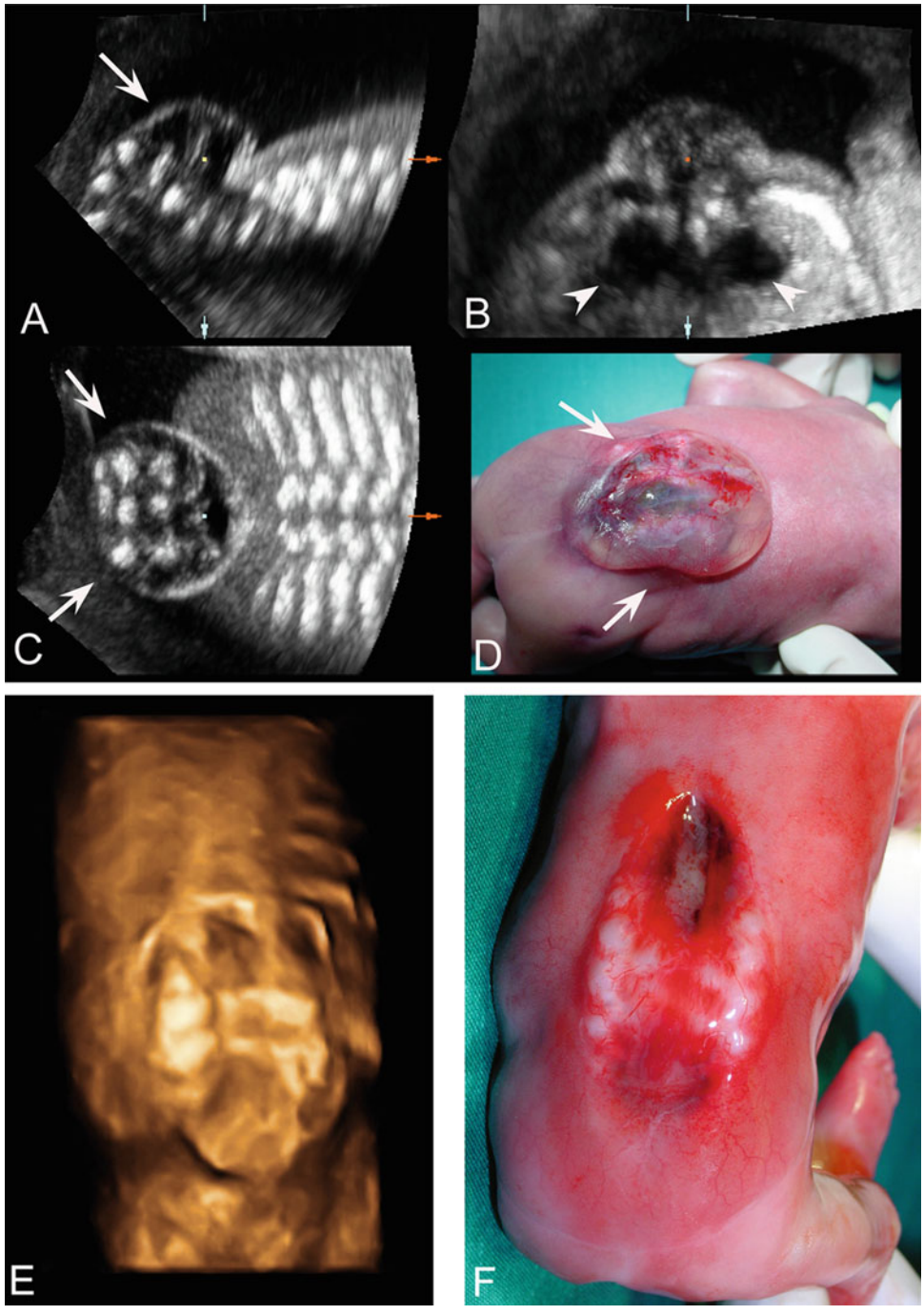

Fig. 63 Complex spina bifida. In some cases, the spinal defect includes also an abnormal convexity of the affected segment, as in this case (21 weeks of gestation). Multiplanar three-dimensional imaging of the defect: (**a**) sagittal view, showing the abnormal spinal convexity at the lumbar level (arrow); (**b**) axial view, showing the "U" sign of the open vertebra, the dorsal meningocele and concurrent bilateral pyelectasis (arrowheads), sign of neurofunctional compromise (the fetus had also talipes); (**c**) coronal view, showing the severe vertebral and cutaneous defect; (**d**) the specimen, after termination of pregnancy; (**e**) another case of complex spina bifida, with severe distortion of the thoraco-lumbar tract of the spine. Three-dimensional imaging shows the wide and complex spinal defect; **f**, confirmation after termination of pregnancy

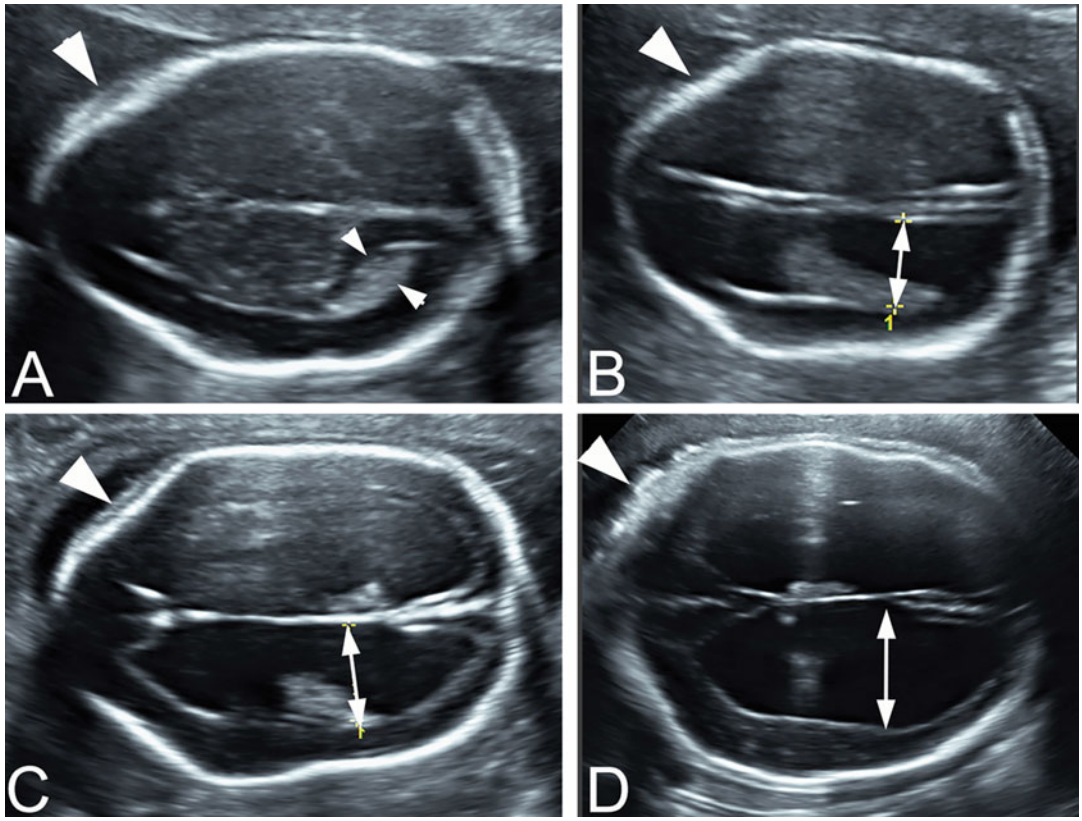

Fig. 64 Ventriculomegaly in open spina bifida. The degree of ventriculomegaly (double arrow) associated with open spinal dysraphisms may vary, from absent (**a**) to severe (**d**). The typical feature is the pointed shape of the frontal horn, which parallels the splaying frontal bones (arrowhead) in the so-called *lemon sign* (see text)

important because the level of the spinal lesion dictates to a certain extent motor and the neurofunctional outcome of fetuses with OSD; and these data can be advantageously employed during prenatal counseling sessions, when the neurosurgeon will need this piece of information to fine-tuning his/her consultation.

Associated anomalies include talipes, pyelectasis, and/or bladder distension with the latter representing signs of neurofunctional damage. The risk of chromosomal anomalies is significant (8–16%) (Kennedy et al. 1998; Sepulveda et al. 2004).

In fetuses with open spina bifida, ventriculomegaly represents a relatively late-onset sign. It appears in the late 2nd trimester in most cases (70%) and worsens thereafter (80–90%) (Fig. 64). In spina bifida, the dilated ventricles have a peculiar shape: they show a pointed frontal horn, which is rather typical. On a transventricular plane, the lateral wall of the frontal horn is therefore parallel with the frontal bone, which shows a flattened outline, consistent with the so-called lemon sign (Fig. 64). This sign, which describes the frontal scalloping, is present in roughly 50% of fetuses with spina bifida, develops early, and is lost in most cases by 24 weeks (Nicolaides et al. 1986).

In any case, a thorough assessment of the fetal brain should be warranted in fetuses with open spina bifida, because ventriculomegaly may also be related to associated CNS malformations (Fig. 65). In fact, both midline anomalies as agenesis of the corpus callosum and migration

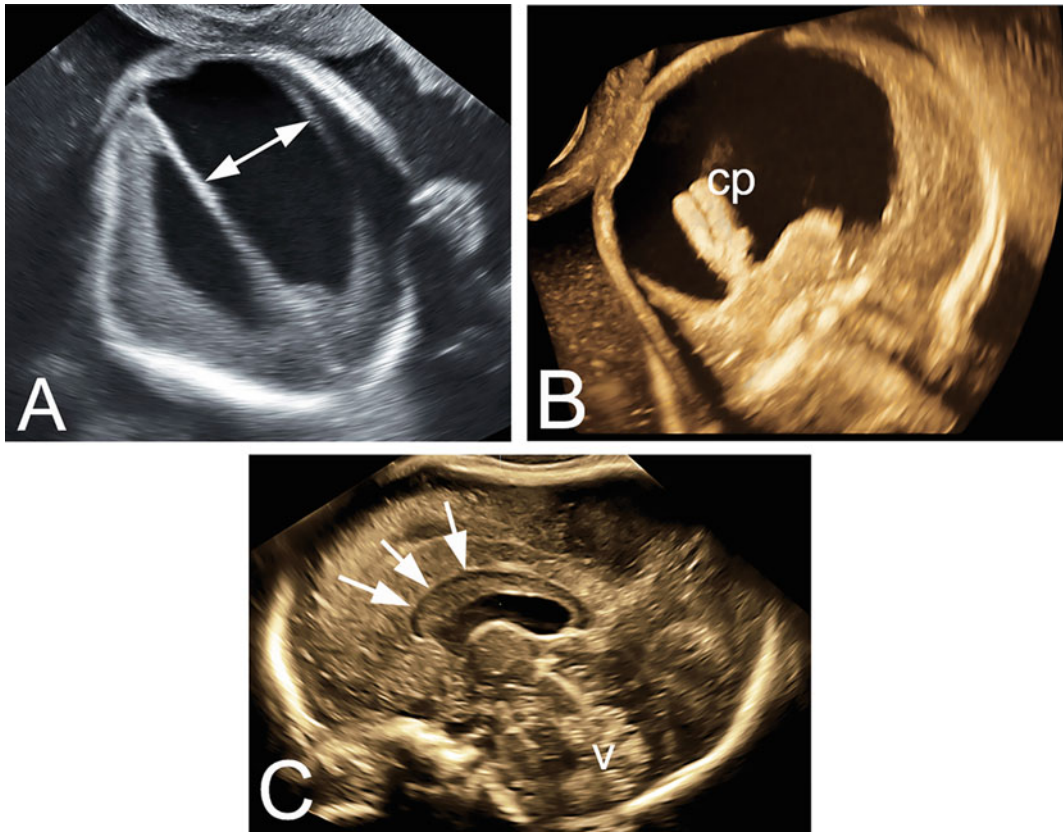

Fig. 65 Open spina bifida may be associated with other CNS lesions. (**a**–**b**) Severe unilateral ventriculomegaly with parenchymal destruction: (**a**) axial view demonstrating the asymmetrical lesion and the abnormal atrial width (double arrow); (**b**) on three-dimensional surface rendering, with a sagittal approach, the dangling choroid plexus (cp) is shown; (**c**) another case, in which a thick, dysraphic corpus callosum (arrows) was associated with an open spina bifida (v: vermis)

defects or also aqueductal stenosis (Fig. 66) may be associated with neural tube defects.

Conclusion

In conclusion, we have shown that the diagnosis of "hydrocephalus" cannot be made with certainty in the fetus. In prenatal life, the most used term is *ventriculomegaly* because this is the sign that can easily be detected and characterized, less so to ascertain whether it is due to obstruction (hydrocephalus) or not. Another concept that we have illustrated in these pages is that in prenatal life the epidemiology of CNS abnormalities is completely different in comparison with neonatal and, above all, pediatric populations. This is due to the fact that termination of pregnancy (in the countries where this option is allowed by law) and spontaneous fetal or early neonatal demise have a deep impact on the prevalence of the various pathologic conditions after birth. In the fetus, the association of ventriculomegaly with other severe CNS and extra-CNS malformations is therefore much more common that in postnatal life.

A final notation regards the issue of the normal and abnormal mechanisms of CSF circulation. In postnatal life, this mechanism is still unclear and

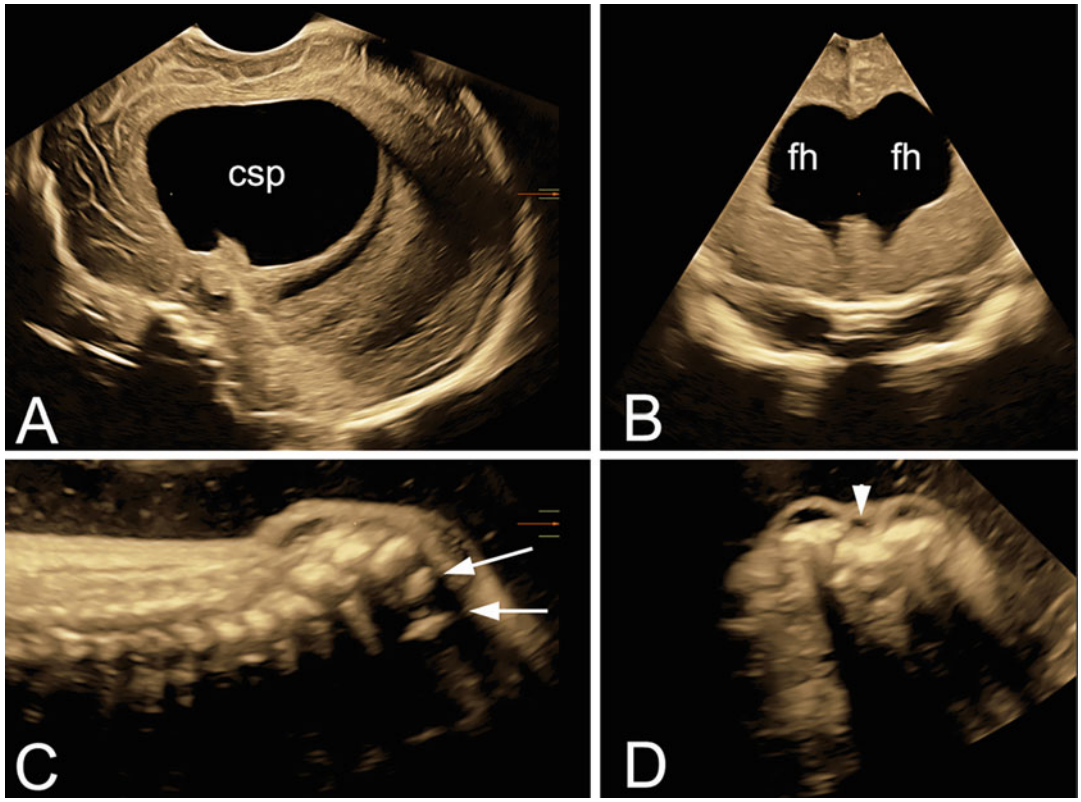

Fig. 66 Ventriculomegaly in open spina bifida. If the degree of ventriculomegaly is severe, the concurrent occurrence of aqueductal stenosis should be considered. 30 weeks of gestation. Three-dimensional multiplanar imaging of the head and spine demonstrates: (**a**) on the midsagittal view, severe enlargement of the cavum septi pellucidi (csp); (**b**) on the coronal view, severe dilatation of the frontal horns (fh), with disruption of the cavum septi pellucidi; (**c**) midsagittal view of the spine, showing severe distortion of the sacral spine (arrows); (**d**) axial view of the spine at the lumbar level shows the typical "U" sign, for the absence of the posterior arches (arrowhead)

in fact various theories have been put forward. In the fetus, the uncertainty is even more pronounced, because of the limited possibility to explore instrumentally the physiology of the CSF circulation, considering also that the Pacchioni granules, that, according to one of the most accredited theories, are considered the main clearance pathway for the CSF, are absent, until almost at the end of gestation. At the same time, with the exception of the lateral ventricles, it is rather challenging if not impossible to evaluate sonographically the Sylvian aqueduct in the fetus. This is why the literature addressing the prenatal counterpart of hydrocephalus is very scant, as mentioned in this chapter.

The take-home message for non-fetal medicine experts is that in prenatal life the overwhelming majority of cases of ventriculomegaly are secondary to other more severe congenital anomalies of the CNS in the context of chromosomal, nonchromosomal, or field developmental abnormalities.

References

Almog B, Gamzu R, Achiron R et al (2003) Fetal lateral ventricular width: what should be its upper limit? A prospective cohort study and reanalysis of the current and previous data. J Ultrasound Med 22:39–43

Bahlmann F, Reinhard I, Schramm T et al (2015) Cranial and cerebral signs in the diagnosis of spina bifida between 18 and 22 weeks of gestation: a German multicentre study. Prenat Diagn 35(3):228–235. https://doi.org/10.1002/pd.4524. Epub 2015 Feb 4

Barkovich AJ, Kjos BO (1989) Revised classification of posterior fossa cysts and cystlike malformations based

on the results of multiplanar MR imaging. AJR 153:1289–1300
Barkovich AJ, Millen KJ, Dobyns WB (2009) A developmental and genetic classification for midbrain-hindbrain malformations. Brain 132(Pt 12):3199–3230
Bayer SA, Altman J (2008) Atlas of human central nervous system development – 5 volume set. CRC Press/Taylor and Francis Group, Boca Raton
Blake JA (1900) The roof and lateral recesses of the 4th ventricle, considered morphologically and embryologically. J Comp Neurol 10:79–108
Brocklehurst G (1969) The development of the human cerebrospinal fluid pathway with particular reference to the roof of the fourth ventricle. J Anat 105 (Pt 3):467–475
Bromley B, Frigoletto FD Jr, Benacerraf BR (1991) Mild fetal lateral cerebral ventriculomegaly: clinical course and outcome. Am J Obstet Gynecol 164:863–867
Bystron I, Blakemore C, Rakic P (2008) Development of the human cerebral cortex: Boulder Committee revisited. Nat Rev Neurosci 9(2):110–122
Cagneaux M, Vasiljevic A, Massoud M et al (2013) Severe second-trimester obstructive ventriculomegaly related to disorders of diencephalic, mesencephalic and rhombencephalic differentiation. Ultrasound Obstet Gynecol 42(5):596–602
Cardoza JD, Goldstein RB, Filly RA (1988) Exclusion of fetal ventriculomegaly with a single measurement: the width of lateral ventricular atrium. Radiology 169:711–714
Cohen-Sacher B, Lerman-Sagie T, Lev D et al (2006) Sonographic developmental milestones of the fetal cerebral cortex: a longitudinal study. Ultrasound Obstet Gynecol 27(5):494–502
De Keersmaecker B, Van Esch H, Van Schoubroeck D et al (2013) Prenatal diagnosis of MPPH syndrome. Prenat Diagn 33(3):292–295
Deloison B, Chalouhi GE, Sonigo P (2012) Hidden mortality of prenatally diagnosed vein of Galen aneurysmal malformation: retrospective study and review of the literature. Ultrasound Obstet Gynecol 40(6):652–658
Emery SP, Hogge WA, Hill LM (2005) Accuracy of prenatal diagnosis of isolated aqueductal stenosis. Prenat Diagn 35:319–324
Garel C (2004) Abnormalities of the fetal cerebral parenchyma: ischaemic and haemorrhagic lesions. In: Garel C (ed) MRI of the fetal brain. Springer-Verlag Berlin Heidelberg, pp 247–262
Gato A, Desmond ME (2009) Why the embryo still matters: CSF and the neuroepithelium as interdependent regulators of embryonic brain growth, morphogenesis and histiogenesis. Dev Biol 327(2):263–272
Hertzberg BS, Kliewer MA, Freed KS et al (1997) Third ventricle: size and appearance in normal fetuses through gestation. Radiology 203(3):641–644
International Society of Ultrasound in Obstetrics & Gynecology Education Committee (2007) Sonographic examination of the fetal central nervous system: guidelines for performing the 'basic examination' and the 'fetal neurosonogram'. Ultrasound Obstet Gynecol 29 (1):109–116
Kennedy D, Chitayat D, Winsor EJT et al (1998) Prenatally diagnosed neural tube defects: ultrasound, chromosome, and autopsy or postnatal findings in 212 cases. Am J Med Genet 77:317–321
Kier EL, Truwit CL (1996) The normal and abnormal genu of the corpus callosum: an evolutionary, embryologic, anatomic, and MR analysis. AJNR Am J Neuroradiol 17(9):1631–1641
Lun MP, Monuki ES, Lehtinen MK (2015) Development and functions of the choroid plexus-cerebrospinal fluid system. Nat Rev Neurosci 16(8):445–457
Mack J, Squier W, Eastman JT (2009) Anatomy and development of the meninges: implications for subdural collections and CSF circulation. Pediatr Radiol 39 (3):200–210
Mangione R, Fries N, Godard P et al (2011) Neurodevelopmental outcome following prenatal diagnosis of an isolated anomaly of the corpus callosum. Ultrasound Obstet Gynecol 37(3):290–295
Melchiorre K, Bhide A, GIka AD et al (2009) Counseling in isolated mild fetal ventriculomegaly. Ultrasound Obstet Gynecol 34:212–224
Monteagudo A, Timor-Tritsch IE (1997) Development of fetal gyri, sulci and fissures: a transvaginal sonographic study. Ultrasound Obstet Gynecol 9(4):222–228
Monteagudo A, Timor-Tritsch IE (2009) Normal sonographic development of the central nervous system from the second trimester onwards using 2D, 3D and transvaginal sonography. Prenat Diagn 29(4):326–339
Mortazavi MM, Griessenauer CJ, Adeeb N et al (2014) The choroid plexus: a comprehensive review of its history, anatomy, function, histology, embryology, and surgical considerations. Childs Nerv Syst 30(2):205–214
Müller F, O'Rahilly R (2003) Segmentation in staged human embryos: the occipitocervical region revisited. J Anat 203(3):297–315
Napolitano R, Maruotti GM, Quarantelli M (2009) Prenatal diagnosis of Seckel syndrome on three-dimensional sonography and magnetic resonance imaging. J Ultrasound Med 28:369–374
Nicolaides KH, Campbell S, Gabbe SG (1986) Ultrasound screening for spina bifida: cranial and cerebellar signs. Lancet 2(8498):72–74
O'Rahilly R, Muller F (1987) Developmental stages in human embryos. Carnegie institution of Washington, Washington, DC
O'Rahilly R, Muller F (1999) Minireview: Summary of the initial development of the human nervous system. Teratology 1999; 60(1):39–41
O'Rahilly R, Muller F (2005) The embryonic human brain: an atlas of developmental stages, 3rd edn. Wiley, New York
O'Rahilly R, Muller F (2010) Developmental stages in human embryos: revised and new measurements. Cells Tissues Organs 192(2):73–84
Ouahba J, Luton D, Garel C et al (2006) Prenatal isolated mild ventriculomegaly: outcome in 167 cases. BJOG 113:1072–1079

Paladini D (2008) Diagnosis of spina bifida and other dysraphic states in the fetus. In: Ozek MM, Cinalli G, Maixner WJ (ed). Spina Bifida. Management and outcome. Springer-Verlag Italia, Milan, p 75–102

Paladini D, Volpe P (2006) Posterior fossa and vermian morphometry in the characterization of fetal cerebellar abnormalities: a prospective three-dimensional ultrasound study. Ultrasound Obstet Gynecol 27 (5):482–489

Paladini D, Sglavo G, Quarantelli M et al (2005) Large infratentorial subdural hemorrhage diagnosed by ultrasound and MRI in a second-trimester fetus. Letter to the Editor. Ultrasound Obstet Gynecol 26:789–796

Paladini D, Quarantelli M, Pastore G (2012) Abnormal or delayed development of the posterior membranous area of the brain: anatomy, ultrasound diagnosis, natural history and outcome of Blake's pouch cyst in the fetus. Ultrasound Obstet Gynecol 39(3):279–287

Paladini D, Pastore G, Cavallaro A et al (2013) Agenesis of the fetal corpus callosum: sonographic signs change with advancing gestational age. Ultrasound Obstet Gynecol 42(6):687–690

Paladini D, Quarantelli M, Sglavo G (2014) Accuracy of neurosonography and MRI in clinical management of fetuses referred with central nervous system abnormalities. Ultrasound Obstet Gynecol 44(2):188–196

Pinto J, Paladini D, Severino M (2016) Delayed rotation of the cerebellar vermis: a pitfall in early second-trimester fetal magnetic resonance imaging. Ultrasound Obstet Gynecol 48(1):121–124

Pugash D, Hendson G, Dunham CP et al (2012) Sonographic assessment of normal and abnormal patterns of fetal cerebral lamination. Ultrasound Obstet Gynecol 40(6):642–651

Rakic S, Zecevic N (2003) Emerging complexity of layer I in human cerebral cortex. Cereb Cortex 13 (10):1072–1083

Rubenstein JL, Shimamura K, Martinez S, Puelles L (1998) Regionalization of the prosencephalic neural plate. Annu Rev Neurosci 21:445–477

Salomon LJ, Ouahba J, Delezoide AL, Vuillard E, Oury JF, Sebag G, Garel C et al (2006) Third-trimester fetal MRI in isolated 10–12 mm ventriculomegaly: is it worth it? BJOG 113:942–947

Sari A, Ahmetoglu A, Dinc H et al (2005) Fetal biometry: size and configuration of the third ventricle. Acta Radiol 46(6):631–635

Sepulveda W, Corral E, Ayala C et al (2004) Chromosomal abnormalities in fetuses with open neural tube defects: prenatal identification with ultrasound. Ultrasound Obstet Gynecol 23:352–356

Strazielle N, Ghersi-Egea JF (2000) Choroid plexus in the central nervous system: biology and physiopathology. J Neuropathol Exp Neurol 59(7):561–574

Streeter GL (1911) Die Entwicklung des Nervensystems. In: Keibel F, Mall FP (eds) Handbuch der Entwicklungsgeschichte des Menschen. Zweiter Band, Hirzel/Leipzig, pp.1–156

Timor-Tritsch IE, Monteagudo A (1996) Transvaginal fetal neurosonography: standardization of the planes and sections by anatomic landmarks. Ultrasound Obstet Gynecol 8(1):42–47

Toi A, Lister WS, Fong KW (2004) How early are fetal cerebral sulci visible at prenatal ultrasound and what is the normal pattern of early fetal sulcal development? Ultrasound Obstet Gynecol 24(7):706–715

Tortori-Donati P, Fondelli MP, Rossi A et al (1996) Cystic malformations of the posterior cranial fossa originating from a defect of the posterior membranous area. Mega cisterna magna and persisting Blake's pouch: two separate entities. Childs Nerv Syst 12(6):303–308

Van den Hof MC, Wilson RD, Diagnostic Imaging Committee, Society of Obstetricians and Gynaecologists of Canada, Genetics Committee, Society of Obstetricians and Gynaecologists of Canada (2005) Fetal soft markers in obstetric ultrasound. J Obstet Gynaecol Can 27:592–636

Vassallo M, Maruotti GM, Quarantelli M et al (2012) Choroid plexus carcinoma: prenatal characterization by 3-dimensional sonography and magnetic resonance imaging, perinatal management, and natural history. J Ultrasound Med 31(2):337–339

Volpe P, Muto B, Passamonti U (2015) Abnormal sonographic appearance of posterior brain at 11–14 weeks and fetal outcome. Prenat Diagn 35(7):717–723

Wilson JT (1937) On the nature and mode of origin of the foramen of Magendie. J Anat 71(Pt 4):423–428